



UNIWERSYTET SZCZECIŃSKI
WYDZIAŁ NAUK ŚCISŁYCH
I PRZYRODNICZYCH



University of Szczecin
Faculty of Pure and Exact Sciences

PhD Thesis

in the Physical Sciences

to receive the academic degree of
Doctor of Physical Sciences

Ricci Cosmologies

Author: Roberto Caroli

PESEL: 93071916093

Supervisor: Prof. Mariusz P. Dąbrowski

Submission date: 13th June 2022

Oświadczenie Doktoranta

Oświadczam, że moja praca pt.: **Ricci Cosmologies**:

- a. została napisana przeze mnie samodzielnie,
- b. nie narusza praw autorskich w rozumieniu ustawy z dnia 14 lutego 1994 roku o prawie autorskim i prawach pokrewnych (Dz.U. 2019 r. poz. 1231) oraz dóbr osobistych chronionych prawem,
- c. nie zawiera danych i informacji, które uzyskałem / uzyskałam w sposób niedozwolony,
- d. nie była podstawą nadania tytułu naukowego lub zawodowego ani mnie ani innej osobie.

Ponadto oświadczam, że treść pracy przedstawionej przeze mnie do obrony, zawarta na przekazanym nośniku elektronicznym jest identyczna z jej wersją drukowaną.

Szczecin, dn. ...13.06.2022.....

.....*Roberto Carli*.....

podpis doktoranta

Oświadczenie

Wyrażam zgody na udostępnienie mojej pracy doktorskiej pt.: **Ricci Cosmologies**.

Szczecin, dn. ...13.06.2022.....

.....*Roberto Carli*.....

podpis doktoranta

Oświadczenie

Akceptuję ostateczną wersję pracy.

Szczecin, dn. ...13.06.2022.....

.....*Maciej P. Dąbrowski*.....

podpis promotora

Abstract

This dissertation deals with the new framework of Ricci Cosmology which has recently emerged from the study of out-of-equilibrium relativistic fluids in curved spacetime.

After briefly recalling the strengths and the challenges of the widely accepted Standard Cosmological Model or Λ CDM, we shortly review the theoretical construction on which the framework of Ricci Cosmology relies.

Next, we introduce different models we have derived in this framework in order to describe the late-time accelerated expansion of the Universe, under the assumption of constant transport coefficients.

The first model considered is Isotropic Ricci Cosmology, in which Ricci pressure terms affect all the matter components filling in the Universe. A departure from perfect fluid redshift scaling is found for each matter component.

Next, we consider two models in which we drop the assumption of the Cosmological Principle: in the first model, we study the consequences of the departure from equilibrium for cosmic fluids on a background described by the Bianchi I Type metric, while in the second model, we consider an inhomogeneous Universe described by the Lemaître-Tolman-Bondi metric.

Then, we study the model of Ricci Vacuum Cosmology in which non-equilibrium Ricci terms affect only the vacuum pressure. As a result of such departure from equilibrium for the vacuum, its energy density depends on the energy densities of matter and radiation. Two subcases are taken into account: in the first, the Ricci vacuum interacts with Cold Dark Matter, while in the second, it interacts with a relativistic species, which we call Dark Radiation.

The last model we consider is the Tilted Ricci Cosmology, in which the observer 4-velocity does not coincide with the fluid 4-velocity, leading to the presence of an energy flux and an anisotropic stress in the fluid as seen by the observer. We study the effects that the non-equilibrium Ricci terms have onto the cosmic fluid and on its energy conditions.

Finally, after introducing the statistical tools for Bayesian Inference and the available cosmological data, we discuss the results of the fit of the Isotropic Ricci Cosmology model against these cosmological data.

Observational bounds on the parameters of the model are found and its capability to relief the Hubble tension at the background level and to describe better than Λ CDM the cosmological data are discussed.

Acknowledgements

First, I would like to thank my supervisor Prof. Mariusz P. Dąbrowski for his patience and time in all the stages of my PhD studies.

A special thank to Prof. Vincenzo Salzano for his help in diving into the observational cosmology methods.

I would like to also thank the mates of this challenging trip at the University of Szczecin in the Cosmology Group Fabian, Samuel, Paolo, and Enrico together with Alessandro from the Institute of Mathematics.

A thank to those that I have known in conferences, doctoral schools, and workshops for the discussions and the shared scientific insights, even virtually.

I would like to thank also my Bachelor and Master theses supervisors, Prof. F. Benatti and Prof. I. Sachs for their support in the last years and all the professors and teachers that have contributed to my education during the years at school and at University: without their contributions, this important milestone in my life would not have been possible.

A special thank to the Apulian crew that makes amazing the summers and the other holidays and smart working periods during my PhD and make me stronger through its difficulties: Alessandro, Angelo, Angioletto, Chiara, Ciccio, Elena, Federica, Francesca, Francesco, Gigi, Ilaria, Ilenia, Marino, Matteo, Michele, Valeria, Vanessa, Vita.

A special thank to my grandparents that have been a source of inspiration and great life examples and to my brother Fulvio and his girlfriend Chiara, and my parents, Mina and Graziano, for their invaluable support.

Declaration

I hereby declare that the contents of this dissertation are original except where references to the work of others have been specified, and have not been submitted in whole or in part for any other qualification or degree in this or any other university. This dissertation is my own work and contains nothing but the results of my work done in collaboration with others, except as specified in the text. This dissertation contains fewer than 65,000 words including appendices, bibliography, footnotes, tables and equations and has fewer than 150 figures.

Roberto Caroli

Roberto Caroli

13.06.2022

Date

Contents

1	Introduction	1
2	Standard Cosmological Model	3
2.1	Ingredients of Standard Cosmological Model	3
2.2	Problems of Standard Cosmological Model	7
3	Relativistic Fluid Dynamics	9
3.1	General Construction	9
3.2	Fluids near equilibrium	10
3.2.1	First order Energy-Momentum Tensor	12
3.2.2	Second order Energy-Momentum Tensor	14
4	Ricci Cosmologies	17
4.1	Isotropic Ricci Cosmology	17
4.1.1	Physical bounds from Thermodynamics	20
4.1.2	Energy conditions in Isotropic Ricci Cosmology	21
	Null Energy Condition (NEC)	21
	Weak Energy Condition (WEC)	22
	Strong Energy Condition (SEC)	22
	Dominant Energy Condition (DEC)	23
4.2	Anisotropic Ricci Cosmology	24
4.3	Inhomogeneous Ricci Cosmology	27
4.4	Ricci Vacuum Cosmology	30
4.4.1	Cold Dark Matter - Ricci Vacuum interaction	32
4.4.2	Dark Radiation - Ricci Vacuum interaction	34
4.5	Tilted Ricci Cosmology	35
4.5.1	Tilted Cosmology	35
4.5.2	Tilted Ricci Cosmology	38
	Null Energy Condition	38
	Weak Energy Condition	39
	Strong Energy Condition	39
	Dominant Energy Condition	40

5	Bayesian Inference and Monte Carlo methods	43
5.1	Frequentist vs Bayesian Probabilities	43
5.2	Bayesian Inference	44
5.2.1	Probability	44
5.2.2	Random variables	45
5.3	Parameter Estimation	45
5.4	Hypothesis Testing	47
5.5	Markov Chain Monte Carlo methods	49
5.5.1	Markov Chain	49
5.5.2	The Metropolis-Hastings algorithm	50
6	Cosmological Probes of Dark Energy	53
6.1	Cosmic distances	53
6.1.1	Luminosity distance	53
6.1.2	Angular diameter distance	54
6.2	Type Ia supernovae	55
6.3	Gamma-Ray Bursts	57
6.4	Cosmic Chronometers	58
6.5	Strong Lensed Quasars	58
6.6	Baryon Acoustic Oscillations	59
6.7	Cosmic Microwave Background	61
7	Ricci Cosmology tested against astronomical data	65
7.1	Assumptions	65
7.2	Data & Statistical Analysis	66
	Data	66
	Statistical Analysis	67
7.3	Results from the fits	68
7.4	Discussion	72
8	Conclusion and Outlook	75
A	Priors derivation of Isotropic Ricci Cosmology parameters	77
A.1	Ansatz 1	77
A.2	Ansatz 2	79
A.3	Ansatz 3	80
A.4	Ansatz 4	81

List of Figures

4.1	Representation of the observer 4- velocity orthogonal to the surface of homogeneity $S(t)$ and making a hyperbolic angle β with the fluid 4-velocity. The tensor $p_{\mu\nu}$ spans the 2-surface in $S(t)$ perpendicular to the vectors c^μ and \tilde{c}^μ . (King and Ellis, 1973)	37
6.1	Angular diameter distance for a source of physical scale r from (Perivolaropoulos and Skara, 2021)	55
7.1	1σ and 2σ contour plots in the parameter plane $\delta_\Lambda - \delta_m$ for the four ansätze (Ansatz 1 - blue; Ansatz 2 - grey; Ansatz 3 - green; Ansatz 4 - red)	70
7.2	1σ and 2σ contour plots in the parameter plane $\delta_r - \delta_m$ for the two ansätze in which $\delta_r \neq 0$ (Ansatz 2 - grey; Ansatz 4 - red)	71

List of Tables

7.1	The table reports the four different ansätze on the reduced second order transport coefficients we have considered.	66
7.2	The table reports the priors on the deviation parameters δ_m, δ_r and δ_Λ we have used in our data analysis. These priors are derived in Appendix A.	66
7.3	In the table, we report the constraints on the parameters of Isotropic Ricci Cosmology with ansatz 1 and Λ CDM, both tested against the same full and late data sets.	69
7.4	In the table, we report the constraints on the parameters of Isotropic Ricci Cosmology with ansatz 2 and Λ CDM, both tested against the same full and late data sets.	70
7.5	In the table, we report the constraints on the parameters of Isotropic Ricci Cosmology with ansatz 3 and Λ CDM, both tested against the same full and late data sets.	71
7.6	In the table, we report the constraints on the parameters of Isotropic Ricci Cosmology with ansatz 4 and Λ CDM, both tested against the same full and late data sets.	72

Chapter 1

Introduction

In Cosmology, the model that best describes the late-time phase of accelerated expansion of our Universe is the *Standard Cosmological Model*, also known as Λ CDM. Despite its strengths, we still face fundamental theoretical issues regarding the physical nature of Cold Dark Matter (CDM) and of the Cosmological Constant Λ . Furthermore, there are new observational challenges due to the growing precision of the cosmological data, among which the most important is represented by the Hubble Tension.

Among the proposals to solve the new and the old puzzles present in Cosmology, the hypothesis of a departure from the perfect fluid description of the cosmic fluid has been proposed and represents the core of the framework of Viscous Cosmology, where a dissipative term proportional to the Hubble constant modifies the bulk pressure of the cosmic fluid. For recent reviews, see (Brevik and Grøn, 2014; Brevik et al., 2017).

The models in Viscous Cosmology may differ for the matter components filling in the Universe affected by the bulk viscosity or in the assumptions made on the bulk viscosity coefficients. Some of these models have revealed successful in describing the late-time accelerated expansion. For recent works, see (Brevik, Obukhov, and Timoshkin, 2015; Barbosa et al., 2015; Mohan, Sasidharan, and Mathew, 2017; Silva and Silva, 2019; Cruz, González, and Palma, 2020; Brevik, Makarenko, and Timoshkin, 2019; Madriz Aguilar et al., 2020). So far, nevertheless, it is still debated whether they can solve the Hubble tension (Anand et al., 2017; Yang et al., 2019; Elizalde et al., 2020; Normann and Brevik, 2021).

From the study of relativistic dynamics of fluids out of equilibrium in a curved background, such bulk viscous term is seen just as a first order departure from equilibrium for the cosmic fluids filling in the Universe. In this framework, the correction to the perfect fluid Energy-Momentum Tensor due to the departure from equilibrium is written in terms of a power expansion of gradients of hydrodynamic fields describing the fluid, i.e. its 4-velocity and its energy density, and the metric of the curved background.

Based on these studies, a new cosmological framework, dubbed Ricci Cosmology, has been proposed, in which second order deviations from equilibrium pressure, due to linear terms in the Ricci scalar and the Ricci tensor are taken into account.

The coefficients in front of such terms are the so-called second order transport coefficients and they parameterise the cosmic fluid response to the new pressure terms. The framework of Ricci Cosmology has been studied for the first time in (Baier, Lahiri, and Romatschke, 2019).

These authors explored the possibility for these modifying bulk pressure terms to support early-time inflationary phase of the Universe without resorting to exotic matter fields.

Instead, in this thesis, we investigate the effects of such modifying bulk pressure terms, dubbed as Ricci pressure terms, in the late-time accelerated epoch of our Universe.

We propose some new models in the framework of Ricci Cosmology with different assumptions on the background metric and on the matter components affected by the new pressure terms in such a framework, and study their features in the description of the evolution of the Universe at the background level.

We test against data the Isotropic Ricci Cosmology model, studying whether such model describes better than Λ CDM model the available cosmological data, and at the same time, relieves the Hubble tension.

Chapter 2

Standard Cosmological Model

In this chapter, we review briefly the pillars on which the Concordance Cosmological Model or Λ CDM relies and we briefly mention some of its unsolved theoretical and observational issues.

2.1 Ingredients of Standard Cosmological Model

In Λ CDM, the theory describing how the metric tensor $g_{\mu\nu}$ describing the geometrical properties of the spacetime, treated as a 4-dimensional manifold, evolves with the evolution of the matter in it, described by the Energy-Momentum Tensor (EMT) $T_{\mu\nu}$, is General Relativity (GR).

The dynamics of the universe is thus described by the Einstein equations (Misner, Thorne, and Wheeler, 1973), given by

$$G_{\mu\nu} = \frac{8\pi G}{c^4} T_{\mu\nu}, \quad (2.1)$$

where the sign convention $(-, +, +, +)$ for the metric $g_{\mu\nu}$ is used, c is the speed of light, G is the Newtonian constant of gravitation and $G_{\mu\nu}$ is the Einstein tensor, which can be written as

$$G_{\mu\nu} \equiv R_{\mu\nu} - \frac{1}{2} g_{\mu\nu} R, \quad (2.2)$$

where $R_{\mu\nu}$ is the Ricci tensor and its trace R is the Ricci scalar.

A body subject only to gravity follows a geodesic curve in a curved spacetime. The Ricci tensor describes how much two nearby geodesics deviate in such a spacetime, whereas the Ricci scalar is a measure of how the area a small sphere deviates from its value in a flat spacetime.

The Ricci tensor can be expressed in terms of the spacetime metric $g_{\mu\nu}$ via the formula

$$R_{\mu\nu} = \partial_\alpha \Gamma_{\mu\nu}^\alpha - \partial_\nu \Gamma_{\alpha\mu}^\alpha + \Gamma_{\mu\nu}^\lambda \Gamma_{\lambda\alpha}^\alpha - \Gamma_{\nu\alpha}^\lambda \Gamma_{\lambda\mu}^\alpha, \quad (2.3)$$

where the Christoffel symbol $\Gamma_{\mu\nu}^\rho$ is given by

$$\Gamma_{\mu\nu}^\rho = \frac{1}{2}g^{\rho\alpha} (\partial_\mu g_{\alpha\nu} + \partial_\nu g_{\alpha\mu} - \partial_\alpha g_{\mu\nu}). \quad (2.4)$$

Physically, one can interpret the Christoffel symbols as terms describing gravitational forces which cause objects to accelerate.

The second ingredient underlining Λ CDM is the *Cosmological Principle*: the Universe is assumed to be homogeneous and isotropic on large scales. This assumption dictates a simple form for the spacetime metric $g_{\mu\nu}$ that goes under the name of Friedmann-Lemaitre-Robertson-Walker (FLRW) metric defined by the following infinitesimal spacetime interval in spherical comoving coordinates r, θ and ϕ

$$ds^2 = -c^2 dt^2 + a^2(t) \left[\frac{dr^2}{1 - Kr^2} + r^2(d\theta^2 + \sin^2\theta d\phi^2) \right], \quad (2.5)$$

where $a(t)$ is scale factor, depending only on cosmic time t . The constant K in the metric (2.5) describes the geometry of the 3-dimensional spatial hypersurface with $K = +1, 0, -1$ indicating a spherical, flat and hyperbolic geometry, respectively.

Numerous evidences point towards to flatness of our Universe spatial background ($K = 0$), which results to be described by the flat FLRW metric

$$ds^2 = -c^2 dt^2 + a^2(t) \delta_{ij} dx^i dx^j, \quad (2.6)$$

with x^i comoving Cartesian coordinates.

For the flat FLRW background, the components of the Ricci tensor and the Ricci scalar are given by

$$R_{00} = -3\frac{\ddot{a}}{a}, \quad (2.7)$$

$$R_{ij} = c^{-2} (\ddot{a}a + 2\dot{a}^2) \delta_{ij}, \quad (2.8)$$

and

$$R = \frac{6}{c^2} \left(\frac{\ddot{a}}{a} + \frac{\dot{a}^2}{a^2} \right), \quad (2.9)$$

where the dot denotes the derivative with respect to the cosmic time t .

So far, we have considered the l.h.s. of Einstein equations (2.1).

On the r.h.s., the EMT $T_{\mu\nu}$ represents the source of the gravitational field and is used to describe in GR the matter components filling the Universe.

In Λ CDM, the form of such tensor for a matter component with energy density ρc^2 , pressure $P(\rho)$ and 4-velocity u_μ

$$T_{\mu\nu} = \rho u_\mu u_\nu + P(\rho) h_{\mu\nu}, \quad (2.10)$$

where $h_{\mu\nu} = g_{\mu\nu} + u_\mu u_\nu / c^2$ is the 3-spatial metric of the hypersurface orthogonal to the fluid 4-velocity. The energy density ρc^2 is the energy density of the fluid as seen by a comoving observer with the fluid 4-velocity u_μ .

GR does not specify anything about requirements matter fluids filling in the Universe must satisfy to be considered physically acceptable. Some further criteria are needed and these are represented by the so-called energy conditions which put conditions on the energy density ρc^2 and its relation with the pressure $P(\rho)$

- Null Energy Condition (NEC)

$$\rho + \frac{P(\rho)}{c^2} \geq 0, \quad (2.11)$$

- Weak Energy Condition (WEC)

$$\rho \geq 0, \quad \text{and} \quad \rho + \frac{P(\rho)}{c^2} \geq 0, \quad (2.12)$$

- Strong Energy Condition (SEC)

$$\rho + \frac{P(\rho)}{c^2} \geq 0, \quad \text{and} \quad \rho + 3\frac{P(\rho)}{c^2} \geq 0, \quad (2.13)$$

- Dominant Energy Condition (DEC)

$$\rho \geq 0, \quad \text{and} \quad \rho \geq \frac{|P(\rho)|}{c^2}. \quad (2.14)$$

These inequalities are only valid in the case of an isotropic metric such as the FLRW metric (2.5) and in particular, the flat FLRW metric (2.6). For a general formulation of energy conditions one can consult (Wald, 1984).

For the matter components filling in the Universe in Λ CDM model, the pressure $P(\rho)$ has the barotropic form given by

$$P(\rho) = w\rho c^2, \quad (2.15)$$

where w is the constant equation of state (EoS) parameter, which has a different value depending on the nature of the fluid. In particular, in Λ CDM we have

- Dust, comprising baryonic matter and Cold Dark Matter (CDM) which has only gravitational interaction with baryonic matter, it is the matter content of the Universe whose pressure can be neglected with respect to its energy density, i.e. $w = 0$;

- Radiation, including photons and other possible relativistic relics from the previous stages of the Universe history, has an EoS $w = \frac{1}{3}$;
- Cosmological Constant (CC) or Λ , a constant energy density pervading the Universe, mostly attributed to the vacuum, has an EoS $w = -1$, representing the simplest form of Dark Energy (DE) violating the SEC and thus, supporting an accelerated expansion of the Universe in the current epoch.

By using the flat FLRW metric (2.6) and the EMT (2.10), the Einstein equations (2.1) give us the Friedmann equations

$$H^2 = \frac{8\pi G}{3}\rho, \quad (2.16)$$

and

$$\dot{H} = -4\pi G \left(\rho + \frac{P(\rho)}{c^2} \right), \quad (2.17)$$

where H is the Hubble parameter, defined as

$$H \equiv \frac{\dot{a}}{a}. \quad (2.18)$$

Furthermore, from the contracted Bianchi identities in GR

$$\nabla_\lambda R^\lambda_\mu = \frac{1}{2}\nabla_\mu R \quad (2.19)$$

the EMT (2.10) satisfies the conservation equation

$$\nabla_\mu T^{\mu\nu} = 0, \quad (2.20)$$

which reduces in FLRW background to the continuity equation

$$\dot{\rho} + 3H \left(\rho + \frac{P(\rho)}{c^2} \right) = 0 \quad (2.21)$$

From the continuity (2.21) the matter components filling the Universe in Λ CDM have the following evolution

$$\text{Radiation: } \rho \propto a^{-4}, \quad (2.22)$$

$$\text{Dust: } \rho \propto a^{-3}, \quad (2.23)$$

$$\text{CC: } \rho \propto \text{const.}, \quad (2.24)$$

which imply that the Universe undergoes to two subsequent eras, a radiation dominated era and a matter dominated era in which the Universe expansion following the Big Bang is decelerated, followed by a third era, the CC dominated era corresponding to our accelerated epoch.

By using the first Friedmann equation (2.16), the Hubble function can be rewritten as

$$H^2(a) = H_0 \left[\Omega_m a^{-3} + \Omega_r a^{-4} + \Omega_\Lambda \right], \quad (2.25)$$

where H_0 is the Hubble parameter, i.e. the Hubble function evaluated at the present scale factor, and the dimensionless energy density parameters are defined by

$$\Omega_c = \frac{\rho_c}{\rho_{crit}}, \quad (2.26)$$

with c ranging on the matter components in the Universe and the critical energy density ρ_{crit} defined by

$$\rho_{crit} = \frac{3H_0^2}{8\pi G}. \quad (2.27)$$

In a flat Universe from the Hubble function (2.25), it is straightforward to check that the dimensionless energy density parameters satisfy

$$\Omega_m + \Omega_r + \Omega_\Lambda = 1. \quad (2.28)$$

2.2 Problems of Standard Cosmological Model

The first fundamental issue that characterises the Standard Cosmological Model regards the theory of gravity on which it relies: GR is an effective theory which is perturbatively nonrenormalizable due to the mass dimension of the gravitational coupling with matter, i.e. the Newtonian gravitational constant G . GR is valid only until energies of the order of the Planck Mass $M_P = 10^{-5}$ g are reached, an energy regime realised in the early Universe. At such regimes we need a quantization of gravity, for which many theories exist, but none of them has experimental confirmation. For more insights on these issues see (Donoghue, 1995).

Even at the classical level, Λ CDM is not completely satisfactory for the description of the late Universe.

One issue regards the still unknown physical nature of CDM: despite the efforts and the current numerous active experiments, we still have proofs of CDM only through indirect gravitational effects at the astrophysical and cosmological levels, while still lacking a direct detection of it. For recent reviews on cosmological aspects see (Rubakov, 2019; Arbey and Mahmoudi, 2021; Green, 2022).

Together with CDM also the physical nature of the cosmological constant is unknown. Usually, it is commonly considered as the contribution of the vacuum to the total energy density. However, this leads to two fundamental issues:

- The *Cosmological Constant problem* or *fine-tuning problem*: the observed value of Λ is smaller than the estimations from Quantum Field Theory (QFT) by 60 – 120 orders of magnitude (Weinberg, 1989).
- The *coincidence problem* which states that despite the fact that CDM and Λ evolve differently, their energy densities have currently the same order of magnitude (Weinberg, 2000).

More recently, as soon as we entered in the era of precision cosmology, next to the aforementioned theoretical issues, observational challenges have started to appear. There are some recent claims regarding the existence of cosmological dipoles (Webb et al., 2011; Perivolaropoulos, 2014; Wilczynska et al., 2020) that lead to rethink about the assumption of the Cosmological Principle.

Furthermore, tensions in the values of the parameters of Λ CDM tested against different sets of cosmological data at both the background and perturbations levels have emerged.

The most important example is the *Hubble tension* that have attracted much attention in the last decade (Perivolaropoulos and Skara, 2021). On one hand, from the CMB anisotropy measurements from *Planck* (Aghanim et al., 2020), for the value of the Hubble parameter H_0 one has $H_0 = (67.36 \pm 0.54) \text{ km s}^{-1}\text{Mpc}^{-1}$, by assuming Λ CDM as the fiducial cosmological model.

On the other hand, the local measurements of the same parameter point towards greater values, among which from the *Hubble Space Telescope* we have $H_0 = (74.03 \pm 1.42) \text{ km s}^{-1}\text{Mpc}^{-1}$ (Riess et al., 2019). This means that among the two values there is a discrepancy of 4.4σ .

Currently, this discrepancy does not seem to be due to systematic effects in either early-time or late-time measurements and may point to new physics beyond Λ CDM (Bernal, Verde, and Riess, 2016; Knox and Millea, 2020).

With the goal of solving the aforementioned issues, in the last decades, a great variety of models, which try to explain the late-time accelerated expansion of the Universe without resorting to the Cosmological Constant Λ , have been proposed (Copeland, Sami, and Tsujikawa, 2006; Clifton et al., 2012) trying to obtain a theory that fits equally well the available cosmological data and addresses simultaneously the Hubble tension problem (Di Valentino et al., 2021). For reviews on the experimental status of some of these theories beyond Λ CDM, see references (Joyce et al., 2015; Huterer and Shafer, 2018).

Chapter 3

Relativistic Fluid Dynamics

In this chapter, we review the basics of Relativistic Fluid Dynamics in curved space-time following (Romatschke and Romatschke, 2019), where a method to describe fluids out-of-equilibrium starting from the perfect fluid EMT (2.10) has been introduced. As shown in the following, such a departure from equilibrium is expressed as a gradient expansion in hydrodynamic fields describing the perfect fluids, i.e. the fluid 4-velocity, the energy density and the background metric.

At the first order in such gradient expansion, one recovers the terms which characterise *Viscous Cosmology*, which is a path that has been widely explored in last decades in order to explain the late time accelerated expansion of our Universe. For recent reviews, see (Brevik and Grøn, 2014; Brevik et al., 2017). For more recent works in the Viscous Cosmology framework see (Mohan, Sasidharan, and Mathew, 2017; Silva and Silva, 2019; Cruz, González, and Palma, 2020; Brevik, Makarenko, and Timoshkin, 2019; Madriz Aguilar et al., 2020) and for attempts to solve the Hubble tension in this framework, see (Anand et al., 2017; Yang et al., 2019; Elizalde et al., 2020; Normann and Brevik, 2021).

Instead, at the second order in gradient expansion, one has more terms among which there are those giving rise to the framework of *Ricci Cosmology* (Baier, Lahiri, and Romatschke, 2019) to the study of which it is devoted the rest of this dissertation.

3.1 General Construction

The first attempts to construct a consistent theory of dissipative fluids on a general curved spacetime are due to Eckart (Eckart, 1940) and Landau and Lifshitz (Landau and Lifshitz, 1987) in the first half of the twentieth century. After these first efforts which have been proven to be plagued with stability and causality problems, in the 1960s Müller (Muller, 1967) and in the 1970s Israel and Stewart (Israel, 1976; Israel and Stewart, 1979) succeeded to solve these issues, as shown in (Hiscock and Lindblom, 1983).

Since then, further developments occurred which culminated in the theory of relativistic fluid dynamics without conserved charges reviewed in (Romatschke and Romatschke, 2019), with an equivalent formulation for a fluid with a $U(1)$ symmetry based on an action principle, proposed in (Kovtun and Shukla, 2018). In the rest of the chapter, we will follow (Romatschke and Romatschke, 2019).

By using a common procedure in statistical mechanics, when we describe a system at sufficiently low energy and large scales, we can completely ignore the microscopic degrees of freedom and describe the system using effective macroscopic degrees of freedom more suitable for our purposes.

Here, we restrict our attention on the description of relativistic fluids. In order to describe them at cosmological scales, we can use the framework of Effective Field Theory (EFT).

In our case, we consider the conserved quantities of the quantum system underlying the fluid, i.e. energy density, momentum and eventually charges as the effective macroscopic degrees of freedom.

Once identified the degrees of freedom, the other ingredients for an EFT description to be considered are the symmetries of the system: for a relativistic system without charges we consider here, the symmetry group is that of the Poincaré group.

After having chosen the degrees of freedom suitable for the description of the system at the energy scale which we are interested in and identified the symmetries characterizing the system under consideration, fluid dynamics is built in three steps. Firstly, fluid dynamics without fluctuations is derived. Then, small deviations from equilibrium are considered giving rise to dissipative fluid dynamics. Finally, far from equilibrium departures are taken into account.

In the following, we will consider only small deviations from equilibrium up to second order on which the framework of Ricci Cosmology, covered in Chapter 4 relies. For full discussion of relativistic fluids, refer to (Romatschke and Romatschke, 2019).

3.2 Fluids near equilibrium

To be more concrete, let us consider an out-of-equilibrium relativistic quantum system with EMT $\hat{T}^{\mu\nu}$, invariant under Poincaré symmetry, on a general background described by the metric $g_{\mu\nu}$.

By taking the expectation value of the quantum EMT averaging on a statistical ensemble, we can describe the system as a fluid in the EFT framework by means of an effective classical EMT $T^{\mu\nu}$.

This EMT is built by using the conserved quantities, i.e. the energy density ρc^2 and the 4-velocity u^μ , which are the fundamental hydrodynamic fields locally defined

as the eigenvalue and the eigenvector of the EMT

$$u_\nu T^{\mu\nu} = -\rho c^2 u^\mu \quad (3.1)$$

and the source $g^{\mu\nu}$ only, for the perfect fluid contribution to the EMT, and gradients of them for the near-equilibrium deviations.

In general, the EMT can be written as

$$T^{\mu\nu} = T_{(0)}^{\mu\nu} + T_{(1)}^{\mu\nu} + T_{(2)}^{\mu\nu} + \dots \quad (3.2)$$

where the subscripts $(0), (1), (2), \dots$ indicate the number of gradients in each term of $T^{\mu\nu}$.

The corrections to the perfect fluid EMT $T_{(0)}^{\mu\nu}$ are conventionally splitted into a traceless part $\pi^{\mu\nu}$, referred to as the shear stress tensor

$$\pi^{\mu\nu} = T_{(1)}^{<\mu\nu>} + T_{(2)}^{<\mu\nu>} + \dots \quad (3.3)$$

where $< \dots >$ indicates symmetrization over the indices and subtraction of the trace and a trace part $\Pi g^{\mu\nu}$, with

$$\Pi = \frac{1}{d-1} \left(T_{(1)\mu}^\mu + T_{(2)\mu}^\mu \right) + \dots \quad (3.4)$$

which is called the bulk stress.

Furthermore, from the EMT (3.2), we can obtain the equation of motion for the fluid as

$$\nabla_\mu T^{\mu\nu} = 0, \quad (3.5)$$

where we can truncate the gradient expansion of $T^{\mu\nu}$ at the order we need to well approximate the dynamics of the fluid under consideration.

In particular, if we consider a fluid free of dissipative effects, we can describe its dynamics with great approximation by using the zeroth-order EMT $T_{(0)}^{\mu\nu}$, satisfying the eigenvalue equation

$$u_\nu T_{(0)}^{\mu\nu} = -\rho c^2 u^\mu, \quad (3.6)$$

where ρ and u^μ in this case are equilibrium quantities, and the equation of motion associated reads

$$\nabla_\mu T_{(0)}^{\mu\nu} = 0 \quad (3.7)$$

In addition, the eigenvalue equation (3.6) constrains the form of the perfect fluid EMT

$$T_{(0)}^{\mu\nu} = \rho u^\mu u^\nu + P(\rho) h^{\mu\nu} \quad (3.8)$$

which coincides with Eqn.(2.10).

When we consider near-equilibrium corrections, the local pressure $P(\rho)$ acquires corrections, which make the fluid EMT no longer isotropic in the local rest-frame.

In general, the space-space components of the fluid EMT gets the form

$$T_{j,LRF}^i = P\delta_j^i + \pi_{j,LRF}^i + \Pi\delta_j^i, \quad (3.9)$$

where $\pi_{j,LRF}^i$ are the space-space components of the shear tensor in the local rest frame.

Thus, the effective pressure in the i direction become

$$P_{eff}^{(i)} = P + \pi_{i,LRF}^i + \Pi \quad (3.10)$$

where in the second term there is no summation over i .

When we neglect anisotropies, that is possible on cosmological scales which we are interested in here, the last equation simplifies to

$$P_{eff} = P + \Pi, \quad (3.11)$$

which is an isotropic non-equilibrium pressure, due to internal friction in a fluid and can be responsible, in the cosmological context for the late-time accelerated expansion of the Universe, as we will point out in the following.

3.2.1 First order Energy-Momentum Tensor

Here, we review the construction of the first order correction $T_{(1)}^{\mu\nu}$, containing only first order terms in the gradient expansion.

Since, as already mentioned, the energy density ρ and the pressure $P(\rho)$ are related by the EoS, one can choose any function of one of these quantities to build gradient corrections, for instance $\ln \rho$.

Thus, the building blocks for the first order correction $T_{(1)}^{\mu\nu}$ to the perfect fluid EMT (3.8) are $\nabla_\mu \ln \rho$ and $\nabla_\mu u_\nu$.

As a remark, we are not taking into account the gradient of the source, the metric $g^{\mu\nu}$, which is identically zero due to metricity condition of GR.

Then, by using the perfect fluid equation of motion (3.7), it is easy to see that not all the gradients are independent: the only linearly independent first order gradients are the comoving spatial gradients $\nabla_\mu^\perp \ln \rho$ and $\nabla_\mu^\perp u_\nu$, with $\nabla_\mu^\perp = h_{\mu\nu} \nabla^\nu$.

Thus, these gradients are grouped into three classes depending on their properties under the action of the Poincaré group: scalars, vectors, and rank-two tensors.

Furthermore, only those vectors and rank-two tensors orthogonal to u^μ are independent.

To the first order, there is only one independent term in each class

$$\nabla_\mu^\perp u^\mu, \quad \nabla_\mu^\perp \ln \rho, \quad \nabla_\mu^\perp u_\nu \quad (3.12)$$

Finally, from Eqns.(3.6) and (3.1), for the first order EMT $T_{(1)}^{\mu\nu}$, we have the condition

$$u_\mu T_{(1)}^{\mu\nu} = 0. \quad (3.13)$$

Now, we can combine the terms in Eqn.(3.12) with the zeroth-order hydrodynamic fields ρ , u^μ and the source $g^{\mu\nu}$ to form the first-order correction $T_{(1)}^{\mu\nu}$ to the perfect fluid EMT $T_{(0)}^{\mu\nu}$ (3.8).

The only possible building blocks for $T_{(1)}^{\mu\nu}$ are

$$h_{\mu\nu} \nabla_\lambda^\perp u^\lambda \quad \text{and} \quad \nabla_{(\mu}^\perp u_{\nu)} = \frac{1}{2} (\nabla_\mu^\perp u_\nu + \nabla_\nu^\perp u_\mu), \quad (3.14)$$

which can be linearly combined, giving rise to the terms

$$h^{\mu\nu} \nabla_\lambda^\perp u^\lambda, \quad \sigma^{\mu\nu} = 2\nabla_{\langle\mu}^\perp u^{\nu\rangle} = 2\nabla_{\perp}^{(\mu} u^{\nu)} - \frac{2}{3} h^{\mu\nu} \nabla_\lambda^\perp u^\lambda \quad (3.15)$$

where $\sigma_{\mu\nu}$ is the traceless shear tensor.

Hence, the first-order EMT in gradient expansion can be written as

$$T_{(1)}^{\mu\nu} = -\eta \sigma^{\mu\nu} - \zeta h^{\mu\nu} \nabla_\lambda^\perp u^\lambda. \quad (3.16)$$

The first term in the last equation is the well-known shear viscosity which becomes relevant in presence of anisotropies, and the second term is the bulk viscosity, which modifies the bulk pressure of the fluid experiencing such departure from equilibrium and, as mentioned in the Introduction, has been used in alternative cosmological models to DE.

The shear viscosity coefficient η and the bulk viscosity coefficient ζ , are collectively called first order transport coefficients and to first order in gradients, the shear stress tensor (3.3) and the bulk stress (3.4) imply the relations

$$\pi_{(1)}^{\mu\nu} = -\eta \sigma^{\mu\nu}, \quad \Pi_{(1)} = -\zeta \nabla_\lambda^\perp u^\lambda \quad (3.17)$$

which are referred to as first order constitutive relations.

3.2.2 Second order Energy-Momentum Tensor

The procedure described in the previous subsection can be applied to obtain higher-order corrections to the perfect fluid EMT from building terms compatible with the Poincaré group, containing a certain number of gradients depending on the order. For instance, in order to obtain the second order correction $T_{(2)}^{\mu\nu}$ to the perfect fluid EMT (3.8) one considers all the independent scalars, and the vectors and the rank-two tensors, orthogonal to u^μ containing exactly two gradients.

There are seven independent scalars

$$\begin{aligned} & \nabla_\mu^\perp \nabla_\perp^\mu \ln \rho, \nabla_\mu^\perp \ln \rho \nabla_\perp^\mu \ln \rho, \sigma^{\mu\nu} \sigma_{\mu\nu}, \Omega_{\mu\nu} \Omega^{\mu\nu}, (\nabla_\mu^\perp u^\mu)^2, \\ & u^\mu u^\nu R_{\mu\nu}, R \end{aligned} \quad (3.18)$$

where $R_{\mu\nu}$ is the Ricci tensor, $R = g^{\mu\nu} R_{\mu\nu}$ is the Ricci scalar and $\Omega_{\mu\nu}$ is the fluid vorticity given by

$$\Omega_{\mu\nu} = \nabla_{[\mu}^\perp u_{\nu]} = \frac{1}{2} (\nabla_\mu^\perp u_\nu - \nabla_\nu^\perp u_\mu), \quad (3.19)$$

and six independent vectors orthogonal to u^μ

$$\nabla_\lambda^\perp \sigma^{\lambda\mu}, \nabla_\lambda^\perp \Omega^{\lambda\mu}, \sigma^{\lambda\mu} \nabla_\lambda^\perp \ln \rho, (\nabla_\lambda^\perp u^\lambda) \nabla_\perp^\mu \ln \rho, \Delta^{\lambda\mu} u^\nu R_{\lambda\nu} \quad (??) \quad (3.20)$$

Regarding the rank-two tensorial terms, multiplying by the metric $g_{\mu\nu}$, the scalars in Eqn.(3.18) can be used to generate symmetric rank two tensors with non-vanishing trace.

Finally, there are eight independent symmetric traceless rank-two tensors orthogonal to u_μ

$$\begin{aligned} & \nabla_\perp^{<\mu} \nabla_\perp^{>\nu} \ln \rho, \nabla_\perp^{<\mu} \ln \rho \nabla_\perp^{>\nu} \ln \rho, \sigma^{\mu\nu} (\nabla_\lambda^\perp u^\lambda), \sigma_\lambda^{<\mu} \sigma^{>\nu\lambda}, \\ & \sigma_\lambda^{<\mu} \Omega^{>\nu\lambda}, \Omega_\lambda^{<\mu} \Omega^{>\nu\lambda}, u_\lambda R^{\lambda<\mu\nu>\rho} u_\rho, R^{<\mu\nu>}. \end{aligned} \quad (3.21)$$

Hence, by considering linear combinations of the terms above (3.18), (??) and (3.21), the second order correction $T_{(2)}^{\mu\nu}$ to the perfect fluid EMT (3.8) can be written down, with the shear tensor $\pi_{(2)}^{\mu\nu}$ and the bulk pressure $\Pi_{(2)}$ given by

$$\begin{aligned} \pi_{(2)}^{\mu\nu} = & \eta \tau_\pi \left[<^* D \sigma^{\mu\nu}> + \frac{\nabla_\lambda^\perp u^\lambda}{3} \sigma^{\mu\nu} \right] + \kappa [R^{<\mu\nu>} - 2u_\lambda u_\rho R^{\lambda<\mu\nu>\rho}] + \lambda_1 \sigma_\lambda^{<\mu} \sigma^{>\nu\lambda} + \\ & + \lambda_2 \sigma_\lambda^{<\mu} \Omega^{>\nu\lambda} + \lambda_3 \Omega_\lambda^{<\mu} \Omega^{>\nu\lambda} + \kappa^* 2u_\lambda u_\rho R^{\lambda<\mu\nu>\rho} + \eta \tau_\pi^* \frac{\nabla_\lambda^\perp u^\lambda}{d-1} \sigma^{\mu\nu} + \\ & + \bar{\lambda}_4 \nabla_\perp^{<\mu} \ln \rho \nabla_\perp^{>\nu} \ln \rho, \end{aligned} \quad (3.22)$$

and

$$\begin{aligned} \Pi_{(2)} = & \zeta \tau_{\Pi} D(\nabla_{\lambda}^{\perp} u^{\lambda}) + \zeta_1 \sigma^{\mu\nu} \sigma_{\mu\nu} + \zeta_2 (\nabla_{\lambda}^{\perp} u^{\lambda})^2 + \zeta_3 \Omega^{\mu\nu} \Omega_{\mu\nu} + \bar{\zeta}_4 \nabla_{\mu}^{\perp} \ln \rho \nabla_{\perp}^{\mu} \ln \rho \\ & + \zeta_5 R + \zeta_6 u^{\lambda} u^{\rho} R_{\lambda\rho}, \end{aligned} \quad (3.23)$$

respectively. The coefficients multiplying each term in the above expressions, are called second order transport coefficients.

The second order constitutive relations (3.22) and (3.23) contain vanishing terms in flat spacetimes, e.g. the terms multiplied by the coefficients κ , κ^* , $\bar{\zeta}_5$, $\bar{\zeta}_6$.

In the next chapters, we will consider the cosmological model, dubbed *Ricci Cosmology*, introduced in (Baier, Lahiri, and Romatschke, 2019) in which the fluids filling the Universe have a modified out-of-equilibrium pressure given by

$$p_{eff} = P(\rho) + \zeta_5 R + \zeta_6 u^{\alpha} u^{\beta} R_{\alpha\beta} \quad (3.24)$$

where $P(\rho)$ is the equilibrium barotropic pressure, ζ_5 and ζ_6 are the only non-zero second order transport coefficients parametrising the deviation from equilibrium, R is the Ricci scalar and $u^{\alpha} u^{\beta} R_{\alpha\beta}$ is the projection of the Ricci tensor along the fluid 4-velocity.

Chapter 4

Ricci Cosmologies

In this chapter, we introduce the models with different assumptions underlying them we have considered in the new framework of Ricci Cosmology to describe the late-time accelerated expansion of the Universe.

4.1 Isotropic Ricci Cosmology

We assume that our Universe is well described at large scales by the flat FLRW metric (2.6) and that the Universe undergo the usual sequence of radiation, dust and CC, dominated eras.

Given a matter component c with energy density $\varepsilon_c = \rho_c c^2$, its effective pressure is modified by the presence of Ricci pressure terms and is given by

$$p_{c,eff} = w_c \rho_c c^2 + \zeta_{5c} R + \zeta_{6c} u^\alpha u^\beta R_{\alpha\beta}, \quad (4.1)$$

where the second order transport coefficients ζ_{5c} and ζ_{6c} are assumed constant and in general different for each matter component.

The Energy-Momentum Tensor is thus given by

$$T_{\mu\nu} = \left(\rho_c + \frac{p_{c,eff}}{c^2} \right) u_\mu u_\nu + p_{c,eff} g_{\mu\nu}. \quad (4.2)$$

From the Einstein equations (2.1), the Friedmann equations for Isotropic Ricci Cosmology governing a Universe filled with a single matter component with energy density ε are

$$\frac{\dot{a}^2}{a^2} = \frac{8\pi G}{3} \rho_c, \quad (4.3)$$

$$- \left(2 \frac{\ddot{a}}{a} + \frac{\dot{a}^2}{a^2} \right) = \frac{8\pi G}{c^2} p_{c,eff}, \quad (4.4)$$

where the effective pressure $p_{c,eff}$ written in terms of the scale factor $a(t)$ and its time derivatives reads

$$p_{c,eff} = p_c + 6 \frac{\xi_{5c}}{c^2} \frac{\dot{a}^2}{a^2} + 3 \left(\frac{2\xi_{5c}}{c^2} - \xi_{6c} \right) \frac{\ddot{a}}{a}. \quad (4.5)$$

By inserting Eqn.(4.5) in the second Friedmann equation (4.4), one easily finds for the scale factor $a(t)$ a power law solution

$$a(t) = (t - t_0)^{\frac{\alpha}{\alpha-\beta}}, \quad (4.6)$$

where the coefficients α and β are modified due to the second-order transport coefficients as

$$\alpha = 3 \left(\xi_{6c} - 2 \frac{\xi_{5c}}{c^2} \right) - \frac{c^2}{4\pi G}, \quad (4.7)$$

and

$$\beta = 2 \frac{\xi_{5c}}{c^2} + \frac{(3w_c + 1)c^2}{8\pi G}. \quad (4.8)$$

In the limit $\xi_{5c} = \xi_{6c} = 0$, Eqn.(4.6) gives the standard Λ CDM solution

$$a(t) = (t - t_0)^{\frac{2}{3(w_c+1)}}. \quad (4.9)$$

Besides this solution, we will find another solution and test it against cosmological data in Chapter 7.

Following (Caroli, Dabrowski, and Salzano, 2021), the Ricci scalar R and the projection of the Ricci tensor $R_{\alpha\beta}$ along the fluid 4-velocity u^α for the FLRW background given in Eqns.(2.7) and (2.9) can be written in terms of the Hubble function as

$$R = \frac{6}{c^2} \left(2H^2 + \dot{H} \right), \quad (4.10)$$

$$u^\alpha u^\beta R_{\alpha\beta} = R_{00} = -3 \left(H^2 + \dot{H} \right). \quad (4.11)$$

From the conservation of the Energy-Momentum Tensor (4.2), we obtain the continuity equation (2.21) for the energy density ε_c for such out-of-equilibrium fluid given by

$$\dot{\rho}_c + 3H \left(\rho_c + \frac{p_{c,eff}}{c^2} \right) = 0, \quad (4.12)$$

with the energy density related to the Hubble function via the first Friedmann equation (4.3), in the epoch dominated by the matter component with energy density ε_c . By inserting the effective pressure (4.1) and the expressions for the Ricci scalar (4.10) and the time-time component of the Ricci tensor (4.11) into continuity equation

(4.12), using the expressions in Eqn.(4.10), one obtains the evolution equation for the energy density as

$$\dot{\rho}_c + 3H \left[\rho_c(1 + w_c) + \frac{6\tilde{\zeta}_{5c}}{c^4}(2H^2 + \dot{H}) - \frac{3\tilde{\zeta}_{6c}}{c^2}(H^2 + \dot{H}) \right] = 0. \quad (4.13)$$

By replacing cosmic time derivatives with redshift derivatives and using the Hubble function (4.3) to express the Hubble function in terms of the energy density, after rearranging the terms, the last equation becomes

$$-(1+z) \frac{d\rho_c(z)}{dz} (1 + 2\hat{\zeta}_{5c} - \hat{\zeta}_{6c}) + [3(1 + w_c) + 8\hat{\zeta}_{5c} - 2\hat{\zeta}_{6c}] \rho_c(z) = 0, \quad (4.14)$$

where the reduced second order transport coefficients

$$\hat{\zeta}_{5c} \equiv \frac{12\pi G\tilde{\zeta}_{5c}}{c^4}, \quad \text{and} \quad \hat{\zeta}_{6c} \equiv \frac{12\pi G\tilde{\zeta}_{6c}}{c^2}, \quad (4.15)$$

have been defined. From the differential equation (4.14), we find for the energy density the following expression

$$\rho_c(z) = \rho_{c0}(1+z)^{\frac{3(1+w_c)+8\hat{\zeta}_{5c}-2\hat{\zeta}_{6c}}{1+2\hat{\zeta}_{5c}-\hat{\zeta}_{6c}}}. \quad (4.16)$$

From the evolution of the generic matter component energy density (4.16), one can see that such matter component acquires an effective EoS parameter given by

$$w_{c,eff} = \frac{w_c + \frac{2}{3}\hat{\zeta}_{5c} + \frac{1}{3}\hat{\zeta}_{6c}}{1 + 2\hat{\zeta}_{5c} - \hat{\zeta}_{6c}} \quad (4.17)$$

The squared Hubble function for a flat Universe filled with dust, radiation and cosmological constant, all having a modified redshift scaling, can thus be written as

$$H^2 = H_0^2 \left[\Omega_m(1+z)^{3+\delta_m} + \Omega_r(1+z)^{4+\delta_r} + \Omega_\Lambda(1+z)^{\delta_\Lambda} \right], \quad (4.18)$$

where the dimensionless energy density parameters are those defined in Eqn. (2.26) with the condition (2.28) and the deviation parameters δ_m , δ_r and δ_Λ for dust, radiation and Λ , respectively, from usual redshift scaling can be easily derived from Eqn.(4.17) as

$$\delta_m = \frac{2\hat{\zeta}_{5m} + \hat{\zeta}_{6m}}{1 + 2\hat{\zeta}_{5m} - \hat{\zeta}_{6m}}, \quad (4.19)$$

$$\delta_r = \frac{2\hat{\zeta}_{6r}}{1 + 2\hat{\zeta}_{5r} - \hat{\zeta}_{6r}}, \quad (4.20)$$

and

$$\delta_\Lambda = \frac{8\hat{\zeta}_{5\Lambda} - 2\hat{\zeta}_{6\Lambda}}{1 + 2\hat{\zeta}_{5\Lambda} - \hat{\zeta}_{6\Lambda}}, \quad (4.21)$$

respectively.

4.1.1 Physical bounds from Thermodynamics

On the deviation parameters (4.19), (4.20) and (4.21), one can impose a physical bound coming from the Second Law of Thermodynamics which states that the entropy of a closed system S never decreases (Barrow, 1988), i.e.

$$\Delta S \geq 0. \quad (4.22)$$

These bounds are considered as priors for the fit of the model with cosmological data presented in Chapter 7.

For the fluid with energy $E = \varepsilon V$ in a volume V , with temperature T and equilibrium pressure p , we apply the First Law of Thermodynamics

$$dE = TdS - pdV, \quad (4.23)$$

in order to obtain the conservation equation for its energy density

$$\dot{\rho} + 3H \left(\rho + \frac{p}{c^2} \right) - \frac{T}{V} \frac{\dot{S}}{c^2} = 0. \quad (4.24)$$

By comparing the last equation with the continuity equation (4.12), we find the following differential equation for the entropy S

$$\frac{T}{V} \dot{S} = -3H \left(\zeta_5 R + \zeta_6 u^\alpha u^\beta R_{\alpha\beta} \right) \quad (4.25)$$

From the thermodynamic relation for enthalpy $H \equiv E + pV = TS$, the entropy can be expressed as

$$S = \left(\rho c^2 + p \right) \frac{V}{T}, \quad (4.26)$$

which combined with Eqn.(4.25), leads to

$$\frac{\dot{S}}{S} = -\frac{3H}{\rho c^2 + p} \left(\zeta_5 R + \zeta_6 u^\alpha u^\beta R_{\alpha\beta} \right) \quad (4.27)$$

This must be valid for each matter component filling in the Universe.

For a matter component with energy density ε_c , barotropic EoS parameter w_c and constant reduced second order transport coefficients $\hat{\zeta}_{5c}$ and $\hat{\zeta}_{6c}$, the entropy S in

terms of the scale factor reads

$$S(a) = S_0 a^{-\frac{1}{1+w_c}} [8\hat{\xi}_{5c} - 2\hat{\xi}_{6c} - \delta_c(2\hat{\xi}_{5c} - \hat{\xi}_{6c})] + 3(2\hat{\xi}_{5c} - \hat{\xi}_{6c}). \quad (4.28)$$

From imposing the Second Law of Thermodynamics (4.22), for each matter component of the Universe and using the expressions for δ_m , δ_r , and δ_Λ found above, we can obtain the constraints on the second order transport coefficients (4.15).

For the cosmological constant, the entropy is given by

$$S(a) = S_0 a^{3(2\hat{\xi}_{5\Lambda} - \hat{\xi}_{6\Lambda})}, \quad (4.29)$$

which increases when $2\hat{\xi}_{5\Lambda} - \hat{\xi}_{6\Lambda} \geq 0$. For dust, the entropy reads

$$S(a) = S_0 a^{-\delta_m}, \quad (4.30)$$

which increases when $\delta_m \leq 0$. Finally, for radiation, it holds

$$S(a) = S_0 a^{-\frac{3}{4}\delta_r}, \quad (4.31)$$

which increases when $\delta_r \leq 0$.

4.1.2 Energy conditions in Isotropic Ricci Cosmology

For a fluid with energy density ε , the effective pressure given by Eqn.(4.1) and barotropic EoS parameter w , the energy conditions for a perfect fluid reported in Chapter 2, get modified as in the following.

Null Energy Condition (NEC)

The Null Energy Condition (NEC) for Isotropic Ricci Cosmology is given by

$$\rho + \frac{p_{eff}}{c^2} \geq 0. \quad (4.32)$$

By using the expressions for the Ricci scalar and the time-time component of Ricci tensor from Eqns.(4.10) and (4.11), one has

$$\rho(1+w) + 6\frac{\tilde{\xi}_5}{c^4} (2H^2 + \dot{H}) - 3\frac{\tilde{\xi}_6}{c^2} (\dot{H} + H^2) \geq 0. \quad (4.33)$$

Further, using the First Friedmann equation (4.3), the definitions of the reduced second order transport coefficients (4.15), and the definition of the deceleration parameter in terms of the Hubble function and its first time derivative

$$q = -\frac{\dot{H}}{H^2} - 1, \quad (4.34)$$

one has the bound

$$1 + w + \frac{2}{3} (4\hat{\zeta}_5 - \hat{\zeta}_6) + \frac{2}{3} (2\hat{\zeta}_5 - \hat{\zeta}_6) (-q - 1) > 0, \quad (4.35)$$

which simplifies to

$$1 + w + \frac{4}{3}\hat{\zeta}_5 - \frac{2}{3} (2\hat{\zeta}_5 - \hat{\zeta}_6) q > 0. \quad (4.36)$$

Thus, for Isotropic Ricci Cosmology, one finds bounds for the deceleration parameter q , that for $2\hat{\zeta}_5 - \hat{\zeta}_6 > 0$ leads to

$$q < \frac{3}{2} \left(1 + w + \frac{4}{3}\hat{\zeta}_5 \right) \frac{1}{2\hat{\zeta}_5 - \hat{\zeta}_6}, \quad (4.37)$$

while for $2\hat{\zeta}_5 - \hat{\zeta}_6 < 0$, one has

$$q > -\frac{3}{2} \left(1 + w + \frac{4}{3}\hat{\zeta}_5 \right) \frac{1}{|2\hat{\zeta}_5 - \hat{\zeta}_6|}. \quad (4.38)$$

Weak Energy Condition (WEC)

For the Weak Energy Condition (WEC) for Isotropic Ricci Cosmology, to the condition in Eqn.(4.32) we have to add the condition

$$\rho \geq 0, \quad (4.39)$$

which is unmodified for Isotropic Ricci Cosmology.

Strong Energy Condition (SEC)

For the Strong Energy Condition (SEC) for Isotropic Ricci Cosmology, to the condition in Eqn.(4.32), one needs to add the condition

$$\rho + 3\frac{p_{eff}}{c^2} \geq 0. \quad (4.40)$$

With the same steps presented above for the NEC, one obtains the expression

$$1 + 3w + 4\hat{\zeta}_5 - 2(2\hat{\zeta}_5 - \hat{\zeta}_6) q > 0, \quad (4.41)$$

which for $2\hat{\zeta}_5 - \hat{\zeta}_6 > 0$ leads to

$$q < \frac{1}{2} (1 + 3w + 4\hat{\zeta}_5) \frac{1}{2\hat{\zeta}_5 - \hat{\zeta}_6}, \quad (4.42)$$

while for $2\hat{\zeta}_5 - \hat{\zeta}_6 < 0$, one has

$$q > -\frac{1}{2} (1 + 3w + 4\hat{\zeta}_5) \frac{1}{|2\hat{\zeta}_5 - \hat{\zeta}_6|}. \quad (4.43)$$

Dominant Energy Condition (DEC)

For the Dominant Energy Condition (DEC) in Isotropic Ricci Cosmology we have two conditions that need to be satisfied. The first one is the positivity of the energy density as for the WEC (4.39) and the second one is given by

$$\rho \geq \frac{|p_{eff}|}{c^2} \quad (4.44)$$

which after the same steps seen for the other energy conditions leads to the inequality

$$1 \geq \left| w + \frac{4}{3}\hat{\zeta}_5 - \frac{2}{3}(2\hat{\zeta}_5 - \hat{\zeta}_6)q \right|. \quad (4.45)$$

The last inequality can be rewritten as

$$1 + w + \frac{4}{3}\hat{\zeta}_5 \geq \frac{2}{3}(2\hat{\zeta}_5 - \hat{\zeta}_6)q \geq -1 + w + \frac{4}{3}\hat{\zeta}_5, \quad (4.46)$$

which gives two different bounds on the deceleration parameter q depending on the sign of $2\hat{\zeta}_5 - \hat{\zeta}_6$: for $2\hat{\zeta}_5 - \hat{\zeta}_6 > 0$, we have

$$\frac{3 \left(-1 + w + \frac{4}{3}\hat{\zeta}_5 \right)}{2(2\hat{\zeta}_5 - \hat{\zeta}_6)} \leq q \leq \frac{3 \left(1 + w + \frac{4}{3}\hat{\zeta}_5 \right)}{2(2\hat{\zeta}_5 - \hat{\zeta}_6)}, \quad (4.47)$$

and for $2\hat{\zeta}_5 - \hat{\zeta}_6 < 0$, one has

$$\frac{3}{2|2\hat{\zeta}_5 - \hat{\zeta}_6|} \left(-1 - w - \frac{4}{3}\hat{\zeta}_5 \right) \leq q \leq \frac{3}{2|2\hat{\zeta}_5 - \hat{\zeta}_6|} \left(1 - w - \frac{4}{3}\hat{\zeta}_5 \right). \quad (4.48)$$

Today, the Universe is undergoing a phase of accelerated expansion for which one has a negative deceleration parameter evaluated at the present time q_0 which can be measured as shown in (Camarena and Marra, 2020). Furthermore, in Isotropic Ricci Cosmology the Universe is dominated by the Cosmological Constant, which

has equilibrium EoS parameter $w_\Lambda = -1$, at the present time. For the late-time accelerated expansion to happen the SEC must be violated. Hence, the inequalities (4.37) and (4.42) for the reduced second order transport coefficients $\hat{\zeta}_{5\Lambda}$ and $\hat{\zeta}_{6\Lambda}$ give us the constraint

$$\frac{1}{q_0} - 2\hat{\zeta}_{5\Lambda} \frac{1-q_0}{q_0} < \hat{\zeta}_{6\Lambda} < -2\hat{\zeta}_{5\Lambda} \frac{1-q_0}{q_0}, \quad (4.49)$$

together with $2\hat{\zeta}_{5\Lambda} - \hat{\zeta}_{6\Lambda} > 0$ from the Second Law of Thermodynamics.

4.2 Anisotropic Ricci Cosmology

In this section, we obtain a solution for Ricci Cosmology when the isotropy assumption is dropped.

For this purpose, we consider the Bianchi I Type metric which is given by

$$ds^2 = -c^2 dt^2 + X^2(t) dx^2 + Y^2(t) dy^2 + Z^2(t) dz^2, \quad (4.50)$$

where $X(t), Y(t), Z(t)$, functions of the cosmic time only, are the directional scale factors different for each principal axis on the 3-spatial hypersurface, determined by the fluid 4-velocity. One can immediately notice that for $X(t) = Y(t) = Z(t) = a(t)$, the metric (4.50) reduces to the flat FLRW (2.6).

We want to find how the effective pressure (3.24) looks like for a fluid near equilibrium filling in the Universe with a background described by the Bianchi I Type metric (4.50). From such a metric one can straightforwardly compute the time-time component of the Ricci tensor, which reads

$$R_{00} = - \left(\dot{H}_X + H_X^2 + \dot{H}_Y + H_Y^2 + \dot{H}_Z + H_Z^2 \right), \quad (4.51)$$

and the Ricci scalar, given by

$$R = \frac{2}{c^2} \left(\dot{H}_X + H_X^2 + \dot{H}_Y + H_Y^2 + \dot{H}_Z + H_Z^2 \right) + \frac{2}{c^2} (H_X H_Y + H_X H_Z + H_Y H_Z) \quad (4.52)$$

in which the Hubble functions along the principal axes $\{x, y, z\}$ have been defined as

$$H_X = \frac{\dot{X}}{X}, \quad H_Y = \frac{\dot{Y}}{Y}, \quad \text{and} \quad H_Z = \frac{\dot{Z}}{Z}. \quad (4.53)$$

Thus, the effective pressure (3.24) can be written as

$$p_{eff} = p + \frac{2\hat{\zeta}_5}{c^2} (H_X H_Y + H_X H_Z + H_Y H_Z) + \left(\frac{2\hat{\zeta}_5}{c^2} - \hat{\zeta}_6 \right) \left(\dot{H}_X + H_X^2 + \dot{H}_Y + H_Y^2 + \dot{H}_Z + H_Z^2 \right), \quad (4.54)$$

where p is the equilibrium pressure.

Following (Akarsu et al., 2019), for the metric (4.50), the Einstein equations (2.1) read as

$$H_X H_Y + H_Y H_Z + H_X H_Z = 8\pi G \rho, \quad (4.55)$$

$$-\dot{H}_Y - H_Y^2 - \dot{H}_Z - H_Z^2 - H_Y H_Z = \frac{8\pi G}{c^2} p_{eff}, \quad (4.56)$$

$$-\dot{H}_Z - H_Z^2 - \dot{H}_X - H_X^2 - H_X H_Z = \frac{8\pi G}{c^2} p_{eff}, \quad (4.57)$$

and

$$-\dot{H}_Y - H_Y^2 - \dot{H}_X - H_X^2 - H_Y H_X = \frac{8\pi G}{c^2} p_{eff}. \quad (4.58)$$

By combining the last equations, one has the Raychaudhuri equation given by

$$\left(\dot{H}_X + H_X^2 + \dot{H}_Y + H_Y^2 + \dot{H}_Z + H_Z^2 \right) = -4\pi G \left(\rho + 3 \frac{p_{eff}}{c^2} \right). \quad (4.59)$$

By using the first component of the Einstein equations (4.55) and the Raychaudhuri equation (4.59), the effective pressure (4.54) can be written as

$$p_{eff} = \frac{p + \frac{2}{3}\hat{\zeta}_5 \rho c^2 + \frac{1}{3}\hat{\zeta}_6 \rho c^2}{1 + 2\hat{\zeta}_5 - \hat{\zeta}_6}, \quad (4.60)$$

where $\hat{\zeta}_5$ and $\hat{\zeta}_6$ are the reduced second order transport coefficients defined in Eqn. (4.15).

By considering the equilibrium pressure p as the barotropic pressure with EoS parameter w , we find an effective EoS parameter w_{eff} which coincides with Eqn.(4.17) found in Section 4.1.

Furthermore, from the conservation of the Energy-Momentum Tensor (4.2), for an isotropic source one gets the continuity equation

$$\dot{\rho} + 3H \left(\rho + \frac{p_{eff}}{c^2} \right) = 0, \quad (4.61)$$

with H denoting the average Hubble function defined as

$$H = \frac{1}{3} (H_X + H_Y + H_Z). \quad (4.62)$$

By substituting the effective pressure (4.54) in the continuity equation (4.61), for the energy density one has the solution

$$\rho(t) = \rho_0 a^{-3(1+w_{eff})}, \quad (4.63)$$

where the average scale factor has been defined as

$$a(t) = (X(t)Y(t)Z(t))^{1/3}. \quad (4.64)$$

In the time-time component of the Einstein equations (4.55), and hence to the energy budget of the Universe, there is a contribution from the expansion anisotropy. This is evaluated in terms of the shear tensor defined in Eqn.(3.15), through the shear scalar

$$\sigma^2 = \frac{1}{2} \sigma_{\mu\nu} \sigma^{\mu\nu}. \quad (4.65)$$

For the Bianchi I Type metric (4.50), the shear scalar can be written in terms of the directional Hubble functions as

$$\sigma^2 = \frac{1}{6} \left[(H_X - H_Y)^2 + (H_Y - H_X)^2 + (H_Z - H_X)^2 \right]. \quad (4.66)$$

With an isotropic source as that considered here, it holds

$$\frac{H_X - H_Y}{c_1} = \frac{H_X - H_Z}{c_2} = \frac{H_Y - H_Z}{c_3} = a^{-3}, \quad (4.67)$$

where c_1 , c_2 and c_3 are integration constants and $a(t)$ is the average scale factor (4.64).

Therefore, the shear scalar (4.66) is simply given by

$$\sigma^2 = \sigma_0^2 a^{-6}, \quad (4.68)$$

with $\sigma_0^2 = \frac{1}{6}(c_1^2 + c_2^2 + c_3^2)$.

Analogously to dimensionless energy density parameters defined in Eqn.(2.26) for dust, radiation and cosmological constant, one can define the density parameter for the contribution of the shear scalar to the energy budget of the Universe as

$$\Omega_\sigma = \frac{\sigma^2}{3H_0^2} \quad (4.69)$$

By using the average redshift, defined by

$$z = -1 + \frac{1}{a}, \quad (4.70)$$

with the average scale factor given by Eqn.(4.64), we can write the time-time component of Einstein equations (4.55)

$$H^2(a) = H_0^2 \left[\Omega_\sigma(1+z)^6 + \Omega_r(1+z)^{4+\delta_r} + \Omega_m(1+z)^{3+\delta_m} + \Omega_\Lambda(1+z)^{\delta_\Lambda} \right] \quad (4.71)$$

with deviation parameters for dust, radiation and cosmological constant given in Eqn.(4.19), (4.20) and (4.21).

The Hubble function in Eqn.(4.71) differ from the Hubble function (4.18) found in Section 4.1 for Isotropic Ricci Cosmology for two features: the Hubble function and the redshift appearing in Eqn.(4.71) are average quantities, and a new term appears, describing the contribution of the expansion anisotropy.

4.3 Inhomogeneous Ricci Cosmology

In this section, we study an inhomogeneous isotropic background which is described by the so-called Lemaître-Tolman-Bondi (LTB) metric (Lemaître, 1933; Tolman, 1934; Bondi, 1947).

The general LTB metric reads

$$ds^2 = -c^2 dt^2 + \frac{(A'(r,t))^2}{1+E(r)} dr^2 + A^2(r,t) \left[d\theta^2 + \sin^2 \theta d\phi^2 \right], \quad (4.72)$$

where the generalised scale factor $A(t,r)$ depends not only on the cosmic time t , but also on the radial coordinate r and $A'(t,r) = \frac{\partial A(t,r)}{\partial r}$, $\dot{A}(t,r) = \frac{\partial A(t,r)}{\partial t}$.

One can immediately notice that for $A(t,r) = a(t)r$ and $E(r) = kr^2$, the metric (4.50) reduces to the general FLRW metric (2.6).

For the rest of discussion, we consider a spatially flat model with $E(r) = 0$.

Following the same lines of the previous section, we compute the time-time component of the Ricci tensor

$$R_{00} = -\frac{\ddot{A}'}{A'} - 2\frac{\ddot{A}}{A}, \quad (4.73)$$

and the Ricci scalar

$$R = 2c^{-2}\frac{\ddot{A}'}{A'} + 4c^{-2}\frac{\ddot{A}}{A} + 4c^{-2}\frac{\dot{A}}{A}\frac{\dot{A}'}{A'} + 2c^{-2}\frac{\dot{A}^2}{A^2}. \quad (4.74)$$

By substituting these expressions in the effective pressure (3.24), one has

$$p_{eff} = p + \xi_5 \left[2c^{-2}\frac{\ddot{A}'}{A'} + 4c^{-2}\frac{\ddot{A}}{A} + 4c^{-2}\frac{\dot{A}}{A}\frac{\dot{A}'}{A'} + 2c^{-2}\frac{\dot{A}^2}{A^2} \right] + \xi_6 \left[-\frac{\ddot{A}'}{A'} - 2\frac{\ddot{A}}{A} \right]. \quad (4.75)$$

Furthermore, the time-time component of Einstein equations (2.1) reads

$$\frac{\dot{A}^2}{A^2} + 2\frac{\dot{A}\dot{A}'}{AA'} = 8\pi G\rho, \quad (4.76)$$

while the $r - r$ component and the $\theta - \theta$ component are given by

$$-\frac{\dot{A}^2}{A^2} - 2\frac{\ddot{A}}{A} = \frac{8\pi G}{c^2}p_{eff}, \quad (4.77)$$

and

$$-\frac{\dot{A}\dot{A}'}{AA'} - \frac{\ddot{A}}{A} - \frac{\ddot{A}'}{A'} = \frac{8\pi G}{c^2}p_{eff}, \quad (4.78)$$

respectively, with the last equation coinciding with the $\phi - \phi$ component for rotational symmetry.

By combining all the components of Einstein equations, one arrives at the Raychaudhuri equation

$$\frac{\ddot{A}'}{A'} + 2\frac{\ddot{A}}{A} = -4\pi G \left(\rho + 3\frac{p_{eff}}{c^2} \right). \quad (4.79)$$

By using the first component of the Einstein equations (4.76) and the Raychaudhuri equation (4.79), the effective pressure (4.75) can be written as

$$p_{eff} = \frac{p + \frac{2}{3}\hat{\zeta}_5\rho c^2 + \frac{1}{3}\hat{\zeta}_6\rho c^2}{1 + 2\hat{\zeta}_5 - \hat{\zeta}_6}, \quad (4.80)$$

which coincides with Eqn.(4.60).

Furthermore, from the conservation of the Energy-Momentum Tensor (4.2), for an isotropic source one gets the continuity equation

$$\dot{\rho} + 3H \left(\rho + \frac{p_{eff}}{c^2} \right) = 0. \quad (4.81)$$

with H denoting the average Hubble function defined as

$$H(t, r) = \frac{1}{3} \left(\frac{\dot{A}'(t, r)}{A'(t, r)} + 2\frac{\dot{A}(t, r)}{A(t, r)} \right). \quad (4.82)$$

By substituting the effective pressure (4.80) in the continuity equation (4.61), for the energy density one has the solution

$$\rho(t, r) = \rho_0(r)a(t, r)^{-3(1+w_{eff})} \quad (4.83)$$

where the average scale factor has been defined as

$$a(t, r) = (A'(t, r)A(t, r)^2)^{1/3}, \quad (4.84)$$

which, in turn, as can be noticed depends also on the radial coordinate r . As for Anisotropic Ricci Cosmology, the time-time component of the Einstein equation takes into account also the contribution to the energy budget of the Universe of the anisotropy expansion that, in this case, is induced by the inhomogeneity. In this case the shear scalar is given by

$$\sigma^2 = \frac{1}{3} \left(\frac{\dot{A}}{A} - \frac{\dot{A}'}{A'} \right)^2. \quad (4.85)$$

A similar condition to that used for Anisotropic Ricci Cosmology for an isotropic source holds

$$\frac{1}{k_1(r)} \left(\frac{\dot{A}'}{A'} - \frac{\dot{A}}{A} \right) = \frac{1}{k_2(r)} \left(\frac{\dot{A}'}{A'} - \frac{\dot{A}}{A} \right) = a(t, r)^{-3}, \quad (4.86)$$

where $k_1(r)$ and $k_2(r)$ are integration constants depending on r .

Therefore, analogously to the previous section, the shear scalar (4.85) is given by

$$\sigma^2 = \sigma_0^2(r)a(t, r)^{-6}, \quad (4.87)$$

with $\sigma_0^2(r) = \frac{1}{3}(k_1^2(r) + 2k_2^2(r))$ and $a(t, r)$, the average scale factor (4.84).

In the same way as done for Anisotropic Ricci Cosmology, one can define the density parameter for the contribution of the shear scalar to the energy budget of the Universe, which has a dependence on the radial coordinate due to the inhomogeneity encoded in the LTB metric. By defining the average redshift,

$$z(t, r) = -1 + \frac{1}{a(t, r)}, \quad (4.88)$$

with the average scale factor given by Eqn.(4.84), we can write the time-time component of Einstein equations (4.76)

$$\frac{H^2(z, r)}{H_0^2(r)} = \Omega_\sigma(r)(1+z)^6 + \Omega_r(r)(1+z)^{4+\delta_r} + \Omega_m(r)(1+z)^{3+\delta_m} + \Omega_\Lambda(r)(1+z)^{\delta_\Lambda}. \quad (4.89)$$

As for the Anisotropic Ricci Cosmology, the Hubble function in Eqn.(4.89) is an average quantity depending on the average redshift (4.88) but now the dimensionless density parameters explicitly depend on the radial coordinate r .

4.4 Ricci Vacuum Cosmology

Let us assume as in Section 4.1 that at large scales our Universe is homogeneous and isotropic, i.e. well described by the flat FLRW metric (2.6) and that our Universe is filled with baryonic matter, CDM and radiation with usual EoS parameters at equilibrium plus a vacuum which is the only matter component whose pressure is modified by the presence of the Ricci Cosmology pressure terms in Eqns.(4.10) and (4.11) with an effective pressure

$$p_{vac}^{eff} = p_0 + \tilde{\zeta}_5 R + \tilde{\zeta}_6 u^\alpha u^\beta R_{\alpha\beta}, \quad (4.90)$$

where p_0 is a constant of the dimension of pressure.

The total EMT with the contributions of matter, radiation, and vacuum reads

$$T_{\mu\nu} = (\rho_m + \rho_r + \rho_{vac})u_\mu u_\nu + (p_r + p_{vac}^{eff})h_{\mu\nu} \quad (4.91)$$

with $h_{\mu\nu} = g_{\mu\nu} + u_\mu u_\nu / c^2$, the 3-spatial metric perpendicular to the fluid 4-velocity u^μ . The dust energy density ρ_m is the sum of the energy density of CDM ρ_{dm} and baryonic matter ρ_b and the radiation energy density ρ_r is the sum of photons energy density ρ_γ and the energy density ρ_{dr} of a component of radiation non-interacting through electromagnetic force, which we call *Dark Radiation* (DR).

The vacuum is characterised by the condition

$$\rho_{vac} + \frac{p_{vac}^{eff}}{c^2} = 0, \quad (4.92)$$

which implies that the evolution of the vacuum energy density in Ricci Vacuum Cosmology is dictated by the pressure p_{vac}^{eff} as

$$\rho_{vac} = -\frac{p_0}{c^2} - \frac{\tilde{\zeta}_5}{c^2} R - \frac{\tilde{\zeta}_6}{c^2} u^\alpha u^\beta R_{\alpha\beta}. \quad (4.93)$$

If one uses the expressions of the Ricci scalar and the time-time component of the Ricci tensor in terms of the Hubble function and its first derivative with respect to cosmic time in Eqns.(4.10) and (4.11), one finds for the vacuum energy density

$$\rho_{vac}(H) = -\frac{p_0}{c^2} - 3 \left(4 \frac{\tilde{\zeta}_5}{c^4} - \frac{\tilde{\zeta}_6}{c^2} \right) H^2 - 3 \left(2 \frac{\tilde{\zeta}_5}{c^4} - \frac{\tilde{\zeta}_6}{c^2} \right) \dot{H}. \quad (4.94)$$

By using the following identifications

$$c_0 = -8\pi G 3c^2 p_0, \quad v = -\frac{8\pi G}{c^2} \left(4\frac{\hat{\xi}_5}{c^2} - \hat{\xi}_6 \right), \quad \text{and} \quad \tilde{v} = -\frac{8\pi G}{c^2} \left(2\frac{\hat{\xi}_5}{c^2} - \hat{\xi}_6 \right), \quad (4.95)$$

the expression for the vacuum energy density coincides with the vacuum energy density of Running Vacuum Model (Sola, 2013; Solà and Gómez-Valent, 2015; Perez et al., 2021).

In order to find a solution for Ricci Vacuum Cosmology, we consider the Friedmann equations that read

$$H^2 = \frac{8\pi G}{3} (\rho_m + \rho_r + \rho_{vac}), \quad (4.96)$$

and

$$3H^2 + 2\dot{H} = -\frac{8\pi G}{c^2} (p_r + p_{vac}^{eff}), \quad (4.97)$$

which combined with the first Friedmann equation, gives us

$$\dot{H} = -4\pi G \left(\rho_m + \frac{4}{3}\rho_r \right). \quad (4.98)$$

Thus, from the first Friedmann equation (4.96) and the first derivative of the Hubble function with respect to cosmic time (4.98), one can find an expression for the Ricci scalar and the time-time component of the Ricci tensor in terms of the energy densities as

$$R = \frac{8\pi G}{c^2} (\rho_m + 4\rho_{vac}), \quad (4.99)$$

and

$$R_{00} = 8\pi G \left(\frac{\rho_m}{2} + \rho_r - \rho_{vac} \right), \quad (4.100)$$

respectively. By substituting the last expressions in the vacuum condition (4.92), and by using the dimensionless reduced second order transport coefficients defined in Eqn.(4.15), one has for the vacuum energy density

$$\rho_{vac} = -\frac{\frac{p_0}{c^2} + \frac{2}{3} \left(\hat{\xi}_5 + \frac{\hat{\xi}_6}{2} \right) \rho_m + \frac{2}{3} \hat{\xi}_6 \rho_r}{1 + \frac{8}{3} \hat{\xi}_5 - \frac{2}{3} \hat{\xi}_6}. \quad (4.101)$$

By using the initial condition

$$\rho_{vac}(a = 1) = \rho_{vac0}, \quad (4.102)$$

the constant p_0 appearing in the effective pressure Eqn.(4.90) can be determined as

$$p_0 = \left[- \left(1 + \frac{8}{3}\hat{\zeta}_5 - \frac{2}{3}\hat{\zeta}_6 \right) \rho_{vac0} - \frac{2}{3}\hat{\zeta}_5 \rho_{m0} - \frac{2}{3}\hat{\zeta}_6 \left(\frac{\rho_{m0}}{2} + \rho_{r0} \right) \right] c^2. \quad (4.103)$$

From the last expression, one can notice that the EoS at the present time t_0 for the vacuum does not coincide with the cosmological constant EoS $w_\Lambda = -1$ but gets modified due to the presence of the Ricci pressure terms (4.10) and (4.11).

By substituting the expression of the constant p_0 (4.103), in the vacuum energy density (4.101), one gets

$$\rho_{vac}(a) = \rho_{vac0} - \frac{\frac{2}{3} \left(\hat{\zeta}_5 + \frac{\hat{\zeta}_6}{2} \right)}{1 + \frac{8}{3}\hat{\zeta}_5 - \frac{2}{3}\hat{\zeta}_6} (\rho_m(a) - \rho_{m0}) + \frac{\frac{2}{3}\hat{\zeta}_6}{1 + \frac{8}{3}\hat{\zeta}_5 - \frac{2}{3}\hat{\zeta}_6} (\rho_r(a) - \rho_{r0}). \quad (4.104)$$

The conservation of the Energy-Momentum Tensor (4.91) leads to the following continuity equation for the fluids filling in the Universe

$$\dot{\rho} + 3H \left(\rho + \frac{p}{c^2} \right) = 0, \quad (4.105)$$

where $\rho = \rho_{dm} + \rho_b + \rho_{dr} + \rho_\gamma + \rho_{vac}$ is the total energy density and $p = p_r + p_{vac}^{eff}$ the total pressure of the matter components.

4.4.1 Cold Dark Matter - Ricci Vacuum interaction

In this subsection, we consider the vacuum interacting with CDM, where the baryon energy density ρ_b and the total radiation energy density ρ_r satisfy the continuity equations

$$\dot{\rho}_b + 3H\rho_b = 0, \quad (4.106)$$

and

$$\dot{\rho}_r + 4H\rho_r = 0, \quad (4.107)$$

which are immediately solved by

$$\rho_b(a) = \rho_{b0} a^{-3}, \quad (4.108)$$

and

$$\rho_r(a) = \rho_{r0} a^{-4}. \quad (4.109)$$

By using the vacuum condition (4.92), the last equations imply that the total continuity equation (4.105) becomes a *continuity equation for CDM interacting with a time*

evolving vacuum

$$\dot{\rho}_{dm} + 3H\rho_{dm} = -\dot{\rho}_{vac}. \quad (4.110)$$

By substituting the vacuum energy density (4.104) and using the baryon energy density (4.108) and the radiation energy density (4.109), one finds for the CDM energy density the solution

$$\rho_{dm}(a) = \left(\rho_{m0} - \frac{8}{3} \frac{\hat{\xi}_6}{1 - 2\hat{\xi}_6} \right) a^{-3-\delta_m} + \frac{8}{3} \frac{\hat{\xi}_6}{1 - 2\hat{\xi}_6} a^{-4} - \rho_{b0} a^{-3}, \quad (4.111)$$

where the deviation parameter δ_m has been defined as

$$\delta_m \equiv \frac{2\hat{\xi}_5 + \hat{\xi}_6}{1 + 2\hat{\xi}_5 - \hat{\xi}_6}, \quad (4.112)$$

and the initial condition $\rho_{dm}(a = 1) = \rho_{dm0}$ has been used.

Therefore, by substituting the energy densities (4.104), (4.108), (4.109), and (4.111) in the first Friedmann equation (4.96), for the Hubble function one has

$$H^2(a) = H_0^2 \left[\psi_1 \Omega_m a^{-3-\delta_m} + \psi_2 \Omega_r a^{-4} + 1 - \psi_3 \Omega_m - \psi_4 \Omega_r \right] \quad (4.113)$$

with the functions of the parameters ψ_1 , ψ_2 , ψ_3 and ψ_4 , defined by

$$\psi_1 \equiv \frac{\left(1 - 2\hat{\xi}_6 \left(1 + \frac{4}{3} \frac{\Omega_r}{\Omega_m} \right) \right) (1 + 2\hat{\xi}_5 - \hat{\xi}_6)}{(1 - 2\hat{\xi}_6) \left(1 + \frac{8}{3} \hat{\xi}_5 - \frac{2}{3} \hat{\xi}_6 \right)}, \quad (4.114)$$

$$\psi_2 \equiv \frac{1}{1 - 2\hat{\xi}_6}, \quad (4.115)$$

$$\psi_3 \equiv \frac{1 + 2\hat{\xi}_5 - \hat{\xi}_6}{1 + \frac{8}{3} \hat{\xi}_5 - \frac{2}{3} \hat{\xi}_6}, \quad (4.116)$$

and

$$\psi_4 \equiv \frac{1 + \frac{8}{3} \hat{\xi}_5 - \frac{4}{3} \hat{\xi}_6}{1 + \frac{8}{3} \hat{\xi}_5 - \frac{2}{3} \hat{\xi}_6}. \quad (4.117)$$

For the Hubble function to be well defined mathematically and physically, we impose the following two conditions

$$\psi_1 \geq 0, \quad \text{and} \quad \psi_2 \geq 0. \quad (4.118)$$

From the second inequality of (4.118), one has

$$\hat{\xi}_6 \leq \frac{1}{2} \quad (4.119)$$

and combining the last equation with the first inequality of (4.118), we have also the following restriction on the region of the parameters

$$\frac{\left(1 - 2\hat{\xi}_6 \left(1 + \frac{4}{3}\frac{\Omega_r}{\Omega_m}\right)\right) (1 + 2\hat{\xi}_5 - \hat{\xi}_6)}{1 + \frac{8}{3}\hat{\xi}_5 - \frac{2}{3}\hat{\xi}_6} \geq 0 \quad (4.120)$$

4.4.2 Dark Radiation - Ricci Vacuum interaction

Let us consider now the case in which dust and photons satisfy the following continuity equations

$$\dot{\rho}_m + 3H\rho_m = 0, \quad (4.121)$$

and

$$\dot{\rho}_\gamma + 4H\rho_\gamma = 0, \quad (4.122)$$

respectively, from which one has the usual energy density evolutions for dust

$$\rho_m(a) = \rho_{m0}a^{-3} \quad (4.123)$$

and for photons

$$\rho_\gamma(a) = \rho_{\gamma0}a^{-4}. \quad (4.124)$$

Thus, the continuity equation (4.105) simplifies to

$$\dot{\rho}_{dr} + 4H\rho_{dr} = -\dot{\rho}_{vac}. \quad (4.125)$$

By substituting the vacuum energy density (4.104), the dust energy density (4.123) together with the photons energy density (4.124) into Eqn.(4.125), one can find the DR energy density given by

$$\rho_{dr}(a) = \left(\rho_{r0} + \frac{2\hat{\xi}_5 + \hat{\xi}_6}{1 + \frac{8}{3}\hat{\xi}_5 + \frac{4}{3}\hat{\xi}_6} \rho_{m0} \right) a^{-4-\delta_r} - \frac{2\hat{\xi}_5 + \hat{\xi}_6}{1 + \frac{8}{3}\hat{\xi}_5 + \frac{4}{3}\hat{\xi}_6} \rho_{m0}a^{-3} - \rho_{\gamma0}a^{-4}, \quad (4.126)$$

where the deviation parameter δ_r has been defined as

$$\delta_r = \frac{8}{3} \frac{\hat{\xi}_6}{1 + \frac{8}{3}\hat{\xi}_5 - \frac{4}{3}\hat{\xi}_6}, \quad (4.127)$$

and the initial condition $\rho_{dr}(a = 1) = \rho_{dr0}$ has been used.

Thus, by substitution of the energy densities (4.104), (4.123), (4.124), and (4.126) in

the first Friedmann equation (4.96), one gets

$$H^2(a) = H_0^2 \left[\chi_1 \Omega_m a^{-3} + \chi_2 \Omega_r a^{-4-\delta_r} + 1 - \chi_3 \Omega_m - \chi_4 \Omega_r \right], \quad (4.128)$$

where the functions of the parameters χ_1 and χ_2 are defined as

$$\chi_1 \equiv \frac{1}{1 + \frac{8}{3} \left(\hat{\zeta}_5 + \frac{\hat{\zeta}_6}{2} \right)}, \quad (4.129)$$

and

$$\chi_2 \equiv \frac{1 + \frac{8}{3} \hat{\zeta}_5 - \frac{4}{3} \hat{\zeta}_6}{1 + \frac{8}{3} \hat{\zeta}_5 - \frac{2}{3} \hat{\zeta}_6} \frac{1 + \frac{8}{3} \left(\hat{\zeta}_5 + \frac{\hat{\zeta}_6}{2} \right) \left(1 + \frac{3}{4} \frac{\Omega_m}{\Omega_r} \right)}{1 + \frac{8}{3} \left(\hat{\zeta}_5 + \frac{\hat{\zeta}_6}{2} \right)}, \quad (4.130)$$

while $\chi_3 \equiv \psi_3$, and $\chi_4 \equiv \psi_4$.

For the Hubble function to be well defined mathematically and physically, one needs two constraints on the functions χ_1 and χ_2 , i.e.

$$\chi_1 \geq 0, \quad \text{and} \quad \chi_2 \geq 0. \quad (4.131)$$

From the first inequality of Eqn.(4.131), we have that the following must hold

$$1 + \frac{8}{3} \left(\hat{\zeta}_5 + \frac{\hat{\zeta}_6}{2} \right) > 0, \quad (4.132)$$

while from the second inequality of Eqn.(4.131), we have the following restriction to the allowed region in the parameter space

$$\frac{1 + \frac{8}{3} \hat{\zeta}_5 - \frac{4}{3} \hat{\zeta}_6}{1 + \frac{8}{3} \hat{\zeta}_5 - \frac{2}{3} \hat{\zeta}_6} \left[1 + \frac{8}{3} \left(\hat{\zeta}_5 + \frac{\hat{\zeta}_6}{2} \right) \left(1 + \frac{3}{4} \frac{\Omega_m}{\Omega_r} \right) \right] \geq 0. \quad (4.133)$$

4.5 Tilted Ricci Cosmology

In this section, after having shortly presented the framework of Tilted Cosmology, we study how the energy conditions in this context are modified under the presence of departure from equilibrium for the cosmic fluid determined by the Ricci pressure terms.

4.5.1 Tilted Cosmology

The relevant feature of the Tilted Cosmology is that the fluid 4-velocity differs from the observer 4-velocity in the Universe.

Let us indicate with u^α the fluid 4-velocity and with n^α the observer 4-velocity. These two 4-velocities define two different 3-spatial hypersurfaces with the metrics given by

$$h_{\mu\nu} = g_{\mu\nu} + \frac{u_\mu u_\nu}{c^2}, \quad (4.134)$$

and

$$\tilde{h}_{\mu\nu} = g_{\mu\nu} + \frac{n_\mu n_\nu}{c^2}, \quad (4.135)$$

respectively, with the metric (4.134) appearing in the Energy-Momentum Tensor (4.2).

Following (King and Ellis, 1973), the relation between the two 4-velocities u^μ and n^μ is specified by the hyperbolic *tilt angle* β

$$u^\mu n_\mu = -\cosh \beta, \quad (4.136)$$

and by the direction of the tilt that can be specified through either the projection of the fluid 4-velocity on the so-called surfaces of homogeneity $S(t)$ described by the metric $\tilde{h}_{\mu\nu}$ (4.135), i.e.

$$\tilde{h}_{\mu\nu} u^\nu = \sinh \beta \tilde{c}_\mu, \quad (4.137)$$

or the projection of the observer 4-velocity on the 3-spatial hypersurface determined by the fluid 4-velocity with metric $h_{\mu\nu}$ (4.134)

$$h_{\mu\nu} n^\nu = -\sinh \beta c_\mu. \quad (4.138)$$

Therefore, the observer 4-velocity n^μ and the fluid 4-velocity u^μ are related by

$$u^\mu = \cosh \beta n^\mu + \sinh \beta \tilde{c}^\mu, \quad (4.139)$$

and

$$n^\mu = \cosh \beta u^\mu - \sinh \beta c^\mu. \quad (4.140)$$

For a clarification of the geometrical construction, see Figure 4.1. In a tilted Universe model, we can rewrite the perfect fluid Energy-Momentum Tensor (2.10) in terms of the observer 4-velocity n^μ and the metric of its 3-spatial hypersurface $h_{\mu\nu}$ by using Eqns.(4.134) and (4.139), as

$$T_{\mu\nu} = \tilde{\rho} n_\mu n_\nu + \tilde{p} \tilde{h}_{\mu\nu} + 2\tilde{q}_{(\mu} n_{\nu)} + \tilde{\pi}_{\mu\nu}, \quad (4.141)$$

where energy density $\tilde{\rho}$ and the pressure \tilde{p} of the fluid as seen by the observer are given by

$$\tilde{\rho} = \rho \cosh^2 \beta + \frac{p}{c^2} \sinh^2 \beta, \quad (4.142)$$

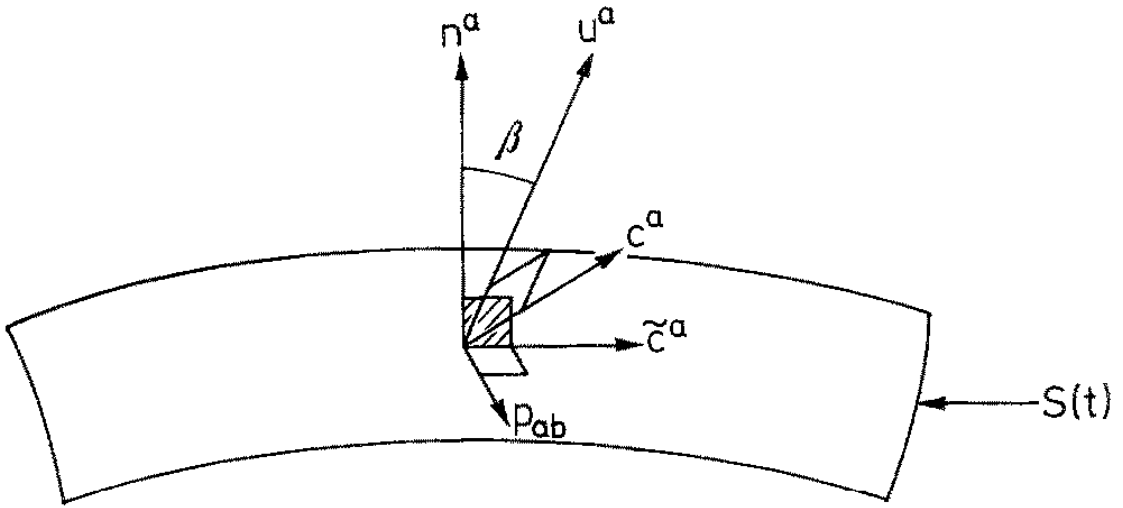


FIGURE 4.1: Representation of the observer 4-velocity orthogonal to the surface of homogeneity $S(t)$ and making a hyperbolic angle β with the fluid 4-velocity. The tensor $p_{\mu\nu}$ spans the 2-surface in $S(t)$ perpendicular to the vectors c^μ and \tilde{c}^μ . (King and Ellis, 1973)

and

$$\tilde{p} = p + \frac{1}{3}(\rho c^2 + p) \sinh^2 \beta, \quad (4.143)$$

respectively.

By inspection of the Energy-Momentum Tensor (4.141), one can further notice that as a result of the non-zero tilt between the fluid and the observer 4-velocities, the observer will experience a non-zero energy flux \tilde{q}_μ and a non-zero shear tensor $\tilde{\pi}_{\mu\nu}$ in his reference frame, given by

$$\tilde{q}_\mu = \left(\rho + \frac{p}{c^2} \right) \sinh \beta \cosh \beta \tilde{c}_\mu, \quad (4.144)$$

and

$$\tilde{\pi}_{\mu\nu} = \left(\rho + \frac{p}{c^2} \right) \sinh^2 \beta \left(\tilde{c}_\mu \tilde{c}_\nu - \frac{1}{3} \tilde{h}_{\mu\nu} \right), \quad (4.145)$$

respectively.

Furthermore, the energy conditions reported in Chapter 2 for a barotropic fluid with EoS parameter w as seen by an observer in Tilted Cosmology get modified, giving us

- for the NEC, $w > -1$ which is unmodified;
- for the WEC,

$$w > -\frac{1}{\sinh^2 \beta} - 1, \quad (4.146)$$

with the tilt angle $\beta \neq 0$;

- for the SEC,

$$w > -\frac{1 + 2 \sinh^2 \beta}{3 + 2 \sinh^2 \beta}; \quad (4.147)$$

- for the DEC,

$$-1 \leq 2 + \frac{1}{3}(1 + w) \sinh^2 \beta \leq 1. \quad (4.148)$$

4.5.2 Tilted Ricci Cosmology

In this subsection, we modify the homogeneous tilted cosmological model of the last subsection considering a fluid with the effective pressure p_{eff} given in Eqn.(3.24), giving rise to the so-called Tilted Ricci Cosmology.

The only effect that the presence of such effective pressure has on the EMT of a fluid as seen by a tilted observer (4.141) is to modify the energy density $\tilde{\rho}$, the pressure \tilde{p} , the energy flux \tilde{q}_μ and the shear tensor $\tilde{\pi}_{\mu\nu}$ by replacing the perfect fluid pressure p with the effective pressure p_{eff} . In particular, the tilted energy density $\tilde{\rho}$ and the tilted pressure \tilde{p} become

$$\tilde{\rho} = \rho \cosh^2 \beta + \frac{p_{eff}}{c^2} \sinh^2 \beta, \quad (4.149)$$

and

$$\tilde{p} = p_{eff} + \frac{1}{3}(\rho c^2 + p_{eff}) \sinh^2 \beta, \quad (4.150)$$

respectively, which reduces to the Ricci Cosmology Energy-Momentum Tensor (4.2) when the tilt angle $\beta = 0$.

In the following, we study how the energy conditions for Isotropic Ricci Cosmology studied in Section 4.1 get modified when one takes into account the tilt angle defined in Eqn.(4.136).

Null Energy Condition

The NEC in Tilted Ricci Cosmology reads

$$\tilde{\rho} + \frac{\tilde{p}}{c^2} > 0. \quad (4.151)$$

By substituting the expressions for the energy density $\tilde{\rho}$ (4.149) and the pressure \tilde{p} (4.150), and using the hyperbolic angle relation $\cosh^2 \beta - \sinh^2 \beta = 1$, we get

$$\left(\rho + \frac{p_{eff}}{c^2} \right) \left[\frac{4}{3} \cosh^2 \beta - \frac{1}{3} \right] > 0. \quad (4.152)$$

From the mathematical properties of hyperbolic functions, the second factor in the last inequality (4.152) is greater than zero for every value of the tilt angle (4.136). Thus, the inequality (4.152) reduces to

$$\rho + \frac{p_{eff}}{c^2} > 0, \quad (4.153)$$

which coincides with the NEC for Isotropic Ricci Cosmology (4.32).

Weak Energy Condition

For the Weak Energy Condition in Tilted Ricci Cosmology, the condition on the tilted energy density to be added to NEC is given by

$$\tilde{\rho} \geq 0, \quad (4.154)$$

that implies

$$\rho \cosh^2 \beta + \frac{p_{eff}}{c^2} \sinh^2 \beta > 0. \quad (4.155)$$

By following similar steps to those done for energy conditions for Isotropic Ricci Cosmology in Section 4.1, one arrives at the inequality

$$\frac{\cosh^2 \beta}{\cosh^2 \beta - 1} + w + \frac{4}{3}\hat{\xi}_5 > \frac{2}{3}(2\hat{\xi}_5 - \hat{\xi}_6)q, \quad (4.156)$$

which for $2\hat{\xi}_5 - \hat{\xi}_6 > 0$ leads to

$$q < \frac{3}{2(2\hat{\xi}_5 - \hat{\xi}_6)} \left[\frac{\cosh^2 \beta}{\cosh^2 \beta - 1} + w + \frac{4}{3}\hat{\xi}_5 \right], \quad (4.157)$$

while for $2\hat{\xi}_5 - \hat{\xi}_6 < 0$, one has

$$q > -\frac{3}{2|2\hat{\xi}_5 - \hat{\xi}_6|} \left[\frac{\cosh^2 \beta}{\cosh^2 \beta - 1} + w + \frac{4}{3}\hat{\xi}_5 \right]. \quad (4.158)$$

Strong Energy Condition

The Strong Energy Condition in Tilted Ricci Cosmology reads

$$\tilde{\rho} + 3\frac{\tilde{p}}{c^2} > 0 \quad (4.159)$$

By substituting the expressions for the tilted energy density $\tilde{\rho}$ (4.149) and the tilted pressure \tilde{p} (4.150), we get

$$\rho \cosh^2 \beta + \frac{p_{eff}}{c^2} \sinh^2 \beta + 3 \frac{p_{eff}}{c^2} + \left(\rho + \frac{p_{eff}}{c^2} \right) \sinh^2 \beta > 0. \quad (4.160)$$

After inserting the expression for the effective pressure p_{eff} (3.24) and using the deceleration parameter q (4.34), one has

$$3 \frac{(2 \cosh^2 \beta - 1) + w(2 \cosh^2 \beta + 1)}{2 \cosh^2 \beta + 1} + 4\hat{\zeta}_5 - (4\hat{\zeta}_5 - 2\hat{\zeta}_6) q > 0. \quad (4.161)$$

The last inequality for $2\hat{\zeta}_5 - \hat{\zeta}_6 > 0$ becomes

$$q < \frac{3}{2(2\hat{\zeta}_5 - \hat{\zeta}_6)} \left[\frac{(2 \cosh^2 \beta - 1)}{2 \cosh^2 \beta + 1} + w + \frac{4}{3}\hat{\zeta}_5 \right], \quad (4.162)$$

while for $2\hat{\zeta}_5 - \hat{\zeta}_6 < 0$, one has

$$q > -\frac{3}{2|2\hat{\zeta}_5 - \hat{\zeta}_6|} \left[\frac{(2 \cosh^2 \beta - 1)}{2 \cosh^2 \beta + 1} + w + \frac{4}{3}\hat{\zeta}_5 \right]. \quad (4.163)$$

The last inequalities for $\beta = 0$ reduce to the inequalities found for SEC for Isotropic Ricci Cosmology in Section 4.1.

Dominant Energy Condition

The Dominant Energy Condition in Tilted Ricci Cosmology reads

$$\tilde{\rho} \geq \frac{|\tilde{p}|}{c^2}. \quad (4.164)$$

By substituting the expressions for the energy density $\tilde{\rho}$ (4.149) and the pressure (4.150), one has

$$\rho \cosh^2 \beta + \frac{p_{eff}}{c^2} \sinh^2 \beta \geq \frac{1}{c^2} \left| p_{eff} + \frac{1}{3} \left(\rho + \frac{p_{eff}}{c^2} \right) c^2 \sinh^2 \beta \right|, \quad (4.165)$$

which is equivalent to

$$-\rho \cosh^2 \beta - \frac{p_{eff}}{c^2} \sinh^2 \beta \leq \frac{p_{eff}}{c^2} + \frac{1}{3} \left(\rho + \frac{p_{eff}}{c^2} \right) \sinh^2 \beta \leq \rho \cosh^2 \beta + \frac{p_{eff}}{c^2} \sinh^2 \beta. \quad (4.166)$$

Let us consider the first inequality given by

$$-\rho \cosh^2 \beta - \frac{p_{eff}}{c^2} \sinh^2 \beta \leq \frac{p_{eff}}{c^2} + \frac{1}{3} \left(\rho + \frac{p_{eff}}{c^2} \right) \sinh^2 \beta. \quad (4.167)$$

A simple rearrangement of the terms leads to

$$\left(\rho + \frac{p_{eff}}{c^2} \right) \left(\cosh^2 \beta + \frac{1}{3} \sinh^2 \beta \right) \geq 0. \quad (4.168)$$

The second factor is always greater than zero, so the only condition is

$$\rho + \frac{p_{eff}}{c^2} > 0, \quad (4.169)$$

which gives the same inequalities as those found for the NEC for Isotropic Ricci Cosmology in Section 4.1. Then, let us consider the second inequality in Eqn.(4.166)

$$\frac{p_{eff}}{c^2} + \frac{1}{3} \left(\rho + \frac{p_{eff}}{c^2} \right) \sinh^2 \beta \leq \rho \cosh^2 \beta + \frac{p_{eff}}{c^2} \sinh^2 \beta. \quad (4.170)$$

After similar steps as those done before, one has

$$3 \left[\frac{1 + \frac{2}{3} \sinh^2 \beta}{1 - \frac{2}{3} \sinh^2 \beta} - w \right] \geq 4\hat{\xi}_5 - (4\hat{\xi}_5 - 2\hat{\xi}_6)q, \quad (4.171)$$

provided that $\sinh^2 \beta \neq \frac{3}{2}$. For $2\hat{\xi} - \hat{\xi}_6 > 0$, the last inequality becomes

$$q \geq -\frac{3}{2} \frac{1}{2\hat{\xi}_5 - \hat{\xi}_6} \left[\frac{1 + \frac{2}{3} \sinh^2 \beta}{1 - \frac{2}{3} \sinh^2 \beta} - w - \frac{4}{3} \hat{\xi}_5 \right], \quad (4.172)$$

while for $2\hat{\xi} - \hat{\xi}_6 < 0$, one has

$$q \leq \frac{3}{2} \frac{1}{|2\hat{\xi}_5 - \hat{\xi}_6|} \left[\frac{1 + \frac{2}{3} \sinh^2 \beta}{1 - \frac{2}{3} \sinh^2 \beta} - w - \frac{4}{3} \hat{\xi}_5 \right]. \quad (4.173)$$

By repeating the same reasoning we follow in Section 4.1 to put the constraint (4.49) onto the reduced second order transport coefficients for Λ for Isotropic Ricci Cosmology, from the NEC (4.37) which is still valid in Tilted Ricci Cosmology, the WEC (4.157) and the violation of the SEC (4.162), for the reduced second order transport coefficients $\hat{\xi}_{5\Lambda}$ and $\hat{\xi}_{6\Lambda}$ we have obtained the following constraint

$$\frac{3}{2 \cosh^2 \beta + 1} \frac{1}{q_0} - 2\hat{\xi}_{5\Lambda} \frac{1 - q_0}{q_0} < \hat{\xi}_{6\Lambda} < -2\hat{\xi}_{5\Lambda} \frac{1 - q_0}{q_0}, \quad (4.174)$$

which for $\beta = 0$ reduces to Eqn.(4.49) and for the tilt angle β , one has

$$\sinh^2 \beta < \frac{3}{2 [-q_0 \hat{\xi}_{6\Lambda} - 2\hat{\xi}_{5\Lambda}(1 - q_0)]}, \quad (4.175)$$

which combined with the second inequality in Eqn.(4.174), gives us the condition

$$\sinh^2 \beta < \frac{3}{2}, \quad (4.176)$$

for the tilt angle β in Tilted Ricci Cosmology.

Chapter 5

Bayesian Inference and Monte Carlo methods

In this chapter, we introduce the methods that are currently widely used in the field of observational cosmology in order to select the model that best fits the available data and put constraints on its parameters.

We start the chapter by introducing Bayesian Inference and its use for parameter estimation and hypothesis testing.

In the second part of the chapter, we will introduce the computational methods to determine posterior probability distributions of parameters and Bayesian factors that go under the name of Monte Carlo methods.

In the following, we mainly follow the discussion in (Kurek, 2012). For more insights and discussion on the statistical tools employed to test cosmological models, see the textbook (Hobson, 2010) and the papers (Trotta, 2007; Verde, 2010; Li, 2013; Sharma, 2017; Trotta, 2017).

5.1 Frequentist vs Bayesian Probabilities

Two different approaches in the interpretation of probabilities have been using in science.

The first one is the so-called *frequentist approach*. In this approach, the probability of an event A is given by the ratio of the number of times it occurs over the total number of events in the limit of an infinite number of experiments.

The underlying key feature in this approach is that the experiment producing the events can be repeated many times in the same conditions.

However, if this approach is well suited for data analysis in particle physics this does not apply to cosmology where we have a single Universe.

In cosmology, in fact we use a different framework to achieve knowledge from measurements of physical interesting quantities. This framework is based on interpreting a probability as a *degree of belief* to be assigned to a proposition, based on the

available information at the time of the experiment.

This approach goes under the name of Bayesian Inference, named after the XVIII century statistician Thomas Bayes.

5.2 Bayesian Inference

5.2.1 Probability

A proposition, usually denoted by a capital Latin letter, is a statement in which a subject and a predicate are combined and to which a value of truth can be assigned. In Aristotelian logic, initiated by Aristotle and further developed in ancient history, a value of either true or false is attributed to propositions and logical combinations of them.

One can extend Aristotelian logic by using plausibility reasoning, assigning a degree of certainty to a proposition, dependent on what is considered to be known. The importance of the plausibility reasoning lies on the fact that we can derive probability from it.

The mathematical rules on which such plausibility reasoning rests have been stated by Cox (Cox, 1946) in the form of mathematically rigorous axioms.

From these axioms one can derive the laws of probability, such as the sum rule and the product rule.

Given I the proposition summarising all the information that one has before a probability is assigned to a proposition and denoted the conditional probability of a proposition A given the prior information I as $p(A|I)$ and the joint probability of two propositions A and B given the information I as $p(A, B|I)$, the sum rule and the product rule can be expressed as

$$p(A|I) + p(\bar{A}|I) = 1, \quad (5.1)$$

with \bar{A} the negation of proposition A and

$$p(A, B|I) = p(A|B, I)p(B|I), \quad (5.2)$$

respectively.

It is straightforward to show that from Eqn.(5.2) the Bayes' theorem follows

$$p(A|B, I) = \frac{p(B|A, I)p(A|I)}{p(B|I)}, \quad (5.3)$$

and from both sum rule (5.1) and product rule (5.2) one obtains the marginalisation rule

$$p(A|I) = p(A, B|I) + p(A, \bar{B}|I), \quad (5.4)$$

that can be generalised to the following expression

$$p(A|I) = \sum_k p(A, B_k|I) = 1. \quad (5.5)$$

where the propositions B_k constitute a discrete mutually exclusive and exhaustive set of propositions such that

$$\sum_k p(B_k|I) = 1 \quad \text{with} \quad p(B_k|B_l, I) = p(B_k|I) \text{ for } k \neq l. \quad (5.6)$$

5.2.2 Random variables

The measurement of a physical observable gives us an outcome that can be considered a continuous random variable.

A continuous random variable X is a function mapping the sample space Ω of possible outcomes of a random process to the space of real numbers.

Such a continuous random variable has a probability distribution associated with it, dubbed probability density function (pdf), denoted by $p(X)$, such that $p(x)dx$ gives the probability that the continuous random variable X assumes the value in the infinitesimal interval $[x, x + dx]$.

For the pdf, one can obtain the cumulative distribution function (cdf), i.e. the probability that the continuous random variable X takes a value smaller than x , as

$$P(x) = \int_{-\infty}^x p(y)dy. \quad (5.7)$$

5.3 Parameter Estimation

We can now use Bayesian Inference for parameter estimation, i.e. infer the value of a parameter of a model given the observed data.

Let us consider a model M which is characterised by a set of parameters $\theta = \{\theta_1, \dots, \theta_n\}$ and we have some data d coming from an experiment.

The probability of the data d given the model M and the parameters θ is given by the *likelihood* $p(d|\theta, M, I)$, where I represents the knowledge prior to the experiment.

In Bayesian Inference, we are interested in the *posterior* $p(\theta|d, M, I)$ which represents the probability distribution of the set of parameters θ given the data d , the model M and the prior information I .

In order to obtain the posterior from the likelihood, we exploit the Bayes' theorem (5.3) derived above

$$p(\boldsymbol{\theta}|d, M, I) = \frac{p(d|\boldsymbol{\theta}, M, I)p(\boldsymbol{\theta}|M, I)}{p(d|M, I)} \quad (5.8)$$

where $p(\boldsymbol{\theta}|M, I)$ is the prior which represent what we know about the set of parameters $\boldsymbol{\theta}$ before we have at our disposal the data d : for instance, this could be the uniform distribution of the parameters in the interval in which they are expected from theoretical considerations or the posterior distribution of the parameters obtained from a previous data analysis. In the denominator of the last equation, we have the *evidence* $p(d|M, I)$. The evidence does not depend on the parameters set $\boldsymbol{\theta}$, and can be ignored for our purposes. The Eqn.(5.8) can thus be restated as a proportionality

$$p(\boldsymbol{\theta}|d, M, I) \propto p(d|\boldsymbol{\theta}, M, I)p(\boldsymbol{\theta}|M, I). \quad (5.9)$$

From the last equation shows that the posterior is proportional to the likelihood weighted by the prior. So Bayes theorem give us a way to update our degrees of belief due to the presence of new data.

Once the joint posterior for the set of the model parameters $\boldsymbol{\theta}$ has been computed, we have all the information about the variables given the data d .

We can then obtain the marginalised posterior distribution for one of the parameters θ_i of the model, by integrating over all the other model parameters

$$p(\theta_i, |d, M, I) = \int_{\theta_1^{\min}}^{\theta_1^{\max}} \cdots \int_{\theta_{i-1}^{\min}}^{\theta_{i-1}^{\max}} \int_{\theta_{i+1}^{\min}}^{\theta_{i+1}^{\max}} \cdots \int_{\theta_N^{\min}}^{\theta_N^{\max}} p(\boldsymbol{\theta}|d, M, I) d\theta_1 \dots d\theta_{i-1} d\theta_{i+1} \dots d\theta_N. \quad (5.10)$$

Other useful information is the expectation value of each parameter θ_i , given by

$$\mu_i = E[\theta_i] = \int_{\theta_1^{\min}}^{\theta_1^{\max}} \cdots \int_{\theta_N^{\min}}^{\theta_N^{\max}} \theta_i p(\boldsymbol{\theta}|d, M, I) d\theta_1 \dots d\theta_N, \quad (5.11)$$

and the uncertainties on the parameters from the *covariance matrix* that can computed as

$$\Sigma_{ij} \equiv E[(\theta_i - \mu_i)(\theta_j - \mu_j)] = \int_{\theta_1^{\min}}^{\theta_1^{\max}} \cdots \int_{\theta_N^{\min}}^{\theta_N^{\max}} (\theta_i - \mu_i)(\theta_j - \mu_j) p(\theta_1, \dots, \theta_N | d, M, I) d\theta_1 \dots \theta_N, \quad (5.12)$$

where the diagonal elements give the variance associated to each parameter θ_i and the off-diagonal elements represent the correlations between two parameters θ_i and θ_j .

While the variance is a good measure of the uncertainty when the posterior is symmetric, in more general situations one uses the *confidence interval*, which is defined to be the smallest interval within which a fraction γ of the posterior distribution is contained

$$\gamma_{\theta_i} = \int_{\theta_i^l}^{\theta_i^u} p(\theta_i|d, M, I) d\theta_i, \quad (5.13)$$

where the integrand is the marginalised posterior distribution (5.10). In the literature, γ_{θ_i} is either chosen to be 0.68 or 0.95 corresponding to 1 and 2 standard deviations for a Gaussian distribution, with a probability that the true estimate lies within the interval $[\theta_i^l, \theta_i^u]$ with a probability of 68% and 95%, respectively.

5.4 Hypothesis Testing

Let us suppose we have two competing models M and N , and we want to decide which one describes the data better.

This decision goes under the name of *hypothesis testing* also known as *model comparison* or *model selection* and can be performed by using the methods of Bayesian inference described above.

Let $p(M|d, I)$ be the posterior probability of the model M given the data d . By using the Bayes' theorem (5.3), we have

$$p(M|d, I) = \frac{p(d|M, I)p(M|I)}{p(d|I)}, \quad (5.14)$$

where $p(M|I)$ is the prior probability of model M given the initial available information. The same can be obtained for the second model N .

Now, we can compute the *odds ratio*, i.e. the ratio of the posterior probabilities of the two models

$$O_N^M \equiv \frac{p(M|d, I)}{p(N|d, I)} = \frac{p(d|M, I)}{p(d|N, I)} \frac{p(M|I)}{p(N|I)}, \quad (5.15)$$

where the factor $p(M|I)/p(N|I)$ is called the *prior odds* indicating our relative initial belief in the models whereas the factor $p(d|M, I)/p(d|N, I)$ is the *Bayes factor*,

$$B_N^M = \frac{p(d|M, I)}{p(d|N, I)}. \quad (5.16)$$

Usually, it is assumed that in the initially available information, there is nothing that leads to a preference between the two models. Therefore, the only important factor to be taken into account in order to do the hypothesis testing is the Bayes factor (5.16). For that one needs to calculate the evidence for both models M and N in

terms of the likelihood and the prior of the considered model. By using the Bayes theorem (5.3), for the model M one can write

$$p(\boldsymbol{\theta}|d, M, I)p(d|M, I) = p(d|\boldsymbol{\theta}, M, I)p(\boldsymbol{\theta}|M, I). \quad (5.17)$$

Then, one can marginalise both sides over $\boldsymbol{\theta}$, i.e.

$$\int p(\boldsymbol{\theta}|d, M, I)p(d|M, I)d\boldsymbol{\theta} = \int p(d|\boldsymbol{\theta}, M, I)p(\boldsymbol{\theta}|M, I)d\boldsymbol{\theta}. \quad (5.18)$$

From the normalization of the posterior and the independence of the evidence $p(d|M, I)$ from the parameter set, one arrives at an expression for the evidence in terms of the likelihood $p(d|\boldsymbol{\theta}, M, I)$ and the prior $p(\boldsymbol{\theta}|M, I)$, given by

$$p(d|M, I) = \int p(d|\boldsymbol{\theta}, M, I)p(\boldsymbol{\theta}|M, I)d\boldsymbol{\theta} \quad (5.19)$$

known as the marginal likelihood.

The logarithm of the Bayes factor is used as information criterion to assess how better a model M fits the data with respect to another model N , following the Jeffreys' Scale (Trotta, 2007): if $\ln B_N^M < 1$, there is no significant evidence in favour of model M ; if $1 < \ln B_N^M < 2.5$, the evidence in favour of the model M is substantial; if $2.5 < \ln B_N^M < 5$, there is strong evidence in favour of model M ; if $\ln B_N^M > 5$, the evidence is decisive, while negative values of $\ln B_N^M$ can be instead interpreted as evidence in favour of model N .

There are two important issues one needs to underline when doing hypothesis testing in the framework of Bayesian Inference, making evident the strengths of this approach with respect to the frequentist approach.

The first one is related to the fact that the model with highest evidence will not be necessarily the preferable one between the two models because the prior odds is included in the odds ratio. We can have, in fact, the case in which prior probabilities of models M and N are different. For instance, if prior belief in model is much lower compared to the other model N , the model M needs to have a particularly good fit to the data.

The second issue regards the different complexities that two models can have. In general, in Bayesian Inference a model with more parameters has not always higher evidence than that of a model with less parameters. Therefore, one has not the freedom to add arbitrary complexity to a model without being penalised, in accordance with Occam's razor.

Even in hypothesis testing, the frequentist and the Bayesian approaches diverge. In the frequentist approach, one accepts or rejects a null hypothesis H_0 based on

the p-value, i.e. the hypothesis H_0 is assumed to be true and one determines how unlikely are the data given this assumption. As illustrated, instead, the Bayesian approach takes the view that does not make sense to reject a model unless there is an alternative model with which the first model can be compared.

5.5 Markov Chain Monte Carlo methods

The posterior probability distribution, which plays a crucial role in parameter estimation and hypothesis testing, as seen in the last sections, most of the times lacks a closed analytical form. Therefore, one needs computational methods to find it. The most widespread procedure used in performing this task is by resorting to Markov Chain Monte Carlo (MCMC) methods. The purpose of a MCMC algorithm is to construct a sequence of points, called a chain, in the parameter space, such that the density of such points is proportional to the posterior pdf. These points are called samples. In the following, we will introduce some basic definitions and the algorithm we have used to obtain the posterior pdf in our data analysis of some models of Ricci Cosmology.

5.5.1 Markov Chain

A Markov Chain is defined as a sequence of random variables $\{X^{(0)}, X^{(1)}, \dots, X^{(M-1)}\}$ such that the probability of the $(t + 1)$ -th element in the chain only depends on the value of the t -th element. The crucial property of Markov chains is that they can be shown to converge to a stationary state, i.e. which does not change with t , where successive elements of the chain are samples from the distribution we want to reconstruct, in our case the posterior $p(\boldsymbol{\theta}|d, M, I)$.

The generation of the elements of the chain is probabilistic in nature, and is described by a transition probability $T(\boldsymbol{\theta}^{(t)}, \boldsymbol{\theta}^{(t+1)})$, giving the probability of moving from point $\boldsymbol{\theta}^{(t)}$ to point $\boldsymbol{\theta}^{(t+1)}$ in parameter space. A sufficient condition to obtain a Markov Chain is that the transition probability satisfy the detailed balance condition

$$p(\boldsymbol{\theta}^{(t)}|d)T(\boldsymbol{\theta}^{(t)}, \boldsymbol{\theta}^{(t+1)}) = p(\boldsymbol{\theta}^{(t+1)}|d)T(\boldsymbol{\theta}^{(t+1)}, \boldsymbol{\theta}^{(t)}), \quad (5.20)$$

from which it is straightforward to see that the ratio of the transition probabilities is inversely proportional to the ratio of the posterior probabilities at the two points.

Once samples from the posterior pdf have been gathered, one can obtain, one can employ usual numerical methods to derive expectation values (5.11) for the model parameters, covariance matrices (5.12), marginalised posterior distributions (5.10) and Bayes factors (5.16), used for Bayesian Inference as outlined in the last sections.

5.5.2 The Metropolis-Hastings algorithm

The MCMC algorithm we have used in our data analyses of Ricci Cosmology models, we will present in Chapters 7 and ?? to sample from the posterior distribution is the Metropolis-Hastings algorithm. This algorithm is one of the most widely used algorithms and has the following steps:

1. Choose randomly an initial point $\boldsymbol{\theta}^{(0)}$ in parameter space, with associated posterior probability

$$p_0 = p(\boldsymbol{\theta}^{(0)} | d, M, I); \quad (5.21)$$

2. Given a proposal distribution $q(\boldsymbol{\theta}^{(0)}, \boldsymbol{\theta}^{(c)})$, draw a candidate point $\boldsymbol{\theta}^{(c)}$ from it. For example, the proposal distribution can be a Gaussian centered around the current point with a fixed width;

3. Compute the posterior distribution at the new candidate point

$$p_c = p(\boldsymbol{\theta}^{(c)} | d, M, I); \quad (5.22)$$

4. Calculate the acceptance probability as

$$\alpha(\boldsymbol{\theta}^{(0)}, \boldsymbol{\theta}^{(c)}) = \min \left(\frac{p_c q(\boldsymbol{\theta}^{(c)}, \boldsymbol{\theta}^{(0)})}{p_0 q(\boldsymbol{\theta}^{(0)}, \boldsymbol{\theta}^{(c)})}, 1 \right) \quad (5.23)$$

with the transition probability $T(\boldsymbol{\theta}^{(0)}, \boldsymbol{\theta}^{(c)})$ appearing in the detailed balance condition (5.20), given by

$$T(\boldsymbol{\theta}^{(0)}, \boldsymbol{\theta}^{(c)}) = q(\boldsymbol{\theta}^{(0)}, \boldsymbol{\theta}^{(c)}) \alpha(\boldsymbol{\theta}^{(0)}, \boldsymbol{\theta}^{(c)}); \quad (5.24)$$

5. Pick a random number u from a uniform distribution in the interval $[0, 1)$
 - If $u \leq \alpha(\boldsymbol{\theta}^{(0)}, \boldsymbol{\theta}^{(c)})$, then accept the candidate point,
 - If $u > \alpha(\boldsymbol{\theta}^{(0)}, \boldsymbol{\theta}^{(c)})$, then reject the candidate point;
6. If the candidate point is rejected, go back to the step 2 with the old point. Otherwise, restart from step 2 with the new point in parameter space.

A simplified version of this algorithm, the Metropolis algorithm uses a symmetric proposal distribution with the acceptance probability simplified to

$$\alpha = \min \left(\frac{p_c}{p_0}, 1 \right). \quad (5.25)$$

A relevant issue for the efficiency in the exploration of the parameter space for the Metropolis-Hastings algorithm regards the optimal scale of the proposal distribution: if the scale of q is too small compared to that of the posterior distribution we are interested in, the algorithm spends too much time locally; if instead the scale of q is too large, we could miss some features of the posterior distribution (Sharma, 2017).

Chapter 6

Cosmological Probes of Dark Energy

In this chapter we review the physics and the observables of the cosmological probes that currently provide us the most relevant sets of data to reconstruct the expansion history of our Universe such as Type Ia Supernovae (SNIa), Gamma-Ray Bursts (GRBs), Cosmic Chronometers (CCs), Strong Lensed Quasars (QSOs), Baryon Acoustic Oscillations (BAO) and Cosmic microwave Background (CMB), that we will use to put observational constraints on the parameters in the Isotropic Ricci Cosmology and in the Ricci Vacuum Cosmology models in the following chapters.

For each probe we are interested in the distances of such objects from us because such distances depend on the cosmological model we consider. Therefore measuring such distances allow us to choose the model best describing our Universe and at the same time put constraints on its parameters.

6.1 Cosmic distances

The two fundamental cosmic distances from which all other cosmological observables are built are the *luminosity distance* and the *angular diameter distance*.

6.1.1 Luminosity distance

Let us consider a luminous cosmological object with an absolute luminosity L , i.e. emitted total power (energy per second). An observer will measure an apparent luminosity l

$$l = \frac{L}{4\pi d_L^2} \quad (6.1)$$

at a distance d_L from the luminous source. Such a distance is the so-called luminosity distance. Such luminosity distance in an expanding flat Universe can be expressed as (Ellis, Maartens, and MacCallum, 2012)

$$d_L(z) = c(1+z) \int_0^z \frac{dz'}{H(z')} \quad (6.2)$$

Such a distance can be written in terms of the apparent magnitude m and the absolute magnitude M of the luminous cosmological object whose apparent luminosity l is measured.

The apparent magnitude m of such astrophysical source is defined as (Perivolaropoulos and Skara, 2021)

$$m = -2.5 \log_{10} \left(\frac{l}{l_0} \right), \quad (6.3)$$

where l_0 is a reference apparent luminosity. The absolute magnitude M of the same source is the apparent magnitude the source would have if it were placed at a distance of 10 pc from the observer.

By using the apparent magnitude (6.3) and the definition of the absolute magnitude M , one obtains the following expression

$$\frac{l_{10}}{l} = 100^{\frac{m-M}{5}} \quad (6.4)$$

where l_{10} is the apparent luminosity of the source as it were at a distance of 10 pc from us.

Thus, from the expression of the apparent luminosity (6.1), one has

$$m - M = 5 \log_{10} \left(\frac{d_L}{10} \right) \quad (6.5)$$

where the difference $m - M$ defines the distance modulus μ . A *standard candle* is an astrophysical object whose absolute magnitude is known. Therefore, for a standard candle, once measured its apparent magnitude, one has its luminosity distance.

6.1.2 Angular diameter distance

Let us consider a source with a physical scale r that subtends an angle θ in the sky as shown in Fig.(6.1). Such an astrophysical source is called *standard ruler* and its physical angular diameter distance D_A is defined as

$$D_A(z) = \frac{r}{\theta}, \quad (6.6)$$

where the angle θ is assumed to be small.

In an expanding flat Universe the physical angular diameter distance can be expressed as (Dodelson, 2003)

$$D_A(z) = \frac{c}{(1+z)} \int_0^z \frac{dz'}{H(z')} \quad (6.7)$$

which is related to the luminosity distance (6.2) by

$$d_L(z) = (1+z)^2 D_A(z) \quad (6.8)$$

which is the so-called *reciprocity formula* (Weinberg, 1972).

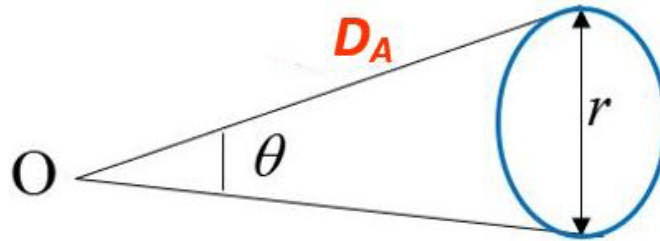


FIGURE 6.1: Angular diameter distance for a source of physical scale r from (Perivolaropoulos and Skara, 2021)

6.2 Type Ia supernovae

One of the most prominent cosmological probe that, as mentioned in Chapter 2, have furnished the first evidence for the accelerated expansion of our Universe are the Type Ia Supernovae (SnIa).

The physical mechanisms at their origin are still debated but there is some consensus on the fact that they are thermonuclear explosions of a rotating carbon-oxygen white dwarf, approaching the Chandrasekhar mass limit ($\sim 1.4M_{\odot}$): this is the mass at which the gravitational attraction is not compensated by the pressure due to nuclear fusion processes inside it and consequently the star collapses and explodes.

For a white dwarf to reach such mass limit, the presence of a companion orbiting star, either another white dwarf or a main sequence star, e.g. a red giant, from which the carbon-oxygen white dwarf can accrete matter, is needed.

This hypothesis is supported mainly by the absence of hydrogen and helium lines and the presence of ionized silicon lines around the maximum in the light spectra produced by these astrophysical objects. For more details on the SnIa spectra see the reference (Parrent, Friesen, and Parthasarathy, 2014).

The usefulness of this kind of supernovae resides on the fact that they are standardizable astrophysical objects, i.e. objects whose absolute brightness is correlated with

other observables and once they are standardized they can be used as *standard candles*.

Not all the SnIa have the same spectrum and therefore cannot be immediately used as standard candle but have slightly different peak apparent magnitudes m which depend on the observed stretch s and colour C via the modified relation

$$5 \log_{10} \left[\frac{H_0}{c} d_L(z, \theta) \right] = m + \alpha s - \beta C - \mathcal{M}, \quad (6.9)$$

where \mathcal{M} is the Hubble diagram offset

$$\mathcal{M} \equiv M + 5 \log_{10} \left[\frac{c}{H_0 \times 1\text{Mpc}} \right] + 25, \quad (6.10)$$

which is a combination of the Hubble parameter H_0 and the absolute magnitude M . The last parameter can be determined through the calibration by using the so-called *cosmic distance ladder* method.

In this approach each step of the distance ladder uses parallax methods and/or the known intrinsic luminosity of a standard candle source to determine the absolute luminosity of a more luminous standard candle residing in the same galaxy. Thus highly luminous standard candles are calibrated for the next step in order to reach out to high redshift luminosity distances. Different astrophysical objects can be used for this purpose:

- Cepheids are primary distance indicators whose distance is determined by means of trigonometric parallax methods. Their use as standard candles is possible because their luminosities are correlated with their periods of variability through the Leavitt law.
- The Tip of the Red Giant Branch (TRGB) stars in the Hertzsprung-Russell diagram are stars that have nearly exhausted the hydrogen in their cores and have just started to burn helium. By using parallax methods, one can standardise their brightness.
- Miras are highly evolved low mass variable stars at the tip of asymptotic giant branch (AGB) stars, whose period-luminosity relation can be calibrated by using the water megamaser as distance indicator

For more details on these steps of the cosmic distance ladder and other ways to calibrate SnIa, see (Perivolaropoulos and Skara, 2021), and references therein.

The sample of calibrated supernovae that is currently widely used is the Pantheon sample containing 1048 SnIa in the redshift interval $0.01 < z < 2.26$ (Scolnic et al., 2018).

6.3 Gamma-Ray Bursts

Another cosmological probe that can be used as a standard candle is given by the Gamma-Ray Bursts (GRBs). They have been proposed as a complementary probe to SnIa because their high energy photons in the γ -ray band are only slightly affected by dust extinction making them observable well beyond the redshift range of the SnIa, up to redshift $z \sim 8 - 9$.

Even if the first detection of a GRB dates back to 1967 by the Vela satellites (Klebesadel, Strong, and Olson, 1973), their physical origin is still debated. One of the most recent discovered GRB has been detected in conjunction with the gravitational wave signal GW170817 observed by the LIGO and Virgo detectors in 2017 (Abbott et al., 2017), marking the beginning of the multimessenger astronomy.

Analogously to the SnIa, they are not standard candles by themselves, but they must be calibrated.

Following (Liu and Wei, 2015), one can notice that the possibility to use GRBs as standard candles is due to the existence of an empirical relation between the cosmological rest-frame spectrum peak energy $E_{p,i} = E_{p,obs}(1+z)$ and the isotropic equivalent radiated energy E_{iso} , given by

$$E_{p,i} = KE_{iso}^m \quad (6.11)$$

with K a constant of proportionality and m a constant exponent. The isotropic equivalent radiated energy is given by

$$E_{iso} = 4\pi d_L^2 S_{bol} (1+z)^{-1}, \quad (6.12)$$

where d_L is the luminosity distance of the GRB and S_{bol} . In order to calibrate GRBs, one uses the Amati relation

$$\log \frac{E_{iso}}{\text{erg}} = \lambda + b \log \frac{E_{p,i}}{300\text{keV}} \quad (6.13)$$

with λ and b are constants to be determined. By using the equation (6.5), one can write the luminosity distance d_L in terms of the distance modulus μ .

After the first attempts made in (Liang and Zhang, 2008; Kodama et al., 2008) and in (Capozziello and Izzo, 2010), only with the work (Liu and Wei, 2015), in which GRBs have been calibrated in a cosmology-independent way by means of Padé approximant, a generalization of Taylor expansion, and use of the Union2.1 SnIa dataset (Suzuki et al., 2012) have become useful as standard candles, giving rise to the *Mayflower* sample, comprising 79 GRBs in the redshift range $1.44 < z < 8.1$.

6.4 Cosmic Chronometers

Alongside standard candles and standard rulers, there exists another technique not based on the cosmic distance ladder used to determine the history of our Universe, independent of the early-Universe physics: Cosmic Chronometers or *standard clocks*. However, analogously to SNIa and GRBs, they are independent of any assumption on the cosmological model describing the Universe.

Astrophysical objects that can be used as CCs are those objects whose evolution history is known. An example of these objects is given by passively-evolving Early-Type Galaxies (ETGs) which are galaxies characterised by a low star formation rate and old stellar populations (Jimenez and Loeb, 2002).

As described in the reference above, differently from other cosmological probes, we can acquire direct information about the Hubble function over redshift ranges, through the formula

$$H(z) = -\frac{1}{1+z} \frac{dz}{dt}. \quad (6.14)$$

The last expression comes from the definition of the scale factor in terms of the redshift

$$a(t) = \frac{a_0}{1+z} \quad (6.15)$$

for $a_0 = 1$.

If we measure the age difference Δt between two passively evolving ETGs, separated by a small redshift interval Δz , then from the Hubble function (6.14) it is possible to infer the actual expansion rate $H(z)$ at each redshift and thus the Hubble constant H_0 .

The complete dataset of CCs can be found in (Moresco et al., 2022).

6.5 Strong Lensed Quasars

Strong gravitationally lensed quasars constitute another cosmological probe to constrain the parameters of a cosmological model.

Strong gravitational lensing was first proposed in (Refsdal, 1964) and it is due to the gravitational deflection of light rays coming from a luminous source when a mass distribution, for instance a massive galaxy or a cluster of galaxies, exists along the line of sight between us and the source. The light rays follow different paths arriving to us at different times and producing multiple images of the source. For an extensive review on this topic, see (Suyu et al., 2018).

Here, we will follow (Perivolaropoulos and Skara, 2021) in order to briefly illustrate how to constrain the cosmological parameters θ of a cosmological model through

the *time-delay distance*.

Given the angular positions of two images of the same source θ_A and θ_B , the time delay Δt_{AB} between the light rays forming them is given by

$$\Delta t_{AB} = \frac{1 + z_L}{c} \frac{D_L D_S}{D_{LS}} [\phi(\theta_A, \beta) - \phi(\theta_B, \beta)], \quad (6.16)$$

where β is the angular position of the source, z_L is the lens redshift, D_L , D_S and D_{LS} are the angular diameter distance (6.7) to the lens, to the source and between the lens and the source, respectively, and $\phi(\theta, \beta)$ is the Fermat potential given by

$$\phi(\theta, \beta) = \frac{(\theta - \beta)^2}{2} - \psi(\theta) \quad (6.17)$$

with $\psi(\theta)$ the effective lensing potential in the image direction.

The time delay distance $D_{\Delta t}$ can be obtained from Eqn.(6.16) dividing the time delay by the difference of the Fermat potential in the images directions θ_A and θ_B

$$D_{\Delta t} = (1 + z_L) \frac{D_L D_S}{D_{LS}} \quad (6.18)$$

The most recent available dataset of strong lensed quasars is the TDCOSMO sample described in (Birrer et al., 2020) which consists of seven strong gravitationally lensed quasars with multiple images, six of which are from H0LiCOW collaboration (Suyu et al., 2017).

6.6 Baryon Acoustic Oscillations

Baryon Acoustic Oscillations (BAO) provide a standard ruler evolving with the Universe since recombination and constitute a very useful cosmological probe in constraining cosmology. The physics on which BAO are based is described in the next, following (Bassett and Hlozek, 2009; Weinberg et al., 2013; Perivolaropoulos and Skara, 2021; Suyu et al., 2018).

Let us consider an overdense region of the primordial plasma made of tightly coupled photons and baryons, comprising electrons and protons, interacting via Compton scattering. Matter outside this region is attracted towards it, while the flow of heat in the opposite direction produces an outward pressure. The interplay between these two forces gives rise to damped oscillations of this plasma, analogous to spherical sound waves moving out of the overdensity with a relativistic sound speed

$$c_s(z) = \frac{c}{\sqrt{3(1 + \bar{R}_b(1 + z)^{-1})}}, \quad (6.19)$$

with \bar{R}_b , the baryon-to-photon density ratio parameter, given by

$$\bar{R}_b = 31500\Omega_b h^2 (T_{CMB}/2.7)^{-4} \quad (6.20)$$

with the CMB temperature $T_{CMB} = 2.726$ K.

At the same time, the non-relativistic CDM, which interacts only gravitationally with baryons, remains near the origin of the overdensity. As soon as the temperature decreases, the Hubble rate overcomes the scattering rate between photons and baryons (decoupling) and protons and electrons start to join forming neutral atoms (recombination).

Therefore, photons start to propagate freely, leaving behind overdense shells of baryons, corresponding to the sound waves wavelengths while baryons and CDM pull each other.

Such a process happens for each overdensity present in the Universe and the distance to the first shell such perturbations travel before the decoupling, is the same for all overdensities and it is referred to as the *sound horizon*.

This phenomenon was detected for the first time in 2005 in the galaxy power spectrum by the 2dF Galaxy Redshift Survey (2dFGRS) (Cole et al., 2005) and by Sloan Digital Sky Survey (SDSS) (Eisenstein et al., 2005), observing greater numbers of galaxies separated by the sound horizon distance.

The sound horizon scale as standard ruler scale is the comoving sound horizon scale at the drag epoch, given by

$$r_s(z_d) = \int_{z_d}^{\infty} \frac{c_s(z)}{H(z)} dz. \quad (6.21)$$

The drag epoch occurs when gravitational instabilities in baryons cannot be further prevented by the photon pressure shortly later than decoupling because Ω_b is small at the drag redshift z_d which can be estimated numerically as done in (Eisenstein and Hu, 1998)

$$z_d = 1291 \frac{\omega_m^{0.251}}{1 + 0.659 \omega_m^{0.828}} [1 + b_1 \omega_b^{b_2}], \quad (6.22)$$

with $\omega_m = \Omega_m h^2$ and $\omega_b = \Omega_b h^2$ and the coefficients b_1 and b_2 given by

$$b_1 = 0.313 \omega_m^{-0.419} [1 + 0.607 \omega_m^{0.6748}], \quad (6.23)$$

and

$$b_2 = 0.238 \omega_m^{0.223}, \quad (6.24)$$

respectively. Given a sample of galaxies, by deriving the sound horizon at the drag epoch $r_s(z_d)$ from the peaks in the CMB angular power spectrum, clustering in both radial and transverse directions gives us information on the Hubble parameter at the effective redshift of the galaxy sample, and on its angular distance to that redshift, respectively.

More explicitly, in radial direction one measures the redshift extent Δz_s which is related to the Hubble function via

$$\Delta z_s = \frac{H(z)r_s(z_d)}{c}, \quad (6.25)$$

while in the transverse direction one measures the angular extent $\Delta\theta_s$, related to the angular diameter distance via

$$\Delta\theta_s = \frac{r_s(z_d)}{D_A(z)}. \quad (6.26)$$

Instead of considering these observables independently, in early BAO measurements (Blake et al., 2012), the following combinations of radial and transverse information on galaxy clustering of the above observables were used:

- the acoustic parameter

$$A(z, \boldsymbol{\theta}) = 100\sqrt{\omega_m} \frac{D_V(z, \boldsymbol{\theta})}{cz}, \quad (6.27)$$

where D_V is the volume distance given by

$$D_V(z, \boldsymbol{\theta}) = \left[(1+z)^2 D_A^2(z, \boldsymbol{\theta}) \frac{cz}{H(z, \boldsymbol{\theta})} \right]^{1/3}, \quad (6.28)$$

- and the Alcock-Paczynski distortion parameter

$$F(z, \boldsymbol{\theta}) = (1+z) \frac{D_A(z, \boldsymbol{\theta})H(z, \boldsymbol{\theta})}{c}. \quad (6.29)$$

6.7 Cosmic Microwave Background

The Cosmic Microwave Background (CMB) is a uniform isotropic radiation with thermal black body spectrum at a temperature of $T_{\text{CMB}} = 2.72548 \pm 0.00057$ K which has been discovered accidentally by American astronomers Arno Penzias and Robert Wilson in 1965 (Penzias and Wilson, 1965), representing one of the firmest proof we have on the Hot Big Bang.

Later studies conducted with satellites COBE¹, WMAP² and Planck³ have confirmed its uniformity, discovering the presence of small temperature anisotropies at the same time, due to small initial inhomogeneities in the matter densities.

The physical mechanism that has generated such radiation is well understood.

As outlined in the previous section, before recombination, electrons and baryons are tightly coupled to photons. As the temperature decreased with the adiabatic expansion of the Universe, it became favourable for electrons to combine with protons, forming hydrogen atoms. With the electrons trapped in neutral hydrogen atoms, the photons can stream away.

What we see in the sky is the so-called *last scattering surface* at which electrons lastly experienced Thomson scattering with electrons. Since then, such photons thermalized giving rise to the thermal black body radiation we detect.

The temperature anisotropies encoded in the CMB angular power spectrum are a great source of information not only about the inflationary parameters but also for Dark Energy. The reason behind this is that, even if the physics involved in the CMB is not affected by Dark Energy, the last matter component affects the distance to the epoch at which recombination takes place, and hence the angular scale of the CMB fluctuations, as for BAO.

In order to put constraints on the new parameters appearing in Isotropic Ricci Cosmology and Ricci Vacuum Cosmology, we will not use the entire angular power spectrum but we will consider only the shift parameters (Wang and Mukherjee, 2007):

- the physical baryon density parameter ω_b ,
- the sound horizon angular scale at recombination defined as

$$l_a(\boldsymbol{\theta}) \equiv \pi \frac{D_M(z_*, \boldsymbol{\theta})}{r_s(z_*, \boldsymbol{\theta})}, \quad (6.30)$$

- the scaled distance to recombination given by

$$R(\boldsymbol{\theta}) \equiv \sqrt{\Omega_m H_0^2} \frac{D_M(z_*, \boldsymbol{\theta})}{c}. \quad (6.31)$$

The comoving distance D_M and the sound horizon r_s are evaluated at the recombination redshift z_* (Hu and Sugiyama, 1996)

$$z_* = 1048 [1 + 0.00124 \omega_b^{-0.738}] (1 + g_1 \omega_m^{g_2}), \quad (6.32)$$

¹https://lambda.gsfc.nasa.gov/product/cobe/spacecraft_description.html

²<https://map.gsfc.nasa.gov>

³https://www.esa.int/Enabling_Support/Operations/Planck

where the factors g_1 and g_2 read

$$g_1 = \frac{0.0783 \omega_b^{-0.238}}{1 + 39.5 \omega_b^{-0.763}}, \quad (6.33)$$

and

$$g_2 = \frac{0.560}{1 + 21.1 \omega_b^{1.81}}, \quad (6.34)$$

respectively.

Chapter 7

Ricci Cosmology tested against astronomical data

In this chapter, we present and discuss the results of the fit of Isotropic Ricci Cosmology whose derivation is presented in Section 4.1 to observational data. We discuss the preliminary assumptions made to assess the viability of the model. Then, we report the data used for the fit and the results we have obtained from it. In the last section, we elaborate on these results.

7.1 Assumptions

In order to examine the feasibility of the Isotropic Ricci Cosmology model to describe our Universe, and determine the relative importance of the two contributions from the Ricci scalar (4.10) and the time-time component of the Ricci tensor (4.11) to the non-equilibrium effective pressure (4.1) for the fluids filling in the Universe, we take into account *four special cases* of this model, making four different ansätze on the constant reduced second order transport coefficients (4.15):

- in Ansatz 1, each term in the effective pressure (4.1) has the same effect in the change of the scaling of dust and cosmological constant while radiation is assumed to remain unaffected by the modifying pressure terms;
- in Ansatz 2, together with dust and cosmological constant, radiation also deviates from conformality due to the pressure terms in the same way as described in Ansatz 1;
- in Ansatz 3, the second order transport coefficients characterising the responses to both terms in the effective pressure (4.1) are equal for each matter components they affect, dust and cosmological constant;

- in Ansatz 4, besides to dust and cosmological constant, radiation is also affected by the Ricci pressure terms in (4.1) in the same fashion as in Ansatz 3.

In Table 7.1, we report the ansätze we have just discussed, while in Table 7.2, we show the priors one has on the deviation parameters δ_m , δ_r and δ_Λ once the different ansätze are made, coming from the physical bound of entropy growth from the Second Law of Thermodynamics for a closed Universe we have considered in Section 4.1. For a complete derivation of such priors see Appendix A.

Assumptions on $\hat{\zeta}_5$ and $\hat{\zeta}_6$	
Ansatz 1	$\hat{\zeta}_{5r} = \hat{\zeta}_{6r} = 0$ and $\hat{\zeta}_{5m} = \hat{\zeta}_{5\Lambda} \equiv \hat{\zeta}_{50}$, $\hat{\zeta}_{6m} = \hat{\zeta}_{6\Lambda} \equiv \hat{\zeta}_{60}$
Ansatz 2	$\hat{\zeta}_{5r} = \hat{\zeta}_{5m} = \hat{\zeta}_{5\Lambda} \equiv \hat{\zeta}_{50}$ and $\hat{\zeta}_{6r} = \hat{\zeta}_{6m} = \hat{\zeta}_{6\Lambda} \equiv \hat{\zeta}_{60}$
Ansatz 3	$\hat{\zeta}_{5r} = \hat{\zeta}_{6r} = 0$ and $\hat{\zeta}_{5m} = \hat{\zeta}_{6m}$, $\hat{\zeta}_{5\Lambda} = \hat{\zeta}_{6\Lambda}$
Ansatz 4	$\hat{\zeta}_{5r} = \hat{\zeta}_{6r}$, $\hat{\zeta}_{5m} = \hat{\zeta}_{5\Lambda}$, $\hat{\zeta}_{6m} = \hat{\zeta}_{6\Lambda}$

TABLE 7.1: The table reports the four different ansätze on the reduced second order transport coefficients we have considered.

Priors on δ_m , δ_r and δ_Λ	
Ansatz 1	$\delta_r = 0$, $\delta_m \leq 0$ and $\delta_m \leq \delta_\Lambda < 3 + \delta_m$
Ansatz 2	$\delta_\Lambda = 4\delta_m - 3\delta_r$, $\delta_m \leq 0$ and $-1 + \delta_m < \delta_r \leq \delta_m$
Ansatz 3	$\delta_r = 0$, $\delta_m \leq 0$ and $\delta_\Lambda \geq 0$
Ansatz 4	$\delta_r \leq 0$, $\delta_m \leq 0$ and $\delta_\Lambda \geq 0$

TABLE 7.2: The table reports the priors on the deviation parameters δ_m , δ_r and δ_Λ we have used in our data analysis. These priors are derived in Appendix A.

7.2 Data & Statistical Analysis

Data

The data from the cosmological probes described in Chapter 6 we have used in the fit of the Isotropic Ricci Cosmology model described in Section 4.1 are given by:

- Type Ia Supernovae (SnIa) from the Pantheon catalogue (Scolnic et al., 2018);
- Gamma Ray Bursts (GRBs) from the Mayflower sample (Liu and Wei, 2015);
- Cosmic Chronometers (CC) (Gómez-Valent and Amendola, 2019);
- Strong Lensed Quasars from H0LiCOW collaboration (Wong et al., 2020);
- measurements of BAO from the following surveys and samples
 - WiggleZ Dark Energy Survey (Blake et al., 2012);
 - the twelfth data release (DR12) of the Baryon Oscillation Spectroscopic Survey (BOSS) of the third phase of the Sloan Digital Sky Survey (SDSS-III) (Alam et al., 2017);
 - CMASS galaxy catalogue of the SDSS-III BOSS DR12 (Nadathur et al., 2019);
 - quasar sample of the fourteenth data release (DR14) of the extended Baryon Oscillation Spectroscopic Survey (eBOSS) of the fourth phase of the Sloan Digital Sky Survey (SDSS-IV) (Ata et al., 2018);
 - correlation of Lyman- α ($\text{Ly}\alpha$) forest absorption and quasars from the SDSS DR14 (Blomqvist et al., 2019; Sainte Agathe et al., 2019)
- measurements of CMB shift parameters (Zhai and Wang, 2019).

Statistical Analysis

For our data analysis, we have considered a posterior distribution made of

- a prior probability which put together the flat priors reported in Table 7.2 and the priors on the Hubble parameter, $h = H_0/100$, $0 < h < 1$ and on the dimensionless energy densities for baryons Ω_b and dust Ω_m , $0 < \Omega_b < \Omega_m < 1$,
- and the likelihood given by

$$\mathcal{L}(d|\boldsymbol{\theta}, M) \propto e^{-\chi^2/2}, \quad (7.1)$$

where M stands for one of the cases corresponding to the different ansätze in Table 7.1 and Λ CDM and the total χ^2 is the sum of each χ^2 associated to each set of data d from the cosmological probe.

For the data d and the total χ^2 , we have considered two different combinations of data sets in order to check whether in Isotropic Ricci Cosmology there is a relief

of the Hubble tension at the background level: we have fitted the four cases of the Isotropic Ricci Cosmology model against the full data set, including all the data sets above, and the late time data set including only late time measurements of cosmological observables (SNeIa, CC, H0LiCOW, GRBs, BAO from WiggleZ), with the χ^2 given by

$$\chi_{full}^2 = \chi_{SNIa}^2 + \chi_{GRB}^2 + \chi_{CC}^2 + \chi_{H0LiCOW}^2 + \chi_{WiggleZ}^2 + \chi_{BAO}^2 + \chi_{CMB}^2 \quad (7.2)$$

and

$$\chi_{late}^2 = \chi_{SNIa}^2 + \chi_{GRB}^2 + \chi_{CC}^2 + \chi_{H0LiCOW}^2 + \chi_{WiggleZ}^2, \quad (7.3)$$

respectively.

We have employed our own implementation of the Metropolis-Hastings algorithm.

7.3 Results from the fits

The results of the fits of our model for the four ansätze are reported in the Tables 7.3, 7.4, 7.5 and 7.6.

At 1σ level, one can notice that the values of the cosmological parameters are indistinguishable from those for Λ CDM for all the four ansätze we have made. From this, one can immediately conclude that for none of the ansätze we have a solution or a relief of the Hubble tension.

For the parameters of the Isotropic Ricci Cosmology model, we have found upper or lower bounds, except for δ_Λ for the ansätze 1 and 2 which is compatible with zero when one considers the late-time data set. As can be seen from the Tables 7.3, 7.4, 7.5 and 7.6, the observational bounds on the deviation parameters and thus the indirect constraints on the reduced second order transport coefficients $\hat{\zeta}_5$ and $\hat{\zeta}_6$ overlap with one another, showing that there is no substantial difference among the cases of the Isotropic Ricci Cosmology model corresponding to the different ansätze.

These observational bounds are less strict when one takes into account only the late-time data sets than those found when one includes in the fit also the early-time data sets which thus show a more constraining power.

In particular, regarding the reduced second order transport coefficients, the fits of the model with the first two ansätze imply that ζ_{50} is compatible with zero, while for ζ_{60} , one should take into account that, together with the lower bounds found from the fit, it holds $\zeta_{60} < 0$ from the physical requirement of the increase of entropy for both cases.

For the last two ansätze, only upper or lower bounds can be put on the reduced second order transport coefficients $\hat{\zeta}_5$ and $\hat{\zeta}_6$ with significantly milder bounds coming

from the fit with only late time data set taken into account.

For the deviation parameters δ_m , δ_r and δ_Λ , in Figures 7.1 and 7.2, we show the 1σ and 2σ contour plots of the posterior, obtained from the fit with the full data set, projected in the parameter plane $\delta_\Lambda - \delta_m$, and in the parameter plane $\delta_r - \delta_m$, respectively. From the comparison of these contours, we confirm that there is no significant observational difference between the ansätze we have considered.

Finally, from the negative values of the Bayesian factors reported in the Tables, one can conclude that none of the four cases corresponding to the four different ansätze in Table 7.1 of Isotropic Ricci Cosmology model has a better fit than Λ CDM to our data sets.

Despite this conclusion, by inspecting the Bayesian factor, one can also notice that for all the ansätze taken into account, the combination of the late-time data sets used in the fit makes Isotropic Ricci Cosmology less disfavoured with respect to Λ CDM than the full data set does, implying that the deviation from usual redshift scaling and thus departure from equilibrium, for the matter components filling in the Universe are more relevant for its late-time accelerated phase.

	Λ CDM	Λ CDM	Ansatz 1	Ansatz 1
	full	late	full	late
h	$0.673^{+0.003}_{-0.003}$	$0.713^{+0.013}_{-0.012}$	$0.668^{+0.004}_{-0.005}$	$0.713^{+0.014}_{-0.014}$
Ω_m	$0.319^{+0.005}_{-0.005}$	$0.292^{+0.017}_{-0.016}$	$0.319^{+0.005}_{-0.005}$	$0.307^{+0.023}_{-0.022}$
δ_m			> -0.001	> -0.241
δ_Λ			< 0.003	$0.141^{0.192}_{-0.153}$
Ω_Λ	$0.681^{+0.005}_{-0.005}$	$0.708^{+0.016}_{-0.017}$	$0.681^{+0.005}_{-0.005}$	$0.693^{+0.022}_{-0.023}$
$\xi_{50}(\text{N})$			$0.96^{9.57}_{-8.69} \times 10^{38}$	$-7.08^{6.37}_{-6.89} \times 10^{40}$
$\xi_{60}(\text{kg/m})$			$> -4.66 \times 10^{22}$	$> -7.90 \times 10^{24}$
$\ln \mathcal{B}_j^i$	0	0	$-1.56^{+0.04}_{-0.04}$	$-0.59^{+0.03}_{-0.03}$

TABLE 7.3: In the table, we report the constraints on the parameters of Isotropic Ricci Cosmology with ansatz 1 and Λ CDM, both tested against the same full and late data sets.

	Λ CDM	Λ CDM	Ansatz 2	Ansatz 2
	full	late	full	late
h	$0.673^{+0.003}_{-0.003}$	$0.713^{+0.013}_{-0.012}$	$0.667^{+0.005}_{-0.005}$	$0.713^{+0.013}_{-0.013}$
Ω_m	$0.319^{+0.005}_{-0.005}$	$0.292^{+0.017}_{-0.016}$	$0.319^{+0.005}_{-0.005}$	$0.306^{+0.023}_{-0.022}$
δ_m			> -0.0007	> -0.244
δ_r			> -0.003	> -0.388
δ_Λ			< 0.007	$0.151^{+0.189}_{-0.160}$
Ω_Λ	$0.681^{+0.005}_{-0.005}$	$0.708^{+0.016}_{-0.017}$	$0.681^{+0.005}_{-0.005}$	$0.694^{+0.022}_{-0.023}$
$\tilde{\zeta}_{50}(\text{N})$			$0.79^{1.59}_{-0.93} \times 10^{39}$	$-6.97^{6.27}_{-6.85} \times 10^{40}$
$\tilde{\zeta}_{60}(\text{kg/m})$			$> -5.39 \times 10^{22}$	$> -8.13 \times 10^{24}$
$\ln \mathcal{B}_j^i$	0	0	$-1.56^{+0.04}_{-0.03}$	$-0.59^{+0.02}_{-0.03}$

TABLE 7.4: In the table, we report the constraints on the parameters of Isotropic Ricci Cosmology with ansatz 2 and Λ CDM, both tested against the same full and late data sets.

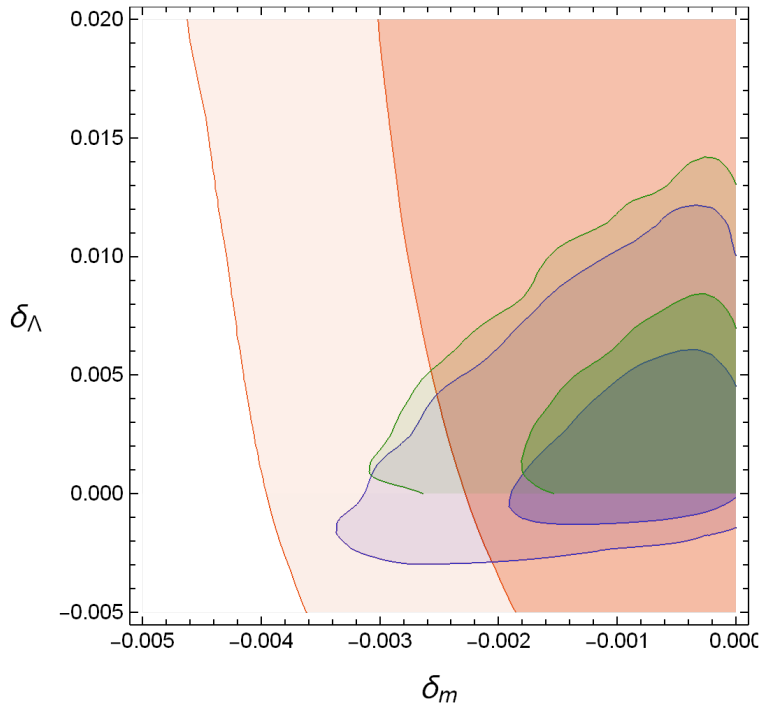


FIGURE 7.1: 1σ and 2σ contour plots in the parameter plane $\delta_\Lambda - \delta_m$ for the four ansätze (Ansatz 1 - blue; Ansatz 2 - grey; Ansatz 3 - green; Ansatz 4 - red)

	Λ CDM	Λ CDM	Ansatz 3	Ansatz 3
	full	late	full	late
h	$0.673^{+0.003}_{-0.003}$	$0.713^{+0.013}_{-0.012}$	$0.667^{+0.004}_{-0.007}$	$0.711^{+0.013}_{-0.013}$
Ω_m	$0.319^{+0.005}_{-0.005}$	$0.292^{+0.017}_{-0.016}$	$0.319^{+0.005}_{-0.005}$	$0.304^{+0.023}_{-0.021}$
δ_m			> -0.001	> -0.256
δ_Λ			< 0.004	< 0.277
Ω_Λ	$0.681^{+0.005}_{-0.005}$	$0.708^{+0.016}_{-0.017}$	$0.681^{+0.005}_{-0.005}$	$0.696^{+0.021}_{-0.023}$
$\tilde{\zeta}_{5m}(\text{N})$			$> -1.03 \times 10^{39}$	$> -2.53 \times 10^{41}$
$\tilde{\zeta}_{5\Lambda}(\text{N})$			$< 2.35 \times 10^{39}$	$< 1.55 \times 10^{41}$
$\tilde{\zeta}_{6m}(\text{kg/m})$			$> -1.14 \times 10^{22}$	$> -2.20 \times 10^{24}$
$\tilde{\zeta}_{6\Lambda}(\text{kg/m})$			$< 2.62 \times 10^{22}$	$< 1.72 \times 10^{24}$
$\ln \mathcal{B}_j^i$	0	0	$-1.53^{+0.03}_{-0.04}$	$-0.68^{+0.02}_{-0.03}$

TABLE 7.5: In the table, we report the constraints on the parameters of Isotropic Ricci Cosmology with ansatz 3 and Λ CDM, both tested against the same full and late data sets.

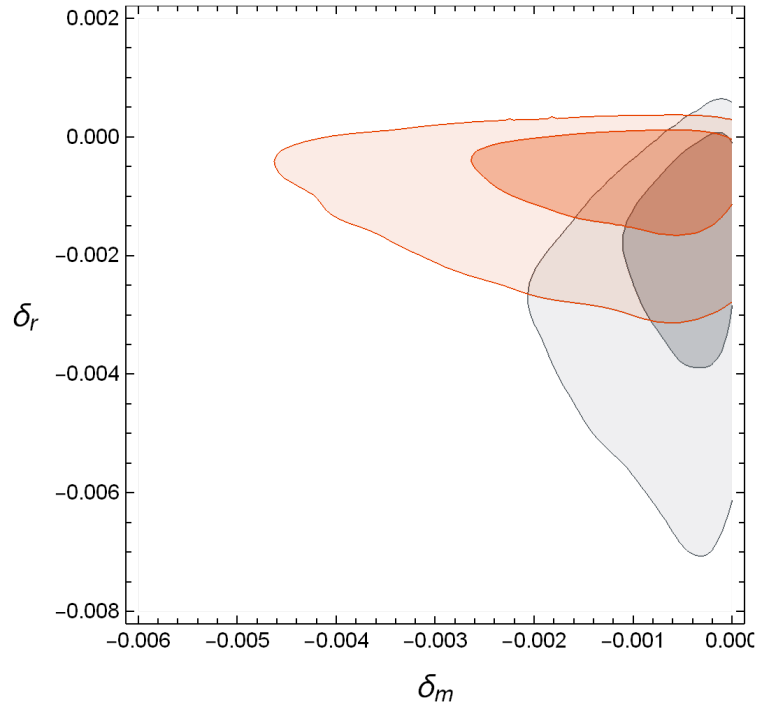


FIGURE 7.2: 1σ and 2σ contour plots in the parameter plane $\delta_r - \delta_m$ for the two ansätze in which $\delta_r \neq 0$ (Ansatz 2 - grey; Ansatz 4 - red)

	Λ CDM	Λ CDM	Ansatz 4	Ansatz 4
	full	late	full	late
h	$0.673^{+0.003}_{-0.003}$	$0.713^{+0.013}_{-0.012}$	$0.701^{+0.012}_{-0.011}$	$0.712^{+0.013}_{-0.013}$
Ω_m	$0.319^{+0.005}_{-0.005}$	$0.292^{+0.017}_{-0.016}$	$0.322^{+0.005}_{-0.005}$	$0.303^{+0.023}_{-0.020}$
δ_m			> -0.002	> -0.245
δ_r			> -0.001	> -199
δ_Λ			< 0.091	< 0.269
Ω_Λ	$0.681^{+0.005}_{-0.005}$	$0.708^{+0.016}_{-0.017}$	$0.678^{+0.005}_{-0.005}$	$0.697^{+0.020}_{-0.023}$
$\xi_{5m}(\text{N})$			$> -1.86 \times 10^{39}$	$> -2.42 \times 10^{41}$
$\xi_{5r}(\text{N})$			$> -1.76 \times 10^{39}$	$> -3.18 \times 10^{42}$
$\xi_{5\Lambda}(\text{N})$			$< 4.95 \times 10^{40}$	$< 1.50 \times 10^{41}$
$\xi_{6m}(\text{kg/m})$			$> -2.08 \times 10^{22}$	$> -2.72 \times 10^{24}$
$\xi_{6r}(\text{kg/m})$			$> -1.96 \times 10^{22}$	$> -3.54 \times 10^{25}$
$\xi_{6\Lambda}(\text{kg/m})$			$< 5.53 \times 10^{23}$	$< 1.67 \times 10^{24}$
$\ln \mathcal{B}_j^i$	0	0	$-2.01^{+0.04}_{-0.03}$	$-0.63^{+0.04}_{-0.03}$

TABLE 7.6: In the table, we report the constraints on the parameters of Isotropic Ricci Cosmology with ansatz 4 and Λ CDM, both tested against the same full and late data sets.

7.4 Discussion

An analogous Hubble function to that derived in Section 4.1 and tested against cosmological data here, has been previously studied in (Bégué, Stahl, and Xue, 2019; Gao, Xue, and Zhang, 2021). In these works, the Hubble function which arises in the framework of *Quantum Field Cosmology* (Weinberg, 2010), is given by Eqn.(2.4) in (Gao, Xue, and Zhang, 2021). In this framework, the modification of the redshift scaling for dust and radiation by the same deviation parameter δ_G is due to the redshift dependence of the gravitational constant while at the same time the cosmological constant acquires dependence on the redshift parameterised by the deviation parameter δ_Λ .

Two models with these features having the same Hubble function have been studied. They differ with the relation among the two deviation parameters δ_G and δ_Λ : in

the first one, the so-called "varying Λ "CDM model or $\tilde{\Lambda}$ CDM, the deviation parameter of matter and radiation is related to the deviation parameter for the cosmological constant through the relation

$$\delta_{\Lambda} \simeq \left(\frac{\Omega_r + \Omega_m}{\Omega_{\Lambda}} \right) \delta_G \quad (7.4)$$

valid at small redshift for $\delta_{\Lambda}, \delta_G \ll 1$, with the consistency relation $\delta_G \delta_{\Lambda} > 0$; in the second one, the so-called extended "varying Λ "CDM model ($e\tilde{\Lambda}$ CDM), the deviation parameters δ_G and δ_{Λ} are independent.

In our model, instead, we have that for the ansätze 1 and 2, the deviation parameters δ_m , δ_r and δ_{Λ} are related through the reduced transport coefficients ζ_{50} and ζ_{60} as shown above, and for the ansätze 3 and 4, it holds $\delta_m \neq \delta_r \neq \delta_{\Lambda}$, and the relation given in Eqn.(7.4) does not hold so that the consistency relation is not compatible with our physical requirements from the Second Law of Thermodynamics for the deviation parameters, which moreover are not constrained to be much smaller than unity.

Nevertheless, the two models $\tilde{\Lambda}$ CDM and $e\tilde{\Lambda}$ CDM, tested against a data set including CMB distance prior data from *Planck 2018*, BAO and SNIa *Pantheon* sample, result to be compatible with Λ CDM, analogously to what we have found for our model tested against a more extended data set.

Similarly, these models can not fit the data better than Λ CDM and cannot solve the Hubble tension, unless the local measurement of the Hubble parameter H_0 by the SH0ES team (Riess et al., 2019) is included into the data set.

Chapter 8

Conclusion and Outlook

In this thesis, we have presented our work in the new framework of Ricci Cosmology, emerged from the study of relativistic dynamics for an out-of-equilibrium fluid in curved spacetime, as a modification of equilibrium pressure at the second order in the expansion of hydrodynamic fields describing it, i.e. its 4-velocity, its energy density and the background metric.

We have derived some models in which the pressure terms involving Ricci scalar and Ricci tensor modify the bulk pressure of the matter components filling in the Universe.

In all of these models, the second-order transport coefficients parametrising the deviation from equilibrium for the bulk pressure are taken to be constant.

The simplest model we have considered is Isotropic Ricci Cosmology, where homogeneity and isotropy of the spacetime is assumed and each matter component, dust, radiation and cosmological constant, has its own bulk pressure modified by the out-of-equilibrium pressure terms.

We have found that, as a result of the presence of such pressure terms, a departure from the perfect fluid redshift scaling for each matter component is obtained. On deviation parameters describing such departures we have put physical bounds from the Second Law of Thermodynamics and we have studied the energy conditions for such a model, finding non trivial relations between the deceleration and the reduced second order transport coefficients.

We have tested this model against cosmological data, finding that it is compatible with Λ CDM, and thus does not lead to a relief of the Hubble tension at the background level and is disfavoured with respect to Λ CDM. Furthermore, observational bounds on the transport coefficients ζ_5 and ζ_6 have been obtained.

Then, we have also studied two solutions in the framework of Ricci Cosmology in which we have dropped the assumptions on which the Cosmological Principle relies.

In the first case, we have considered an anisotropic but homogeneous Universe, described by the Bianchi I Type metric. In the second case, we have studied an isotropic

but inhomogeneous Universe, described by the Lemaître-Tolman-Bondi metric. In both cases, we have found a Hubble function which includes a correction from anisotropic expansion coming from the anisotropy of the cosmic background in the first case and from the anisotropy induced by the inhomogeneity in the second case. The Cosmological Principle was again assumed in Ricci Vacuum Cosmology in which the Ricci pressure terms affect only the vacuum, giving rise to a model analogous to the widely investigated Running Vacuum Model. The running of the vacuum in our case came from the fact that the vacuum was out of equilibrium and its energy density depended on the radiation and dust energy densities. For this model, two cases have been taken into account: in the first one, the vacuum interacted only with Cold Dark Matter, while in the second one, it interacted with Dark Radiation. In both cases, a deviation for the redshift scaling of the interacting species has been found. Another feature of this model was that dust and radiation contributed to the energy budget of the Universe through effective dimensionless energy density parameters.

Then, we have shown how the new pressure terms modify the scenario of Tilted Cosmology at the level of the Energy-Momentum Tensor of the cosmic fluid as seen by the observer and the energy conditions for the cosmic fluid.

Further steps into the exploration of the framework of Ricci Cosmology that we leave for future investigations is testing the Anisotropic Ricci Cosmology, the Inhomogeneous Ricci Cosmology and the Ricci Vacuum Cosmology models against cosmological data in order to study whether these models can fit the data better than Λ CDM and possibly relieve the Hubble tension.

Appendix A

Priors derivation of Isotropic Ricci Cosmology parameters

The general expressions for the deviation parameters parametrising the modification of the usual scaling with the redshift for matter components in terms of the constant reduced second order transport coefficients for dust, radiation and cosmological constant are given by

$$\delta_m = \frac{2\hat{\zeta}_{5m} + \hat{\zeta}_{6m}}{1 + 2\hat{\zeta}_{5m} - \hat{\zeta}_{6m}}, \quad (\text{A.1})$$

$$\delta_r = \frac{2\hat{\zeta}_{6r}}{1 + 2\hat{\zeta}_{5r} - \hat{\zeta}_{6r}}, \quad (\text{A.2})$$

and

$$\delta_\Lambda = \frac{8\hat{\zeta}_{5\Lambda} - 2\hat{\zeta}_{6\Lambda}}{1 + 2\hat{\zeta}_{5\Lambda} - \hat{\zeta}_{6\Lambda}}, \quad (\text{A.3})$$

respectively.

Now, we specialize them to the four ansätze considered for Isotropic Ricci Cosmology considered in Chapter 7.

A.1 Ansatz 1

For Ansatz 1, the assumptions on the reduced second order transport coefficients are

$$\hat{\zeta}_{5\Lambda} = \hat{\zeta}_{5m} \equiv \hat{\zeta}_{50}, \quad \hat{\zeta}_{6\Lambda} = \hat{\zeta}_{6m} \equiv \hat{\zeta}_{60}, \quad \text{and} \quad \hat{\zeta}_{5r} = \hat{\zeta}_{6r} = 0. \quad (\text{A.4})$$

As a result, the deviation parameter for radiation is zero, while the other two deviation parameters have the following expressions

$$\delta_r = 0, \quad \delta_m = \frac{2\hat{\zeta}_{50} + \hat{\zeta}_{60}}{1 + 2\hat{\zeta}_{50} - \hat{\zeta}_{60}}, \quad \text{and} \quad \delta_\Lambda = \frac{8\hat{\zeta}_{50} - 2\hat{\zeta}_{60}}{1 + 2\hat{\zeta}_{50} - \hat{\zeta}_{60}}. \quad (\text{A.5})$$

From the entropy growth condition for dust and cosmological constant studied in Section 4.1, we have

$$\delta_m \leq 0 \quad \text{and} \quad 2\hat{\zeta}_{50} - \hat{\zeta}_{60} \geq 0. \quad (\text{A.6})$$

By using these inequalities in the second of Eqn.(A.5), we have

$$2\hat{\zeta}_{50} + \hat{\zeta}_{60} \leq 0. \quad (\text{A.7})$$

One can invert the relations for the deviation parameters δ_m and δ_Λ (A.5), obtaining the following expressions for the reduced second order transport coefficients in terms of the deviation parameters

$$\hat{\zeta}_{50} = \frac{\delta_m + \frac{1}{2}\delta_\Lambda}{2(3 + \delta_m - \delta_\Lambda)} \quad \text{and} \quad \hat{\zeta}_{60} = \frac{2\delta_m - \frac{1}{2}\delta_\Lambda}{3 + \delta_m - \delta_\Lambda}. \quad (\text{A.8})$$

By substituting the relations in Eqn.(A.8) in the inequality (A.7), one has

$$\frac{3\delta_m}{3 + \delta_m - \delta_\Lambda} \leq 0, \quad (\text{A.9})$$

which together with $\delta_m \leq 0$ from the Second Law of Thermodynamics, implies

$$\delta_\Lambda < 3 + \delta_m. \quad (\text{A.10})$$

From the second inequality in Eqn.(A.6), it holds

$$\frac{\delta_\Lambda - \delta_m}{3 + \delta_m - \delta_\Lambda} \geq 0, \quad (\text{A.11})$$

and by using Eqn.(A.10), one further has the bound

$$\delta_\Lambda \geq \delta_m. \quad (\text{A.12})$$

From inequalities (A.10) and (A.12), we have the following prior for δ_Λ

$$\delta_m \leq \delta_\Lambda < 3 + \delta_m. \quad (\text{A.13})$$

From the expressions in Eqn.(A.8) and the last equation we arrive for the reduced second order transport coefficient $\hat{\zeta}_{60}$ at the following bound

$$\hat{\zeta}_{60} < 0. \quad (\text{A.14})$$

In order to derive a bound on the other reduced second order transport coefficient ζ_{50} , one combines the bound (A.14) with the second inequality in Eqn.(A.6) and the inequality (A.7), finding

$$-\frac{|\hat{\zeta}_{60}|}{2} \leq \hat{\zeta}_{50} \leq \frac{|\hat{\zeta}_{60}|}{2} \quad (\text{A.15})$$

A.2 Ansatz 2

For Ansatz 2, the assumptions on the reduced second order transport coefficients for dust, radiation and cosmological constant are

$$\hat{\zeta}_{5\Lambda} = \hat{\zeta}_{5m} = \hat{\zeta}_{5r} \equiv \hat{\zeta}_{50}, \quad \hat{\zeta}_{6\Lambda} = \hat{\zeta}_{6m} = \hat{\zeta}_{6r} \equiv \hat{\zeta}_{60}, \quad (\text{A.16})$$

with the deviation parameters given by

$$\delta_m = \frac{2\hat{\zeta}_{50} + \hat{\zeta}_{60}}{1 + 2\hat{\zeta}_{50} - \hat{\zeta}_{60}}, \quad (\text{A.17})$$

$$\delta_r = \frac{2\hat{\zeta}_{60}}{1 + 2\hat{\zeta}_{50} - \hat{\zeta}_{60}}, \quad (\text{A.18})$$

and

$$\delta_\Lambda = \frac{8\hat{\zeta}_{50} - 2\hat{\zeta}_{60}}{1 + 2\hat{\zeta}_{50} - \hat{\zeta}_{60}}. \quad (\text{A.19})$$

One can easily see that the deviation parameter δ_Λ (A.19) can be written in terms of the other two deviation parameters δ_m (A.17) and δ_r (A.18) as

$$\delta_\Lambda = 4\delta_m - 3\delta_r. \quad (\text{A.20})$$

In this case, the physical bounds priors from the increase of entropy are given by

$$2\hat{\zeta}_{50} - \hat{\zeta}_{60} \geq 0, \quad \delta_m \leq 0 \quad \text{and} \quad \delta_r \leq 0. \quad (\text{A.21})$$

From the first two inequalities as for Ansatz 1, it holds one finds

$$2\hat{\zeta}_{50} + \hat{\zeta}_{60} \leq 0, \quad (\text{A.22})$$

which coincides with the inequality (A.7) found above.

By inverting the expressions for the deviation parameters δ_m (A.17) and δ_r (A.18), we have

$$\hat{\zeta}_{50} = \frac{-\delta_r + 2\delta_m}{4(1 - \delta_m + \delta_r)} \quad \text{and} \quad \hat{\zeta}_{60} = \frac{\delta_r}{2(1 - \delta_m + \delta_r)}. \quad (\text{A.23})$$

and the inequality (A.22) can thus be rewritten in terms of δ_m and δ_r as

$$\frac{\delta_m}{(1 - \delta_m + \delta_r)} \leq 0, \quad (\text{A.24})$$

which for $\delta_m \leq 0$, gives us a lower bound for the deviation parameter δ_r

$$\delta_r > -1 + \delta_m. \quad (\text{A.25})$$

Furthermore, from the first inequality in Eqn.(A.21), and the lower bound (A.25), one gets for the deviation parameter δ_r the following upper bound

$$\delta_r \leq \delta_m. \quad (\text{A.26})$$

Thus, the physical bounds on the radiation deviation parameter δ_r are given by

$$-1 + \delta_m < \delta_r \leq \delta_m. \quad (\text{A.27})$$

For the reduced second order transport coefficients, from the first and third inequalities in Eqn.(A.21), one has

$$\hat{\zeta}_{60} \leq 0, \quad (\text{A.28})$$

which combined with the first inequality in Eqn.(A.21) and the inequality (A.22), leads to the bound for the reduced second order transport coefficient ζ_{50}

$$-\frac{|\hat{\zeta}_{60}|}{2} \leq \zeta_{50} \leq \frac{|\hat{\zeta}_{60}|}{2}. \quad (\text{A.29})$$

A.3 Ansatz 3

For Ansatz 3, the assumptions on the reduced second order transport coefficients are

$$\hat{\zeta}_{5\Lambda} = \hat{\zeta}_{6\Lambda}, \quad \hat{\zeta}_{5m} = \hat{\zeta}_{6m}, \quad \text{and} \quad \hat{\zeta}_{5r} = \hat{\zeta}_{6r} = 0. \quad (\text{A.30})$$

Thus, the deviation parameters for dust (A.1) and cosmological constant (A.3) read

$$\delta_m = \frac{3\hat{\zeta}_{5m}}{1 + \hat{\zeta}_{5m}} \quad \text{and} \quad \delta_\Lambda = \frac{6\hat{\zeta}_{5\Lambda}}{1 + \hat{\zeta}_{5\Lambda}}, \quad (\text{A.31})$$

while $\delta_r = 0$.

Therefore, the physical bounds from the entropy growth are given by

$$\delta_m \leq 0, \quad \text{and} \quad \hat{\zeta}_{5\Lambda} \geq 0, \quad (\text{A.32})$$

which imply the following bounds for the reduced second order transport coefficient $\hat{\zeta}_{5m}$ and the deviation parameter δ_Λ

$$-1 < \hat{\zeta}_{5m} < 0, \quad \text{and} \quad \delta_\Lambda \geq 0. \quad (\text{A.33})$$

A.4 Ansatz 4

For Ansatz 4, the assumptions on the reduced second order transport coefficients are

$$\hat{\zeta}_{5\Lambda} = \hat{\zeta}_{6\Lambda}, \quad \hat{\zeta}_{5m} = \hat{\zeta}_{6m}, \quad \text{and} \quad \hat{\zeta}_{5r} = \hat{\zeta}_{6r}. \quad (\text{A.34})$$

Thus, the deviation parameters (A.1), (A.2), and (A.3) read

$$\delta_m = \frac{3\hat{\zeta}_{5m}}{1 + \hat{\zeta}_{5m}}, \quad \delta_\Lambda = \frac{6\hat{\zeta}_{5\Lambda}}{1 + \hat{\zeta}_{5\Lambda}} \quad \text{and} \quad \delta_r = \frac{2\hat{\zeta}_{5r}}{1 + \hat{\zeta}_{5r}}. \quad (\text{A.35})$$

The physical bounds from the increase of entropy from the Second Law of Thermodynamics are thus given by

$$\delta_r \leq 0, \quad \delta_m \leq 0, \quad \text{and} \quad \hat{\zeta}_{5\Lambda} \geq 0. \quad (\text{A.36})$$

The last inequalities imply the following bounds for the deviation parameter δ_Λ and the reduced second order transport coefficients $\hat{\zeta}_{5r}$ and $\hat{\zeta}_{5m}$

$$\delta_\Lambda \geq 0, \quad -1 < \hat{\zeta}_{5m} < 0, \quad \text{and} \quad -1 < \hat{\zeta}_{5r} < 0, \quad (\text{A.37})$$

with the first two inequalities coinciding with the priors found for Ansatz 3.

Bibliography

- Abbott, B. P. et al. (2017). “Multi-messenger Observations of a Binary Neutron Star Merger”. In: *Astrophys. J. Lett.* 848.2, p. L12. DOI: [10.3847/2041-8213/aa91c9](https://doi.org/10.3847/2041-8213/aa91c9). arXiv: [1710.05833](https://arxiv.org/abs/1710.05833) [astro-ph.HE].
- Aghanim, N. et al. (2020). “Planck 2018 results. VI. Cosmological parameters”. In: *Astron. Astrophys.* 641, A6. DOI: [10.1051/0004-6361/201833910](https://doi.org/10.1051/0004-6361/201833910). arXiv: [1807.06209](https://arxiv.org/abs/1807.06209) [astro-ph.CO].
- Akarsu, Özgür et al. (2019). “Constraints on a Bianchi type I spacetime extension of the standard Λ CDM model”. In: *Phys. Rev. D* 100.2, p. 023532. DOI: [10.1103/PhysRevD.100.023532](https://doi.org/10.1103/PhysRevD.100.023532). arXiv: [1905.06949](https://arxiv.org/abs/1905.06949) [astro-ph.CO].
- Alam, Shadab et al. (2017). “The clustering of galaxies in the completed SDSS-III Baryon Oscillation Spectroscopic Survey: cosmological analysis of the DR12 galaxy sample”. In: *Mon. Not. Roy. Astron. Soc.* 470.3, pp. 2617–2652. DOI: [10.1093/mnras/stx721](https://doi.org/10.1093/mnras/stx721). arXiv: [1607.03155](https://arxiv.org/abs/1607.03155) [astro-ph.CO].
- Anand, Sampurn et al. (2017). “Cosmic viscosity as a remedy for tension between PLANCK and LSS data”. In: *JCAP* 11, p. 005. DOI: [10.1088/1475-7516/2017/11/005](https://doi.org/10.1088/1475-7516/2017/11/005). arXiv: [1708.07030](https://arxiv.org/abs/1708.07030) [astro-ph.CO].
- Arbey, A. and F. Mahmoudi (2021). “Dark matter and the early Universe: a review”. In: *Prog. Part. Nucl. Phys.* 119, p. 103865. DOI: [10.1016/j.pnpnp.2021.103865](https://doi.org/10.1016/j.pnpnp.2021.103865). arXiv: [2104.11488](https://arxiv.org/abs/2104.11488) [hep-ph].
- Ata, Metin et al. (2018). “The clustering of the SDSS-IV extended Baryon Oscillation Spectroscopic Survey DR14 quasar sample: first measurement of baryon acoustic oscillations between redshift 0.8 and 2.2”. In: *Mon. Not. Roy. Astron. Soc.* 473.4, pp. 4773–4794. DOI: [10.1093/mnras/stx2630](https://doi.org/10.1093/mnras/stx2630). arXiv: [1705.06373](https://arxiv.org/abs/1705.06373) [astro-ph.CO].
- Baier, Rudolf, Sayantani Lahiri, and Paul Romatschke (July 2019). “Ricci cosmology”. In: arXiv: [1907.02974](https://arxiv.org/abs/1907.02974) [gr-qc].
- Barbosa, C.M.S. et al. (Dec. 2015). “Viscous Cosmology”. In: *12th International Conference on Gravitation, Astrophysics and Cosmology*. arXiv: [1512.00921](https://arxiv.org/abs/1512.00921) [astro-ph.CO].
- Barrow, John D. (1988). “String-Driven Inflationary and Deflationary Cosmological Models”. In: *Nucl. Phys. B* 310, pp. 743–763. DOI: [10.1016/0550-3213\(88\)90101-0](https://doi.org/10.1016/0550-3213(88)90101-0).
- Bassett, Bruce A. and Renee Hlozek (Oct. 2009). “Baryon Acoustic Oscillations”. In: arXiv: [0910.5224](https://arxiv.org/abs/0910.5224) [astro-ph.CO].

- Bégué, Damien, Clément Stahl, and She-Sheng Xue (2019). “A model of interacting dark fluids tested with supernovae and Baryon Acoustic Oscillations data”. In: *Nucl. Phys. B* 940, pp. 312–320. DOI: [10.1016/j.nuclphysb.2019.01.001](https://doi.org/10.1016/j.nuclphysb.2019.01.001). arXiv: [1702.03185](https://arxiv.org/abs/1702.03185) [astro-ph.CO].
- Bernal, Jose Luis, Licia Verde, and Adam G. Riess (2016). “The trouble with H_0 ”. In: *JCAP* 10, p. 019. DOI: [10.1088/1475-7516/2016/10/019](https://doi.org/10.1088/1475-7516/2016/10/019). arXiv: [1607.05617](https://arxiv.org/abs/1607.05617) [astro-ph.CO].
- Birrer, S. et al. (2020). “TDCOSMO - IV. Hierarchical time-delay cosmography – joint inference of the Hubble constant and galaxy density profiles”. In: *Astron. Astrophys.* 643, A165. DOI: [10.1051/0004-6361/202038861](https://doi.org/10.1051/0004-6361/202038861). arXiv: [2007.02941](https://arxiv.org/abs/2007.02941) [astro-ph.CO].
- Blake, Chris et al. (2012). “The WiggleZ Dark Energy Survey: Joint measurements of the expansion and growth history at $z < 1$ ”. In: *Mon. Not. Roy. Astron. Soc.* 425, pp. 405–414. DOI: [10.1111/j.1365-2966.2012.21473.x](https://doi.org/10.1111/j.1365-2966.2012.21473.x). arXiv: [1204.3674](https://arxiv.org/abs/1204.3674) [astro-ph.CO].
- Blomqvist, Michael et al. (2019). “Baryon acoustic oscillations from the cross-correlation of Ly α absorption and quasars in eBOSS DR14”. In: *Astron. Astrophys.* 629, A86. DOI: [10.1051/0004-6361/201935641](https://doi.org/10.1051/0004-6361/201935641). arXiv: [1904.03430](https://arxiv.org/abs/1904.03430) [astro-ph.CO].
- Bondi, H. (1947). “Spherically symmetrical models in general relativity”. In: *Mon. Not. Roy. Astron. Soc.* 107, pp. 410–425. DOI: [10.1093/mnras/107.5-6.410](https://doi.org/10.1093/mnras/107.5-6.410).
- Brevik, I., A. N. Makarenko, and A. V. Timoshkin (2019). “Viscous accelerating universe with nonlinear and logarithmic equation of state fluid”. In: *Int. J. Geom. Meth. Mod. Phys.* 16.10, p. 1950150. DOI: [10.1142/S0219887819501500](https://doi.org/10.1142/S0219887819501500). arXiv: [1907.02280](https://arxiv.org/abs/1907.02280) [gr-qc].
- Brevik, I., V.V. Obukhov, and A.V. Timoshkin (2015). “Dark Energy Coupled with Dark Matter in Viscous Fluid Cosmology”. In: *Astrophys. Space Sci.* 355, pp. 399–403. DOI: [10.1007/s10509-014-2163-9](https://doi.org/10.1007/s10509-014-2163-9). arXiv: [1410.2750](https://arxiv.org/abs/1410.2750) [gr-qc].
- Brevik, Iver and Øyvind Grøn (Sept. 2014). “Relativistic Viscous Universe Models”. In: *Recent Advances in Cosmology*. Ed. by Anderson Travena and Brady Soren. arXiv: [1409.8561](https://arxiv.org/abs/1409.8561) [gr-qc].
- Brevik, Iver et al. (2017). “Viscous Cosmology for Early- and Late-Time Universe”. In: *Int. J. Mod. Phys. D* 26.14, p. 1730024. DOI: [10.1142/S0218271817300245](https://doi.org/10.1142/S0218271817300245). arXiv: [1706.02543](https://arxiv.org/abs/1706.02543) [gr-qc].
- Camarena, David and Valerio Marra (2020). “Local determination of the Hubble constant and the deceleration parameter”. In: *Phys. Rev. Res.* 2.1, p. 013028. DOI: [10.1103/PhysRevResearch.2.013028](https://doi.org/10.1103/PhysRevResearch.2.013028). arXiv: [1906.11814](https://arxiv.org/abs/1906.11814) [astro-ph.CO].

- Capozziello, Salvatore and Luca Izzo (2010). "A cosmological independent calibration of the E_p -Eiso correlation for Gamma Ray Bursts". In: *Astron. Astrophys.* 519, A73. DOI: [10.1051/0004-6361/201014522](https://doi.org/10.1051/0004-6361/201014522). arXiv: [1003.5319](https://arxiv.org/abs/1003.5319) [astro-ph.CO].
- Caroli, Roberto, Mariusz P. Dabrowski, and Vincenzo Salzano (2021). "Ricci cosmology in light of astronomical data". In: *Eur. Phys. J. C* 81.10, p. 881. DOI: [10.1140/epjc/s10052-021-09666-9](https://doi.org/10.1140/epjc/s10052-021-09666-9). arXiv: [2105.10933](https://arxiv.org/abs/2105.10933) [gr-qc].
- Clifton, Timothy et al. (2012). "Modified Gravity and Cosmology". In: *Phys. Rept.* 513, pp. 1–189. DOI: [10.1016/j.physrep.2012.01.001](https://doi.org/10.1016/j.physrep.2012.01.001). arXiv: [1106.2476](https://arxiv.org/abs/1106.2476) [astro-ph.CO].
- Cole, Shaun et al. (2005). "The 2dF Galaxy Redshift Survey: Power-spectrum analysis of the final dataset and cosmological implications". In: *Mon. Not. Roy. Astron. Soc.* 362, pp. 505–534. DOI: [10.1111/j.1365-2966.2005.09318.x](https://doi.org/10.1111/j.1365-2966.2005.09318.x). arXiv: [astro-ph/0501174](https://arxiv.org/abs/astro-ph/0501174).
- Copeland, Edmund J., M. Sami, and Shinji Tsujikawa (2006). "Dynamics of dark energy". In: *Int. J. Mod. Phys. D* 15, pp. 1753–1936. DOI: [10.1142/S021827180600942X](https://doi.org/10.1142/S021827180600942X). arXiv: [hep-th/0603057](https://arxiv.org/abs/hep-th/0603057).
- Cox, R. T. (1946). "Probability, Frequency and Reasonable Expectation". In: *American Journal of Physics* 14.1, pp. 1–13. DOI: [10.1119/1.1990764](https://doi.org/10.1119/1.1990764). eprint: <https://doi.org/10.1119/1.1990764>. URL: <https://doi.org/10.1119/1.1990764>.
- Cruz, Norman, Esteban González, and Guillermo Palma (2020). "Exact analytical solution for an Israel–Stewart cosmology". In: *Gen. Rel. Grav.* 52.6, p. 62. DOI: [10.1007/s10714-020-02712-z](https://doi.org/10.1007/s10714-020-02712-z). arXiv: [1812.05009](https://arxiv.org/abs/1812.05009) [gr-qc].
- Di Valentino, Eleonora et al. (Mar. 2021). "In the Realm of the Hubble tension – a Review of Solutions". In: DOI: [10.1088/1361-6382/ac086d](https://doi.org/10.1088/1361-6382/ac086d). arXiv: [2103.01183](https://arxiv.org/abs/2103.01183) [astro-ph.CO].
- Dodelson, Scott (2003). *Modern Cosmology*. Academic Press, Elsevier Science.
- Donoghue, John F. (June 1995). "Introduction to the effective field theory description of gravity". In: *Advanced School on Effective Theories*. arXiv: [gr-qc/9512024](https://arxiv.org/abs/gr-qc/9512024).
- Eckart, Carl (1940). "The Thermodynamics of irreversible processes. 3.. Relativistic theory of the simple fluid". In: *Phys. Rev.* 58, pp. 919–924. DOI: [10.1103/PhysRev.58.919](https://doi.org/10.1103/PhysRev.58.919).
- Eisenstein, Daniel J. and Wayne Hu (1998). "Baryonic features in the matter transfer function". In: *Astrophys. J.* 496, p. 605. DOI: [10.1086/305424](https://doi.org/10.1086/305424). arXiv: [astro-ph/9709112](https://arxiv.org/abs/astro-ph/9709112).
- Eisenstein, Daniel J. et al. (2005). "Detection of the Baryon Acoustic Peak in the Large-Scale Correlation Function of SDSS Luminous Red Galaxies". In: *Astrophys. J.* 633, pp. 560–574. DOI: [10.1086/466512](https://doi.org/10.1086/466512). arXiv: [astro-ph/0501171](https://arxiv.org/abs/astro-ph/0501171).

- Elizalde, Emilio et al. (2020). “Analysis of the H_0 tension problem in the Universe with viscous dark fluid”. In: *Phys. Rev. D* 102.12, p. 123501. DOI: [10.1103/PhysRevD.102.123501](https://doi.org/10.1103/PhysRevD.102.123501). arXiv: [2006.01879](https://arxiv.org/abs/2006.01879) [gr-qc].
- Ellis, George F. R., Roy Maartens, and Malcolm A. H. MacCallum (2012). *Relativistic cosmology*. English. United Kingdom: Cambridge University Press. ISBN: 9780521381154. DOI: [10.1017/CB09781139014403](https://doi.org/10.1017/CB09781139014403).
- Gao, Li-Yang, She-Sheng Xue, and Xin Zhang (Jan. 2021). “Relieving the H_0 tension with a new interacting dark energy model”. In: arXiv: [2101.10714](https://arxiv.org/abs/2101.10714) [astro-ph.CO].
- Gómez-Valent, Adrià and Luca Amendola (May 2019). “ H_0 from cosmic chronometers and Type Ia supernovae, with Gaussian processes and the weighted polynomial regression method”. In: *15th Marcel Grossmann Meeting on Recent Developments in Theoretical and Experimental General Relativity, Astrophysics, and Relativistic Field Theories*. arXiv: [1905.04052](https://arxiv.org/abs/1905.04052) [astro-ph.CO].
- Green, Anne M. (2022). “Dark matter in astrophysics/cosmology”. In: *SciPost Phys. Lect. Notes* 37, p. 1. DOI: [10.21468/SciPostPhysLectNotes.37](https://doi.org/10.21468/SciPostPhysLectNotes.37). arXiv: [2109.05854](https://arxiv.org/abs/2109.05854) [hep-ph].
- Hiscock, W.A. and L. Lindblom (1983). “Stability and causality in dissipative relativistic fluids”. In: *Annals Phys.* 151, pp. 466–496. DOI: [10.1016/0003-4916\(83\)90288-9](https://doi.org/10.1016/0003-4916(83)90288-9).
- Hobson, M.P. (2010). *Bayesian Methods in Cosmology*. Cambridge University Press.
- Hu, Wayne and Naoshi Sugiyama (1996). “Small scale cosmological perturbations: An Analytic approach”. In: *Astrophys. J.* 471, pp. 542–570. DOI: [10.1086/177989](https://doi.org/10.1086/177989). arXiv: [astro-ph/9510117](https://arxiv.org/abs/astro-ph/9510117).
- Huterer, Dragan and Daniel L Shafer (2018). “Dark energy two decades after: Observables, probes, consistency tests”. In: *Rept. Prog. Phys.* 81.1, p. 016901. DOI: [10.1088/1361-6633/aa997e](https://doi.org/10.1088/1361-6633/aa997e). arXiv: [1709.01091](https://arxiv.org/abs/1709.01091) [astro-ph.CO].
- Israel, W. (1976). “Nonstationary irreversible thermodynamics: A Causal relativistic theory”. In: *Annals Phys.* 100, pp. 310–331. DOI: [10.1016/0003-4916\(76\)90064-6](https://doi.org/10.1016/0003-4916(76)90064-6).
- Israel, W. and J.M. Stewart (1979). “Transient relativistic thermodynamics and kinetic theory”. In: *Annals Phys.* 118, pp. 341–372. DOI: [10.1016/0003-4916\(79\)90130-1](https://doi.org/10.1016/0003-4916(79)90130-1).
- Jimenez, Raul and Abraham Loeb (2002). “Constraining cosmological parameters based on relative galaxy ages”. In: *Astrophys. J.* 573, pp. 37–42. DOI: [10.1086/340549](https://doi.org/10.1086/340549). arXiv: [astro-ph/0106145](https://arxiv.org/abs/astro-ph/0106145).
- Joyce, Austin et al. (2015). “Beyond the Cosmological Standard Model”. In: *Phys. Rept.* 568, pp. 1–98. DOI: [10.1016/j.physrep.2014.12.002](https://doi.org/10.1016/j.physrep.2014.12.002). arXiv: [1407.0059](https://arxiv.org/abs/1407.0059) [astro-ph.CO].

- King, A. R. and G. F. R. Ellis (1973). "Tilted homogeneous cosmological models". In: *Commun. Math. Phys.* 31, pp. 209–242. DOI: [10.1007/BF01646266](https://doi.org/10.1007/BF01646266).
- Klebesadel, Ray W., Ian B. Strong, and Roy A. Olson (1973). "Observations of Gamma-Ray Bursts of Cosmic Origin". In: *Astrophys. J. Lett.* 182, pp. L85–L88. DOI: [10.1086/181225](https://doi.org/10.1086/181225).
- Knox, Lloyd and Marius Millea (2020). "Hubble constant hunter's guide". In: *Phys. Rev. D* 101.4, p. 043533. DOI: [10.1103/PhysRevD.101.043533](https://doi.org/10.1103/PhysRevD.101.043533). arXiv: [1908.03663](https://arxiv.org/abs/1908.03663) [astro-ph.CO].
- Kodama, Yoshiki et al. (2008). "Gamma-Ray Bursts in $1.8 < z < 5.6$ Suggest that the Time Variation of the Dark Energy is Small". In: *Mon. Not. Roy. Astron. Soc.* 391, p. 1. DOI: [10.1111/j.1745-3933.2008.00508.x](https://doi.org/10.1111/j.1745-3933.2008.00508.x). arXiv: [0802.3428](https://arxiv.org/abs/0802.3428) [astro-ph].
- Kovtun, Pavel and Ashish Shukla (2018). "Kubo formulas for thermodynamic transport coefficients". In: *JHEP* 10, p. 007. DOI: [10.1007/JHEP10\(2018\)007](https://doi.org/10.1007/JHEP10(2018)007). arXiv: [1806.05774](https://arxiv.org/abs/1806.05774) [hep-th].
- Kurek, Aleksandra (2012). "Testing and selection cosmological models with acceleration". PhD thesis. Jagiellonian University, Krakow.
- Landau, L. D. and E. M. Lifshitz (Jan. 1987). *Fluid Mechanics, Second Edition: Volume 6 (Course of Theoretical Physics)*. 2nd ed. Course of theoretical physics / by L. D. Landau and E. M. Lifshitz, Vol. 6. Butterworth-Heinemann. ISBN: 0750627670. URL: <http://www.worldcat.org/isbn/0750627670>.
- Lemaître, G. (1933). "The expanding universe". In: *Annales Soc. Sci. Bruxelles A* 53, pp. 51–85. DOI: [10.1023/A:1018855621348](https://doi.org/10.1023/A:1018855621348).
- Li, Tjonnie Guang Feng (2013). "Extracting Physics from Gravitational Waves: Testing the Strong-field Dynamics of General Relativity and Inferring the Large-scale Structure of the Universe". PhD thesis. Vrije Universiteit, Amsterdam.
- Liang, Nan and Shuang Nan Zhang (2008). "Cosmology-Independent Distance Moduli of 42 Gamma-Ray Bursts between Redshift of 1.44 and 6.60". In: *AIP Conf. Proc.* 1065.1. Ed. by Yong-Feng Huang, Zi-Gao Dai, and Bing Zhang, pp. 367–372. DOI: [10.1063/1.3027949](https://doi.org/10.1063/1.3027949). arXiv: [0808.2655](https://arxiv.org/abs/0808.2655) [astro-ph].
- Liu, Jing and Hao Wei (2015). "Cosmological models and gamma-ray bursts calibrated by using Padé method". In: *Gen. Rel. Grav.* 47.11, p. 141. DOI: [10.1007/s10714-015-1986-1](https://doi.org/10.1007/s10714-015-1986-1). arXiv: [1410.3960](https://arxiv.org/abs/1410.3960) [astro-ph.CO].
- Madriz Aguilar, José Edgar et al. (2020). "Scalar field unification of interacting viscous dark fluid from a geometrical scalar–tensor theory of gravity". In: *Phys. Dark Univ.* 30, p. 100706. DOI: [10.1016/j.dark.2020.100706](https://doi.org/10.1016/j.dark.2020.100706). arXiv: [2007.05846](https://arxiv.org/abs/2007.05846) [gr-qc].
- Misner, Charles W., K. S. Thorne, and J. A. Wheeler (1973). *Gravitation*. San Francisco: W. H. Freeman. ISBN: 978-0-7167-0344-0, 978-0-691-17779-3.

- Mohan, N. D Jerin, Athira Sasidharan, and Titus K. Mathew (2017). “Bulk viscous matter and recent acceleration of the universe based on causal viscous theory”. In: *Eur. Phys. J. C* 77.12, p. 849. DOI: [10.1140/epjc/s10052-017-5428-y](https://doi.org/10.1140/epjc/s10052-017-5428-y). arXiv: [1708.02437](https://arxiv.org/abs/1708.02437) [gr-qc].
- Moresco, Michele et al. (Jan. 2022). “Unveiling the Universe with Emerging Cosmological Probes”. In: arXiv: [2201.07241](https://arxiv.org/abs/2201.07241) [astro-ph.CO].
- Muller, Ingo (1967). “Zum Paradoxon der Wärmeleitungstheorie”. In: *Z. Phys.* 198, pp. 329–344. DOI: [10.1007/BF01326412](https://doi.org/10.1007/BF01326412).
- Nadathur, Seshadri et al. (2019). “Beyond BAO: Improving cosmological constraints from BOSS data with measurement of the void-galaxy cross-correlation”. In: *Phys. Rev. D* 100.2, p. 023504. DOI: [10.1103/PhysRevD.100.023504](https://doi.org/10.1103/PhysRevD.100.023504). arXiv: [1904.01030](https://arxiv.org/abs/1904.01030) [astro-ph.CO].
- Normann, Ben David and Iver Håkon Brevik (2021). “Can the Hubble tension be resolved by bulk viscosity?” In: *Mod. Phys. Lett. A* 36.27, p. 2150198. DOI: [10.1142/S0217732321501984](https://doi.org/10.1142/S0217732321501984). arXiv: [2107.13533](https://arxiv.org/abs/2107.13533) [gr-qc].
- Parrent, J., B. Friesen, and M. Parthasarathy (2014). “A review of type Ia supernova spectra”. In: *Astrophys. Space Sci.* 351, pp. 1–52. DOI: [10.1007/s10509-014-1830-1](https://doi.org/10.1007/s10509-014-1830-1). arXiv: [1402.6337](https://arxiv.org/abs/1402.6337) [astro-ph.HE].
- Penzias, A. A. and R. W. Wilson (July 1965). “A Measurement of Excess Antenna Temperature at 4080 Mc/s.” In: 142, pp. 419–421. DOI: [10.1086/148307](https://doi.org/10.1086/148307).
- Perez, Javier de Cruz et al. (Oct. 2021). “BD- Λ CDM and Running Vacuum Models: Theoretical background and current observational status”. In: arXiv: [2110.07569](https://arxiv.org/abs/2110.07569) [astro-ph.CO].
- Perivolaropoulos, Leandros (2014). “Large Scale Cosmological Anomalies and Inhomogeneous Dark Energy”. In: *Galaxies* 2, pp. 22–61. DOI: [10.3390/galaxies2010022](https://doi.org/10.3390/galaxies2010022). arXiv: [1401.5044](https://arxiv.org/abs/1401.5044) [astro-ph.CO].
- Perivolaropoulos, Leandros and Foteini Skara (May 2021). “Challenges for Λ CDM: An update”. In: arXiv: [2105.05208](https://arxiv.org/abs/2105.05208) [astro-ph.CO].
- Refsdal, S. (1964). “On the possibility of determining Hubble’s parameter and the masses of galaxies from the gravitational lens effect”. In: *Mon. Not. Roy. Astron. Soc.* 128, p. 307.
- Riess, Adam G. et al. (2019). “Large Magellanic Cloud Cepheid Standards Provide a 1% Foundation for the Determination of the Hubble Constant and Stronger Evidence for Physics beyond Λ CDM”. In: *Astrophys. J.* 876.1, p. 85. DOI: [10.3847/1538-4357/ab1422](https://doi.org/10.3847/1538-4357/ab1422). arXiv: [1903.07603](https://arxiv.org/abs/1903.07603) [astro-ph.CO].

- Romatschke, Paul and Ulrike Romatschke (May 2019). *Relativistic Fluid Dynamics In and Out of Equilibrium*. Cambridge Monographs on Mathematical Physics. Cambridge University Press. ISBN: 978-1-108-48368-1, 978-1-108-75002-8. DOI: [10.1017/9781108651998](https://doi.org/10.1017/9781108651998). arXiv: [1712.05815](https://arxiv.org/abs/1712.05815) [nucl-th].
- Rubakov, V. A. (Dec. 2019). “Cosmology and Dark Matter”. In: *2019 European School of High-Energy Physics*. arXiv: [1912.04727](https://arxiv.org/abs/1912.04727) [hep-ph].
- Sainte Agathe, Victoria de et al. (2019). “Baryon acoustic oscillations at $z = 2.34$ from the correlations of Ly α absorption in eBOSS DR14”. In: *Astron. Astrophys.* 629, A85. DOI: [10.1051/0004-6361/201935638](https://doi.org/10.1051/0004-6361/201935638). arXiv: [1904.03400](https://arxiv.org/abs/1904.03400) [astro-ph.CO].
- Scolnic, D.M. et al. (2018). “The Complete Light-curve Sample of Spectroscopically Confirmed SNe Ia from Pan-STARRS1 and Cosmological Constraints from the Combined Pantheon Sample”. In: *Astrophys. J.* 859.2, p. 101. DOI: [10.3847/1538-4357/aab9bb](https://doi.org/10.3847/1538-4357/aab9bb). arXiv: [1710.00845](https://arxiv.org/abs/1710.00845) [astro-ph.CO].
- Sharma, Sanjib (2017). “Markov Chain Monte Carlo Methods for Bayesian Data Analysis in Astronomy”. In: *Ann. Rev. Astron. Astrophys.* 55, pp. 213–259. DOI: [10.1146/annurev-astro-082214-122339](https://doi.org/10.1146/annurev-astro-082214-122339). arXiv: [1706.01629](https://arxiv.org/abs/1706.01629) [astro-ph.IM].
- Silva, W. J. C. da and R. Silva (2019). “Extended Λ CDM model and viscous dark energy: A Bayesian analysis”. In: *JCAP* 05, p. 036. DOI: [10.1088/1475-7516/2019/05/036](https://doi.org/10.1088/1475-7516/2019/05/036). arXiv: [1810.03759](https://arxiv.org/abs/1810.03759) [astro-ph.CO].
- Sola, Joan (2013). “Cosmological constant and vacuum energy: old and new ideas”. In: *J. Phys. Conf. Ser.* 453. Ed. by Taxiarchis Papakostas and Demetrios A Pliakis, p. 012015. DOI: [10.1088/1742-6596/453/1/012015](https://doi.org/10.1088/1742-6596/453/1/012015). arXiv: [1306.1527](https://arxiv.org/abs/1306.1527) [gr-qc].
- Solà, Joan and Adrià Gómez-Valent (2015). “The Λ CDM cosmology: From inflation to dark energy through running Λ ”. In: *Int. J. Mod. Phys. D* 24, p. 1541003. DOI: [10.1142/S0218271815410035](https://doi.org/10.1142/S0218271815410035). arXiv: [1501.03832](https://arxiv.org/abs/1501.03832) [gr-qc].
- Suyu, S.H. et al. (2017). “H0LiCOW – I. H0 Lenses in COSMOGRAIL’s Wellspring: program overview”. In: *Mon. Not. Roy. Astron. Soc.* 468.3, pp. 2590–2604. DOI: [10.1093/mnras/stx483](https://doi.org/10.1093/mnras/stx483). arXiv: [1607.00017](https://arxiv.org/abs/1607.00017) [astro-ph.CO].
- Suyu, Sherry H. et al. (2018). “Cosmological distance indicators”. In: *Space Sci. Rev.* 214.5, p. 91. DOI: [10.1007/s11214-018-0524-3](https://doi.org/10.1007/s11214-018-0524-3). arXiv: [1801.07262](https://arxiv.org/abs/1801.07262) [astro-ph.CO].
- Suzuki, N. et al. (2012). “The Hubble Space Telescope Cluster Supernova Survey: V. Improving the Dark Energy Constraints Above $z > 1$ and Building an Early-Type-Hosted Supernova Sample”. In: *Astrophys. J.* 746, p. 85. DOI: [10.1088/0004-637X/746/1/85](https://doi.org/10.1088/0004-637X/746/1/85). arXiv: [1105.3470](https://arxiv.org/abs/1105.3470) [astro-ph.CO].
- Tolman, Richard C. (1934). “Effect of inhomogeneity on cosmological models”. In: *Proc. Nat. Acad. Sci.* 20, pp. 169–176. DOI: [10.1073/pnas.20.3.169](https://doi.org/10.1073/pnas.20.3.169).

- Trotta, Roberto (2007). “Applications of Bayesian model selection to cosmological parameters”. In: *Mon. Not. Roy. Astron. Soc.* 378, pp. 72–82. DOI: [10.1111/j.1365-2966.2007.11738.x](https://doi.org/10.1111/j.1365-2966.2007.11738.x). arXiv: [astro-ph/0504022](https://arxiv.org/abs/astro-ph/0504022).
- (Jan. 2017). “Bayesian Methods in Cosmology”. In: arXiv: [1701.01467](https://arxiv.org/abs/1701.01467) [[astro-ph.CO](https://arxiv.org/abs/astro-ph)].
- Verde, Licia (2010). “Statistical methods in cosmology”. In: *Lect. Notes Phys.* 800, pp. 147–177. DOI: [10.1007/978-3-642-10598-2_4](https://doi.org/10.1007/978-3-642-10598-2_4). arXiv: [0911.3105](https://arxiv.org/abs/0911.3105) [[astro-ph.CO](https://arxiv.org/abs/astro-ph)].
- Wald, Robert M (1984). *General relativity*. Chicago, IL: Chicago Univ. Press. URL: <https://cds.cern.ch/record/106274>.
- Wang, Yun and Pia Mukherjee (2007). “Observational Constraints on Dark Energy and Cosmic Curvature”. In: *Phys. Rev. D* 76, p. 103533. DOI: [10.1103/PhysRevD.76.103533](https://doi.org/10.1103/PhysRevD.76.103533). arXiv: [astro-ph/0703780](https://arxiv.org/abs/astro-ph/0703780).
- Webb, J. K. et al. (2011). “Indications of a spatial variation of the fine structure constant”. In: *Phys. Rev. Lett.* 107, p. 191101. DOI: [10.1103/PhysRevLett.107.191101](https://doi.org/10.1103/PhysRevLett.107.191101). arXiv: [1008.3907](https://arxiv.org/abs/1008.3907) [[astro-ph.CO](https://arxiv.org/abs/astro-ph)].
- Weinberg, David H. et al. (2013). “Observational Probes of Cosmic Acceleration”. In: *Phys. Rept.* 530, pp. 87–255. DOI: [10.1016/j.physrep.2013.05.001](https://doi.org/10.1016/j.physrep.2013.05.001). arXiv: [1201.2434](https://arxiv.org/abs/1201.2434) [[astro-ph.CO](https://arxiv.org/abs/astro-ph)].
- Weinberg, S. (1972). *Gravitation and cosmology*. New York: John Wiley and Sons.
- Weinberg, Steven (1989). “The Cosmological Constant Problem”. In: *Rev. Mod. Phys.* 61. Ed. by Jong-Ping Hsu and D. Fine, pp. 1–23. DOI: [10.1103/RevModPhys.61.1](https://doi.org/10.1103/RevModPhys.61.1).
- (Feb. 2000). “The Cosmological constant problems”. In: *4th International Symposium on Sources and Detection of Dark Matter in the Universe (DM 2000)*, pp. 18–26. arXiv: [astro-ph/0005265](https://arxiv.org/abs/astro-ph/0005265).
- (2010). “Asymptotically Safe Inflation”. In: *Phys. Rev. D* 81, p. 083535. DOI: [10.1103/PhysRevD.81.083535](https://doi.org/10.1103/PhysRevD.81.083535). arXiv: [0911.3165](https://arxiv.org/abs/0911.3165) [[hep-th](https://arxiv.org/abs/hep-th)].
- Wilczynska, Michael R. et al. (2020). “Four direct measurements of the fine-structure constant 13 billion years ago”. In: *Sci. Adv.* 6.17, eaay9672. DOI: [10.1126/sciadv.aay9672](https://doi.org/10.1126/sciadv.aay9672). arXiv: [2003.07627](https://arxiv.org/abs/2003.07627) [[astro-ph.CO](https://arxiv.org/abs/astro-ph)].
- Wong, Kenneth C. et al. (2020). “H0LiCOW – XIII. A 2.4 per cent measurement of H0 from lensed quasars: 5.3 σ tension between early- and late-Universe probes”. In: *Mon. Not. Roy. Astron. Soc.* 498.1, pp. 1420–1439. DOI: [10.1093/mnras/stz3094](https://doi.org/10.1093/mnras/stz3094). arXiv: [1907.04869](https://arxiv.org/abs/1907.04869) [[astro-ph.CO](https://arxiv.org/abs/astro-ph)].
- Yang, Weiqiang et al. (2019). “Challenging bulk viscous unified scenarios with cosmological observations”. In: *Phys. Rev. D* 100.10, p. 103518. DOI: [10.1103/PhysRevD.100.103518](https://doi.org/10.1103/PhysRevD.100.103518). arXiv: [1906.04162](https://arxiv.org/abs/1906.04162) [[astro-ph.CO](https://arxiv.org/abs/astro-ph)].
- Zhai, Zhongxu and Yun Wang (2019). “Robust and model-independent cosmological constraints from distance measurements”. In: *JCAP* 07, p. 005. DOI: [10.1088/1475-7516/2019/07/005](https://doi.org/10.1088/1475-7516/2019/07/005). arXiv: [1811.07425](https://arxiv.org/abs/1811.07425) [[astro-ph.CO](https://arxiv.org/abs/astro-ph)].

Streszczenie rozprawy doktorskiej

Uniwersytet Szczeciński
Instytut Fizyki

mgr Roberto Caroli

Tytuł rozprawy doktorskiej: **Kosmologie Ricciego**

Promotor: prof. dr hab. Mariusz P. Dąbrowski

W rozprawie rozważa się nowy rodzaj kosmologii, zwanej kosmologią Ricciego, która pojawia się jako konsekwencja uwzględnienia relatywistycznych płynów nierównowagowych w zakrzywionej czasoprzestrzeni.

Po krótkim przypomnieniu zalet i wyzwań powszechnie akceptowanego Standardowego Modelu Kosmologicznego Λ CDM, przedstawiona jest konstrukcja teoretyczna, na której opierają się kosmologie Ricciego. Następnie przedstawiamy różne modele, które wyprowadziliśmy w ramach tej kosmologii w celu opisanego przyspieszonej ekspansji Wszechświata w późnym okresie jego ewolucji i przy założeniu stałych współczynników równań transportu płynu.

Pierwszym rozważanym modelem jest izotropowa kosmologia Ricciego, w której człon związany z ciśnieniem Ricciego wpływa na wszystkie składniki materii wypełniające Wszechświat. Dla każdego rodzaju materii mamy tutaj do czynienia z odejściem od skalowania przesunięcia ku czerwieni charakterystycznego dla płynu doskonałego.

W następnym kroku rozważamy dwa modele, w których odrzucone jest założenie o spełnianiu zasady kosmologicznej: w pierwszym modelu badane są konsekwencje adaptacji nierównowagowych płynów kosmicznych w czasoprzestrzeni opisanej przez metrykę typu Bianchi I, natomiast w modelu drugim rozważamy ich następstwa dla niejednorodnego wszechświata opisanego metryką Lemaître'a-Tolmana-Bondiego.

Dalej badamy model próżniowy Ricciego, w którym człony nierównowagowego ciśnienia Ricciego wpływają tylko na ciśnienie próżni związanej ze stałą kosmologiczną. W wyniku takiego odstępstwa od stanu równowagi dla próżni, jej gęstość energii zależy także od gęstości energii materii i gęstości energii promieniowania. Pod uwagę brane są tutaj dwa podprzypadki: w pierwszym próżnia Ricciego oddziałuje z zimną ciemną materią, podczas gdy w drugim oddziałuje z relatywistycznym typem materii, który nazywamy ciemnym promieniowaniem.

Ostatnimi rozważanymi przez nas modelami są kosmologie nachylone Ricciego,

w których czteropędność obserwatora nie pokrywa się z czteropędnością płynu kosmicznego, co prowadzi do obecności strumienia energii i anizotropowego naprężenia w płynie, które mogą być zmierzone przez obserwatora. Poza tym badamy wpływ nierównowagowych członów Ricciiego na płyn kosmiczny oraz na związane z jego własnościami warunki energetyczne.

W końcu, po wprowadzeniu narzędzi statystycznych potrzebnych do wnioskowania bayesowskiego i zastosowaniu dostępnych danych kosmologicznych, omawiamy wyniki dopasowania modelu izotropowej kosmologii Ricciiego do tych danych.

W rezultacie znajdujemy obserwacyjne ograniczenia na parametry modeli kosmologii Ricciiego i poddajemy pod dyskusję ich zdolność do rozwiązania problemu niezgodności pomiaru parametru Hubble'a oraz lepszego niż w modelu standardowym Λ CDM dopasowania danych kosmologicznych.

Słowa kluczowe: kosmologie Ricciiego, relatywistyczne płyny nierównowagowe, współczynniki równań transportu drugiego rzędu, ciśnienia efektywne

Data, podpis 13.06.2022 *Roberto Caroli*

Summary of the Doctoral Thesis

University of Szczecin
Institute of Physics

Roberto Caroli M.Sc.

PhD Thesis entitled: **Ricci Cosmologies**

Supervisor: Prof. Mariusz P. Dąbrowski

This dissertation deals with the new framework of Ricci Cosmology which has recently emerged from the study of out-of-equilibrium relativistic fluids in curved spacetime.

After briefly recalling the strengths and the challenges of the widely accepted Standard Cosmological Model or Λ CDM, we shortly review the theoretical construction on which the framework of Ricci Cosmology relies.

Next, we introduce different models we have derived in this framework in order to describe the late-time accelerated expansion of the Universe, under the assumption of constant transport coefficients.

The first model considered is Isotropic Ricci Cosmology, in which Ricci pressure terms affect all the matter components filling in the Universe. A departure from perfect fluid redshift scaling is found for each matter component.

Next, we consider two models in which we drop the assumption of the Cosmological Principle: in the first model, we study the consequences of the departure from equilibrium for cosmic fluids on a background described by the Bianchi I Type metric, while in the second model, we consider an inhomogeneous Universe described by the Lemaitre-Tolman-Bondi metric.

Then, we study the model of Ricci Vacuum Cosmology in which non-equilibrium Ricci terms affect only the vacuum pressure. As a result of such departure from equilibrium for the vacuum, its energy density depends on the energy densities of matter and radiation. Two subcases are taken into account: in the first, the Ricci vacuum interacts with Cold Dark Matter, while in the second, it interacts with a relativistic species, which we call Dark Radiation.

The last model we consider is the Tilted Ricci Cosmology, in which the observer 4-velocity does not coincide with the fluid 4-velocity, leading to the presence of an energy flux and an anisotropic stress in the fluid as seen by the observer. We study the effects that the non-equilibrium Ricci terms have onto the cosmic fluid and on its energy conditions.

Finally, after introducing the statistical tools for Bayesian Inference and the

available cosmological data, we discuss the results of the fit of the Isotropic Ricci Cosmology model against these cosmological data.

Observational bounds on the parameters of the model are found and its capability to relief the Hubble tension at the background level and to describe better than CDM the cosmological data are discussed.

Keywords: Ricci Cosmology, relativistic out-of-equilibrium fluid, second-order transport coefficients, effective pressure

Date, signature 13.06.2022 *Roberto Coniti*